Western Graduate&PostdoctoralStudies

Western University
Scholarship@Western

Electronic Thesis and Dissertation Repository

7-24-2015 12:00 AM

Ginsenosides, Glycosidases and the Ginseng-Pythium Interaction

Dimitre A. Ivanov
The University of Western Ontario

Supervisor
Dr. Mark A. Bernards
The University of Western Ontario

Graduate Program in Biology
A thesis submitted in partial fulfillment of the requirements for the degree in Doctor of Philosophy
© Dimitre A. Ivanov 2015

Follow this and additional works at: https://ir.lib.uwo.ca/etd

 Part of the Agriculture Commons, Biology Commons, and the Plant Biology Commons

Recommended Citation

Ivanov, Dimitre A., "Ginsenosides, Glycosidases and the Ginseng-Pythium Interaction" (2015). *Electronic Thesis and Dissertation Repository*. 2994.
https://ir.lib.uwo.ca/etd/2994

This Dissertation/Thesis is brought to you for free and open access by Scholarship@Western. It has been accepted for inclusion in Electronic Thesis and Dissertation Repository by an authorized administrator of Scholarship@Western. For more information, please contact wlswadmin@uwo.ca.

GINSENOSIDES, GLYCOSIDASES AND THE GINSENG-PYTHIUM INTERACTION

(Thesis format: Integrated Article)

by

Dimitre A. Ivanov

Graduate Program
in
Biology

A thesis submitted in partial fulfillment
of the requirements for the degree of
Doctor of Philosophy

The School of Graduate and Postdoctoral Studies
The University of Western Ontario
London, Ontario, Canada

© Dimitre A. Ivanov 2015

ABSTRACT

Ginsenosides, the triterpenoid saponins produced by American ginseng (*Panax quinquefolius* L.), have been extensively studied for their medicinal value, however, their function in the rhizosphere remains largely unknown. Like other saponins, ginsenosides possess mild fungitoxic activity toward some common ginseng pathogens. However, numerous oomycete root pathogens of ginseng, most notably *Pythium irregulare* Buisman, are able to partially deglycosylate the 20 (S)-protopanaxadiol ginsenosides Rb1, Rd and gypenoside XVII via extracellular glycosidases (ginsenosidases), leading to the formation of a common product, ginsenoside F2. In this thesis the potential role(s) of these extracellular ginsenosidases and the ginsenoside products they produce (ie. ginsenoside F2) in the ginseng-*P. irregulare* pathosystem are examined. Treatment of the roots of ginseng plants with a relatively high dose of ginsenosides results in a delay of infection by *P. irregulare,* as monitored *in vivo* by a non-invasive chlorophyll fluorescence imaging method adapted to track the progression of a root pathogen in perennial plants. Furthermore, there is a correlation between the virulence of *P. irregulare* on ginseng and ginsenosidase activity and the presence of ginsenosides may act as a trigger for the production of these specific ginsenosidases, although the mechanism regulating this is unknown. Previously it was hypothesized that ginsenoside F2 acts as the main chemoattractant/growth stimulator in *P. irregulare*, however, data obtained showed *in vitro* inhibition of *P. irregulare* growth caused by ginsenoside F2, which was overcome with time. This has cast doubt on the initial hypothesis however, it is possible that the inhibition in growth may be overcome through a physiological/structural change in *P. irregulare* signalled by exposure to ginsenoside F2 which may be related to signalling and increased pathogenicity. This suggests that ginsenosides may serve to alter the growth and metabolism of *P. irregulare* which may serve to facilitate infection. In conjunction with the above work, amino-acid sequence data of the purified ginsenosidases was used to clone and sequence a putative ß-glucosidase designated as PiGH1-x from *P. irregulare* which *in silico* analysis suggests may encode previously isolated ß-1,2 glycosidases from P. irregulare. This will allow for future studies of the molecular triggers that that could be involved in facilitating the infection of ginseng by *P. irregulare*.

Key Words: *Pythium irregulare*, *Panax quinquefolius*, glycosidases, ginsenosides, biotic stress, pathogenicity, chlorophyll fluorescence imaging, oomycetes, disease monitoring

CO-AUTHORSHIP

Chapter 2: Ivanov, D.A., Bernards, M.A., 2012. Ginsenosidases and the pathogenicity of *Pythium irregulare*. Phytochemistry 78, 44-53.

Bernards, M.A. - principal investigator, provided guidance for experimental design and critical comments for final manuscript.

Chapter 3: Ivanov, D.A., Bernards, M.A., Chlorophyll Fluorescence Imaging as a Tool to Monitor the Progress of a Root Pathogen in a Perennial Plant.
(Submitted to Plant, Cell and Environment)

Bernards, M.A. - principal investigator, provided guidance for experimental design and critical comments for final manuscript.

Chapter 4: Ivanov, D.A., Georgakopoulos, J.R.C., Bernards, M.A., Chemoattractant Potential of Ginsenosides in the Ginseng - *P. irregulare* Pathosystem.

Georgakopoulos, J.R.C. - ginsenoside soil migration experiment, assisted with chlorophyll fluorescence measurments

Bernards, M.A. - principal investigator, LC-MS ginsenoside analysis, provided guidance for experimental design and critical comments for final manuscript.

Chapter 5: Ivanov, D.A., Bernards, M.A., Sequencing and Preliminary Bioinformatics Analysis of a Potential Ginsenoside Metabolising ß-glucosidase from *P. irregulare.*

Bernards, M.A. - principal investigator, 3D - modelling, provided guidance for experimental design and critical comments for final manuscript

DEDICATION

I dedicate this thesis to my parents

Tanya D. Ivanova and Alexander G. Ivanov

ACKNOWLEDGEMENTS

Completing my PhD would not have been possible without the support and guidance that I received during my studies, and so I wish to acknowledge the following individuals:

First and foremost, I would like to thank my supervisor and mentor, Dr. Mark A. Bernards. Mark welcomed me into his lab many years ago to do an undergraduate project, which was then followed up by my Ph.D. project. His enthusiasm and love for research was contagious, and became the reason I decided to pursue graduate studies. I am grateful for the guidance, support, wisdom and time that he has contributed throughout the years. It has been a pleasure and an honour to be one of Mark's students.

The members of my advisory committee, Dr. R. Greg Thorn, Dr. Susanne Kohalmi and Dr. Dan Brown, for their time, suggestions and encouragement as well as Anica Bjelica for her expertise, technical knowledge and assistance.

The members of the Bernards lab especially Meg Haggitt for her help and guidance over the years and Jorge Georgakopoulos for his tireless assistance in the lab. As well I would like to thank Pooja Sharma, Rachel White and Azul Sosa for their assistance in plant pathogenicity rating and for their support throughout the years. My gratitude is also extended to my colleagues from the 4th floor of NCB, who were an endless source of friendship during my Ph.D. studies.

Lastly, I want to extend a heartfelt and special thank you to my parents and sister, for their endless love and support throughout my life and experience as a graduate student.

I also gratefully acknowledge the funding I received during my graduate studies, from both NSERC and WGRS.

TABLE OF CONTENTS

LIST OF TABLES

LIST OF FIGURES

LIST OF SUPPORTING INFORMATION

LIST OF ABBREVIATIONS

Φ_{PSII}	Quantum yield of photochemical energy conversion in PS II
Φ_{NO}	Quantum yield of non-regulated non-photochemical energy loss in PS II
Φ_{NPQ}	Quantum yield of regulated non-photochemical energy loss in PS II
F	Fluorescence yield measured briefly before application of a Saturation Pulse
F_m	Maximal fluorescence yield of dark-adapted sample with all PS II centers closed
F'_m	Maximal fluorescence yield of illuminated sample with all PS II centers closed
F_o	Minimal fluorescence yield of dark-adapted sample with all PS II centers open
F'_o	Minimal fluorescence yield of illuminated sample with all PS II centers open
F_v	Variable fluorescence of dark-adapted sample, F_m - F_o
F_v/F_m	Maximum quantum efficiency of PS II photochemistry
F'_q	Photochemical quenching of fluorescence with PS II centers open, F'_m - F
NPQ	Non-photochemical quenching parameter describing regulated dissipation of excess energy
PAM	Pulse-Amplitude-Modulation
PAR	Photosynthetically active radiation measured in µmol quanta m^{-2} s^{-1}
PS I	Photosystem I, which does not show variable fluorescence yield
PS II	Photosystem II, which shows variable fluorescence yield
q_L	Parameter estimating the fraction of open PS II centers based on a Lake-model
SP	Saturation Pulse serving for transient full closure of PS II centers

Chapter 1: General Introduction

1.1. *Pythium irregulare* - Root pathogen of ginseng

The genus *Pythium* belongs to the phylum *Oomycota* and contains many well known species of necrotrophic plant pathogens that infect various field and hydroponically grown crops, including root crops (eg., ginseng), deciduous fruit trees, vegetables, cereals and ornamentals (Reeleder and Brammall 1994; Chamswarng and Cook 1985; Gull et al. 2004; Ingram and Cook 1990; Martin and Loper 1999; Mazzola et al. 2002; Moorman et al. 2002). However, there are also a large number of species within this genus that are saprotrophic and occupy a wide range of terrestrial and aquatic habitats (Van der Platts-Nietrink 1981; Martin and Loper 1999; Abdelghani et al. 2004). Oomycetes form fungal-like hyphae and have a growth pattern similar to fungi, however, molecular and morphological studies have classified these organisms within the kingdom Stramenopila alongside photosynthetic organisms like diatoms and brown algae (Baldauf et al. 2000; Hardham 2007). The main morphological characteristic oomycetes share with these other protists within the Stramenopila is the presence of tubular hairs on the anterior flagellum of their motile spores (zoospores) (Van de Peer and de Wachter 1997). The production of motile spores, however, is only one of several differences that distinguish oomycetes from true fungi. Others include the inability of most oomycetes to synthesize sterols, the presence of cellulose instead of chitin in their cell walls, the formation of coenocytic hyphae and the diploid nature of their vegetative life cycle (Tyler et al. 2006; Attard et al. 2008; Latijnhouwers et al. 2003; Hardham 2007).

Phytopathogenic *Pythium* and *Phytophthora* species have been shown to vary in host range with some such as *Pythium ultimum and Pythium aphanidermatum* exhibiting a broad host range and others like *Pythium graminicola* being more restricted (Martin and Loper 1999). However, all *Pythium* spp. infect mainly juvenile and succulent tissues, which restricts their parasitism to seedlings or to the feeder roots and root tips of older plants as well as to watery fruits and stem tissues (Hendrix and Cambell 1973). Furthermore, they infect all dicots as well as some monocots (Weiland et al. 2013) and economic losses from just one species, *Phytophthora infestans*, accounts for about $5 billion USD in lost economic productivity per year (Strange and Scott 2005).

Pythium irregulare Buisman is a further example of a *Pythium* spp. with a very broad host range spanning both angiosperms and gymnosperms from many plant families, such as the *Asteraceae, Fabaceae, Primulaceae, Chenopodiaceae* and *Cucurbitaceae* for dicots and Poaceae for monocots (Middleton 1943). It is also the biggest commercial threat to the cultivation of American ginseng (*Panax quinquefolius* L.) (Howard et al. 1994), whose interaction with *P. irregulare* is the focus of study in this thesis. This destructive soil-borne pathogen causes severe pre-emergence damping-off and post-emergence root rot, most commonly in one- and two-year old ginseng plants (Krupa and Dommergues 1994). Symptoms are an olivaceous, water-soaked rot of the stem, causing stems to collapse and the complete maceration of secondary roots and tips of tap roots until a reddish-brown colour is attained (Reeleder and Brammall 1994). The disease severity depends on environmental factors, with *P. irregulare* as well as other *Pythium* spp. generally showing greater virulence at lower temperatures (below 20°C) and higher soil moisture (Hendrix and Campbell 1973). Furthermore, *Pythium* infection has been shown to increase following addition of residues and high-carbohydrate amendments to soil (Trujillo and Hine 1965; Liu and Vaughn 1966). The accumulation of *Pythium* propagules in soil has also been linked to the occurrence of replant and decline diseases in perennial crops, including ginseng (Hendrix and Campbell 1973; Mai and Abawi 1981).

The ability to control and mitigate the diseases caused by *Pythium* infection is an ongoing area of study. This is because oomycetes are resistant to many available fungicides that either target membrane sterols or inhibit chitin synthase (Griffith et al. 1991; Latijnhouwers et al. 2003). In fact, phenylamide fungicides such as metalaxyl, which interfere with RNA synthesis, are the only control agents that have been used successfully against oomycetes (Schwinn and Staub 1995). However, isolates of *Pythium* and *Phytophthora* species resistant to these chemicals are already prevalent (Attard et al. 2008). For this reason, further research is needed to understand the physiological and molecular processes that affect the interactions between oomycetes and their host species, in order to develop better disease protection strategies.

1.2. American ginseng (*Panax quinquefolius*)

1.2.1. Morphology and horticulture

Ginseng has been used as an herbal medicine in East Asia for thousands of years and holds an important position in oriental medicine (Kiefer and Pantuso 2003). This has been taken into account even in the genus name itself as the word *Panax* is derived from the Greek word "panakos" meaning "all-heal". Ginseng is a member of the *Araliaceae* family and is a slow growing perennial plant which is cultivated for the high medicinal value of its root. There are 17 known species of ginseng in the genus *Panax*, all of which are considered medicinal (Wen and Zimmer 1996; Small and Catling 1999). However, only two species are heavily cultivated for commercial purposes: American ginseng (*Panax quinquefolius*) indigenous to the rich, moist and mature deciduous forests of South-eastern Canada and the Eastern and Midwestern United States (McGraw et al. 2013) and Asian ginseng (*Panax ginseng* C.A. Mey.) indigenous to China, South Korea and Japan (Hu et al. 1980). Of these two species however, American ginseng is believed to have superior medicinal qualities (McGraw et al 2013).

Commercial cultivation of American ginseng in Canada dates back to the 19th century, and coincided with the industrial scale over-harvesting of wild ginseng populations in North America (Proctor and Bailey 1987; McGraw et al. 2013). For this reason, wild populations of ginseng in North America are extremely rare and most ginseng today is produced through intensive field cultivation under artificial shade structures, with roots being harvested after 3-5 years of growth (McGraw et al. 2013; You et al. 2015).

The underground morphology of American ginseng is characterized by a thick and often branched taproot that quickly narrows to an apical rhizome that allows vertical stem growth (Lewis and Zenger 1982). Scars on the rhizome caused by annual loss of the aerial stem are well-marked and can be used to determine the age of the plant, with the maximum age of ginseng in wild populations estimated at 25-30 years (Anderson et al 1993). When they emerge, aerial stems are usually deciduous and at maturity reach a height of 20-70 cm. At the summit of the stem there is a formation of three or four whorled "leaves" that consist of a petiole with three to five palmately divided leaflets (Lewis and Zenger 1982). However, seedlings (one-year old plants) initially have only three leaflets.

Reproduction in American ginseng is usually sexual and the inflorescence consists of small greenish-white flowers that form on a single umbel emerging from the mid axis of the leaves. However, during commercial cultivation it is recommended that flowers are removed (either chemically or mechanically) because this can increase root weight 25-30% and subsequently raise revenue (Proctor et al. 1999; Fiebig et al. 2005). If the inflorescence is not removed, the fruits are typically formed in clusters and consist of red globose berries about 1 cm in diameter that usually contain two seeds (Lewis and Zenger 1982; Schluter and Punja 2000). Germination of seeds for plant propagation requires a stratification period consisting of exposure to chilling temperatures for 2 winter seasons, or about 20 months (Lewis and Zenger 1982; Anderson et al 1993). However, for commercial purposes this can be reduced to 8 months if conditions are simulated (Baranov 1966).

In a commercial sense the shape of ginseng roots is important for market value and usually the presence of concentric circles or wrinkles on roots is a desirable trait (Westerveld 2010). However, the shape of ginseng roots is usually determined in the first two years of life and this makes root diseases particularly problematic for ginseng cultivation (Westerveld 2010). This is because root rot caused by fungal and oomycete pathogens like *Cylindrocarpon destructans, Phytophthora cactorum* and *Pythium irregulare* can destroy or alter the shape of ginseng seedlings and young plants, thus affecting the overall quality of cultivated roots (Reeleder and Brammall 1994). These diseases often cause a 30 to 60% loss in ginseng yield globally and among them, *Pythium irregulare* has been shown to be one of the most destructive soil-borne pathogens affecting commercial ginseng gardens (Howard et al. 1994; Reeleder and Brammall 1994; Punja 1997).

1.2.2. Active compounds

There are numerous classes of secondary metabolites that can be found in ginseng, yet the principal pharmacological properties of these plants are attributed to a class of triterpenoid saponins called ginsenosides (Small and Catling 1999). The synthesis of these compounds is unique to the genus *Panax* (Wen and Zimmer 1996; Jia and Zhao 2009). However, the composition and quantity of ginsenosides may vary depending on species (Lewis 1988), growing environment (Betz et al. 1998), plant age (Soldati and Tanaka 1984) or even plant structure as ginsenosides can be found within the main roots, secondary roots, stem, leaves, flowers and fruit of ginseng (Qu et al. 2009). To date more than 40 different

ginsenosides have been isolated from ginseng roots (Cheng et al. 2007), the source of commercial ginseng extracts, with the most abundant in American ginseng being Rg1 **8**, Re **7**, Rb1 **1**, Rb2 **2**, Rc **3** and Rd **4** (Qu et al. 2009) (Fig. 2.1). These compounds make up approximately 3 to 8% of the dry weight of the root **(**Court et al. 1996) and 2 to 4% of the leaves (Li et al. 1996**)**.

Ginsenosides, with the exception of one oleanane-type saponin, are steroidal triterpenoid saponins based on a tetracyclic dammarane carbon skeleton with mono- and dissacharide carbohydrate moieties attached through hydroxyl groups on the parent aglycone (Attele et al. 1999; Teng et al. 2002; Liang and Zhao 2008). The dammarane-type ginsenosides can be further classified into two groups as either 20(S)-protopanaxadiol (eg., Rb1 **1**, Rb2 **2**, Rc **3** and Rd **4**) or 20 (S)-protopanaxatriol (eg., Re **7** and Rg1 **8**) ginsenosides, based on the hydroxylation pattern of the parent triterpenoid and the attachment position of the saccharide side chains. These dammarane-type ginsenosides are considered bidesmosidic because they contain two saccharide side chains, typically at the C-3 and C-20 positions for protopanaxadiols and at the C-6 and C-20 positions for protopanaxatriols (Hostettmann and Marston 1995). There are also examples of monodesmosidic ginsenosides, however, these are extremely rare.

The attachment site of the carbohydrate moieties, the number of hydroxyl groups and stereochemistry all influence the pharmacological activity of ginsenosides and contribute to their diverse effects on human physiology (Attele et al. 1999). These include adaptogenic effects that help with relief of stress (Kelly 1999) as well as biological effects on the central nervous system (Christensen 2009) and cardiovascular system (Wang et al. 2007) to name a few. However, more work is needed to further elucidate and establish the validity of some medicinal claims attributed to ginseng consumption (O'Hara et al. 1998).

1.3. Plant-oomycete interactions

1.3.1. Infection cycle

Efficient spore production and dispersal is a prerequisite for successful infection of any host plant by an oomycete. To do this oomycetes produce asexual multinucleate sporangia (sometimes referred as conidia), that can germinate directly by producing hyphae that can penetrate the host, or indirectly, by producing motile zoospores (Hardham 2007). During zoosporogenesis, sporangia undergo cytoplasmic cleavage which results in the

formation of wall-less, uninucleate zoopspores that possess two flagella of unequal length, which are subsequently released through apical papillae (Latijnhouwers et al. 2003; Hardham 2007). Zoospores are then dispersed through water-rich soils or droplets and there are indications that chemotaxis, electrotaxis and autoaggregation play a role in guiding spores to potential plant hosts though not necessarily to specific species (Morris et al. 1998; Tyler 2002; Gow et al. 2004).

When zoospores reach the host they encyst after shedding their flagella and attaching themselves to the host surface by secreting a high-molecular-weight adhesive protein (Hardham and Gubler 1990; Robold and Hardham 2005). Cyst germination then takes place and a germ tube with a specialized infection structure, called an appressorium, penetrates the anticlinal or periclinal cell walls of the host (Soylu and Soylu 2003; Slusarenko and Schlaich 2003). These oomycete appressoria are generally smaller than those of true fungi, are not melanized or pigmented and are separated from the germ tube by false septa (Endo and Colt 1974; Kramer et al. 1997). However, as in true fungi, their formation is induced by topological features on the host surface and they can exert mechanical pressure similar to that of fungal appressoria in order to penetrate host tissue (Bircher and Hohl 1997; Money et al. 2004).

Penetration of the host epidermis is also facilitated by the secretion of cell wall-degrading enzymes and other proteins from the apex of the germ tubes or infecting hyphae (Endo and Colt 1974; Jarvis et al. 1981). However, once penetration has occurred the colonization strategy differs depending on the lifestyle of the pathogen. Necrotrophic pathogens grow both inter- and intracellularly and feed on dead and dying tissue, while biotrophic and hemibiotrophic pathogens, in the biotrophic phase, attempt to minimize disruption to host cells (Hardham 2007). In all cases, nutrients are retrieved from the host through the formation of haustoria in mesophyllic or cortical cells, which interfere with the metabolism and organization of the cell (Mendgen and Hahn 2002). Haustoria are spherical, lobed or digit-like structures which infiltrate plant cells through degradation of the cell wall and invagination of the plant plasma membrane (Enkerli et al. 1997).

However, in response to this pathogen infection, plants can produce cell wall-degrading enzymes, proteases and other pathogenicity related proteins targeting pathogens (Latijnhouwers et al. 2003). They can also increase cytosolic calcium concentrations, form

appositions underneath the hyphae, produce reactive oxygen species or initiate hypersensitive cell death (Hardham 2007).

1.3.2. Molecular overview of oomycete pathogenicity

The infection of a host plant by a plant pathogen, such as an oomycete, may be regarded as a battle where the main weapons are proteins and other chemical compounds produced by the organisms. This interaction is characterized by the response of one organism to a substance, such as an infection protein, produced by another organism. For this reason, recognition of these compounds is the first step in any plant-pathogen interaction. Therefore, at the molecular level, recognition means the interaction between a substance and its receptor and subsequently the transduction of a signal generated by that receptor (Tyler 2002, Ferreira et al. 2006; Stukenbrock and McDonald 2009).

To date there have been numerous studies exploring the recognition mechanisms between oomycete pathogens like various *Pythium* and *Phytophthora* species and their hosts. Recognition of the host by the pathogen relies on the detection of the chemical, electrical and physical properties of plant tissues by oomycetes and their zoospores. This can occur either through host-specific recognition, an example of which is the chemoattraction of zoospores produced by *Aphanomyces euteiches* toward the isoflavone prunetin produced by *Prunus emarginata* the Oregon cherry (Horio et al. 1992). Or alternatively, recognition can occur through non-specific recognition, where detection of substrates such as amino acids (Musgrave et al. 1977) and calcium (Donaldson and Deacon 1993) or physical phenomenon such as electric fields (Morris and Gow 1993) can influence zoospore taxis, encystment, cyst germination and hyphal chemotropism, leading the pathogen to potential infection sites.

Meanwhile, the recognition of pathogens by host species has also been examined. Numerous biochemical and genetic studies have focused on isolating pathogenic compounds and the genes that encode them which trigger defence responses in host plants (Tyler 2002, Ferreira et al. 2006). Plants recognize invading pathogens through evolved mechanisms that sense conserved motifs in pathogen derived components such as cell wall-degrading enzymes or structural compounds like chitin, which are generally termed elicitors (Dixon and Lamb 1990; Attard et al. 2008; Stuckenbrock and McDonald 2009). In some oomycetes, like various *Phytophthora* and *Pythium* species, carbohydrates, proteins and other small

molecules have been classified in this category and have been extensively studied (Hahn 1996).

Elicitors are recognized by host plants to varying degrees depending on the source, for example, glucans and fatty acids elicit plant defence responses in numerous plant species (Mithoefer et al. 1996; Bostock et al. 1986; Tyler 2002). Whereas others, like elicitins, which are small (approximately 10 kDa) sterol binding proteins, trigger plant defence responses in a very narrow host range (Tyler 2002). Elicitins that induce the hypersensitive response in host plants have been shown to be important components of the signal pathways that lead to pathogen recognition. Simply put, recognition by a host of elicitin proteins secreted by a specific pathogen, can initiate a co-evolved response that allows a host species to initiate preventive defensive strategies against infection by that pathogen. This is an example of the gene-for-gene interactions that can lead to systemic acquired resistance against numerous plant pathogens in various host species (Kamoun et al. 1994; Panabieres; 1995; Keller et al. 1999).

It should be noted that compounds from both host plants and pathogens play an important role in plant-oomycete interactions and in addition to recognition, they may also have a direct role in pathogenicity (Kamoun et al. 1993). However, more study is needed to determine the underlying mechanisms of pathogenicity in many plant pathogens in order to facilitate disease prevention.

1.3.3. Role of root exudates in rhizosphere interactions

Plant roots are known to influence the composition of soil microbes (Miethling et al. 2000; Grayston et al. 2001) and it has been suggested that secondary metabolites secreted from plant tissue are the leading cause in the alteration of rhizosphere microbial composition (Nicol et al. 2002; Broeckling et al. 2008; Saunder and Kohn 2009). The exact composition of these root exudates varies between plant species, but the majority consists of low molecular weight compounds such as amino acids, organic acids, sugars, phenolics and other secondary metabolites and to a lesser extent high-molecular weight compounds such as polysaccharides, alkaloids and proteins (Walker et al. 2003).

This wide range of molecules can be exuded into the rhizosphere in large quantities by plant roots, with up to 21% of total photosynthetically-fixed carbon transferred into the soil depending on the plant species, in the form of various compounds (Marschner 1995).

The wide array of compounds secreted allows plants to send a diverse array of signals to microorganisms in the surrounding soil. Being the main mode of communication, exudate components are used to initiate symbiotic associations with soil-borne organisms, like mycorrhizae, they can act as defence compounds limiting infection or they can be utilized as nutrient sources by beneficial organisms (Nardi et al. 2000; Hirsch et al. 2001; Bouwmeester et al. 2007).

1.3.3.1 Fungicidal activity of saponins

Saponins are secondary metabolites secreted by plants that have been shown to function as biologically active phytochemicals towards a diverse range of organisms (Sparg et al. 2004). They are a class of natural compounds whose aglycones are either triterpenoid- or steroid derived and which as a group possess soap-like properties (Dewick 1997). Structural diversity of saponins is enhanced by the number and placement of carbohydrate moieties around the aglycone, leading to saponins being either mono- or bidesmosidic (ie. containing one or two sugar side-chains respectively). These carbohydrate moieties can consist of either monosaccharides or higher order oligomers composed of glucose, arabinose, galactose, rhamnose and xylose as well as sugar acids.

From an ecological perspective however, saponin compounds from numerous plant species have been shown to act as constitutive plant defences (i.e. phytoanticipins) against fungal pathogens (Osbourn 1996; 2003). The most well known examples of anti-fungal saponins include the monodesmosidic triterpenoid saponin Avenacin A-1, the main root saponin produced by oat roots, and the glycoalkaloid saponin α-tomatine which is found in tomato. Avenacin A-1 has been shown act against infection by the fungal pathogen *Gaeumannomyces graminis* var. *tritici* and various pathogenic *Fusarium* spp. (Papadopoulou et al. 1999) while α-tomatine which is found in relatively high concentrations in unripe tomato fruits and even ginsenosides isolated from American ginseng, have been shown to be fungitoxic (Steel and Drysdale 1988; Hostettman and Marston 1995; Nicol et al. 2002; 2003).

The fungitoxic activity of Avenacin A-1, α-tomatine and other saponins is derived from their ability to form complexes with membrane sterols and disrupt the integrity of biological membranes (Keukens et al. 1995; Stine et al. 2006). This has been shown to cause the formation of pores and leakage of cell contents in various fungal isolates, presumably because saponins can interact with ergosterol, the main membrane sterol in true fungi (Weete

et al. 1989; Keukens et al. 1995; Stine et al. 2006). However, not all saponins are equally fungitoxic as studies have shown that monodesmosidic, amphiphilic saponins are more fungitoxic than bidesmosidic saponins and that removal of sugar moieties from monodesmosidic saponins results in lower toxicity (Morrissey and Osbourn 1999; Simons et al. 2006). It should also be noted, that oomycete pathogens have been shown to be unaffected by saponin toxicity *in vitro*, probably due to their lack of ergosterol which it appears provides them "innate resistance" (Osbourn 1999).

1.4. Glycosidases

1.4.1. Saponin-detoxifying glycosidases

Saponin-detoxifying glycosidases, often called saponinases, are pathogen produced enzymes able to deglycosylate saponin molecules, often leading to their detoxification/degradation. Numerous pathogenic fungi and oomycetes produce saponinases and the production of these enzymes has been shown to determine host specificity (Bowyer et al. 1995; Crombie et al. 1986). This has been shown by studies of the cereal infecting fungus *G. graminis* var. *avenae*, which requires the production of an extracellular glycosidase that detoxifies the oat triterpenoid saponin avenacin A-1, in order to infect the saponin containing host (Bowyer et al. 1995; Osbourn et al 1991). Likewise it has been shown that the tomato leaf spot fungus *Septoria lycopersici* produces an extracellular tomatinase capable of converting the glycoalkaloid saponin α-tomatine into the compound ß2-tomatine which is less toxic to it (Sandrock and van Eten 1998; Martin-Hernandez et al. 2000).

Interestingly, the enzymes produced by these two organisms specifically target the saponins produced by their respective hosts, even though these enzymes exhibit similar modes of action by hydrolyzing the ß(1-2) linkages of terminal D-glucose molecules (Osbourn et al. 1995). However, it has also been shown that tomatinases from other fungi such as *Botrytis cinera, Fusarium solani* and *Alternaria solani*, that share α-tomatine as a substrate, cleave different carbohydrate moieties from the substrate in order to detoxify it (Quidde et al. 1998; Lairini and Ruiz-Rubio 1998; Sch□nbeck and Schl□sser 1976). Similarly, saponin hydrolases isolated from the soybean pathogen *Neocosmospora vasinfecta* and the saprotrophs *Aspergillus oryzae* and *Eupenicillium brefeldianum,* have been shown to

deglycosylate soybean saponins, but have different specific activities (Watanabe et al. 2004; 2005).

The majority of the saponinases isolated and characterized to date, from a wide assortment of fungal organisms, belong to glycosyl hydrolase family 3 (Osbourn 1996). However, knowledge about the hydrolytic enzymes secreted by other plant pathogenic organisms, like oomycetes, remains very limited (Brunner et al. 2002). Furthermore the role of glycosyl hydrolases in the infection process of various organisms appears to not be universal. In fungal pathogens, it has been shown that while saponin deglycosylation is a component of the infection process, it may not be sufficient by itself for pathogenicity, as different organisms that deglycosylate saponins from the same host have been shown to have varying infection rates (Watanabe et al. 2005). Meanwhile, some oomycetes, which are believed to have innate resistance against saponin toxicity, have been found to produce saponin hydrolases (Yousef and Bernards 2006). This means that saponinases may play a more complex role in oomycete pathogenicity than just detoxifying saponins.

1.4.2. Deglycosylation of ginsenosides by *Pythium irregulare*

As mentioned briefly, ginsenosides produced by American ginseng have been shown to act as allelochemicals (Nicol et al. 2002; 2003). This is because, like other triterpenoid saponins, ginsenosides have been shown to possess antifungal properties, being able to inhibit the growth of saprophytes from the genus *Trichoderm*a and foliar pathogens such as *Alternaria panax, in vitro* (Nicol et al. 2002). However, these compounds have also been shown to promote the growth of severe ginseng pathogens like the oomycetes *Pythium irregulare* and *Phytophthora cactorum* (Nicol et al. 2003). It has therefore been proposed that ginseng saponins act as host recognition factors and/or allelopathic stimulators for the growth of these pathogens and that this may account for the susceptibility of American ginseng to infection by them (Nicol et al. 2003).

Further studies focusing on *P. irregulare*, done to elucidate the underlying mechanism of this observed growth stimulation, discovered that this organism was able to selectively deglycosylate the 20 (S)-protopanaxadiol ginsenosides (Rb1, Rb2, Rc, Rd and Gypenoside XVII) but none of the 20 (S)-protopanaxatriol ginsenosides (Yousef and Bernards 2006). This was accomplished via three isolated and now partially characterised extracellular ß-glucosidases and resulted in the formation and partial assimilation of

ginsenoside F2 by *P. irregulare*. Production of these glycosidases was shown to be induced when *P. irregulare* was exposed to ginsenosides *in vitro,* and it was also determined that these enzymes have differing catalytic activities (Yousef and Bernards 2006; Neculai et al. 2009). Glycosidase G1 isolated from *P. irregulare* was shown to have ß(1 - 6) glucosidase activity, while glycosidases G2 and G3 were shown to have ß(1 - 2) glucosidase activity (Yousef and Bernards 2006; Neculai et al. 2009).

It is still unclear however, if or how the deglycosylation of ginsenosides contributes to the growth stimulation of *P. irregulare, in vitro*. One possible explanation is that enzymatic conversion of ginsenosides into the common metabolite F2 increases *P. irregulare* growth in the same manner that exposure to ergosterol stimulates growth in this oomycete (Yousef and Bernards 2006). It is known that oomycetes are unable to synthesize sterols and rely on exogenous sterols for growth and development (Nes et al 1986). Ginsenosides are structurally and biosynthetically similar to sterols, and after deglycosylation, it is possible that sterol binding elicitin-like proteins (Huet et al 1995) could transport ginsenoside F2 into the hyphae of the pathogen, which could trigger its growth (Yousef and Bernards 2006). However, the production of specific ginsenosidases by *P. irregulare* cultures in response to ginsenoside exposure supports the idea that the secretion of these enzymes may represent an important step in the recognition of the host by this pathogen. This is further supported by the observation that *P. irregulare* isolates obtained from different plant hosts show different levels of induced ginsenosidase activity, with those isolated from ginseng showing higher levels than those from other hosts (Neculai 2008. Therefore it is possible that there is a link between the ability of various *P. irregulare* isolates to deglycosylate ginsenosides and their pathogenicity towards ginseng.

1.5. Chlorophyll fluorescence imaging of plant-pathogen interactions

Necrotrophic root pathogens like *P. irregulare* can cause extensive root damage to crops like ginseng and other species, yet early diagnosis and tracking of these pathogens in various host species is extremely difficult due to the delayed appearance of visual symptoms in the aerial portions of plants and the inability to assess root health *in vivo.* For this reason chlorophyll fluorescence imaging could, potentially, be applied as a non-invasive technique to study the feedback effects that root pathogen infection has on leaves *in vivo,* with tremendous implications for monitoring disease in perennial root crops like ginseng.

1.5.1. PAM fluorometry

The saturation pulse method used by pulse amplitude modulating (PAM) fluorometers, provides a non-destructive means of analyzing the photosynthetic performance of plants (Schreiber et al. 1986). PAM fluorometry allows one to measure the efficiency with which absorbed light is used for photosynthesis by monitoring the quantum yield of energy conversion in the photosystem II (PSII) reaction centre of plants, which is affected by various intrinsic and environmental parameters, like physiological health, light conditions and various stress factors. More precisely, this method uses visible light to elicit chlorophyll (Chl) excitation and then monitors chlorophyll fluorescence in the 690-740 nm range (Schreiber et al. 1986; Lichtenthaler and Miehé 1997; Oxborough and Baker 1997; Lichtenthaler et al. 2005). In modern PAM fluorometry systems, this visible light is usually generated by light emitting diodes (LEDs). These LEDs generate the pulse-modulated measuring light, provide for the actinic illumination driving photosynthesis and also generate the saturating pulses which are then used to derive the key fluorescence intensity levels Fo, Fo', Fm, Fm' and Fs, which are the basis for deriving all other chlorophyll fluorescence parameters reflecting the physiological status of the plant (Schreiber et al. 1986; Genty et al. 1989; Govindjee 1995; Kramer et al. 2004; Baker 2008).

1.5.2. Chlorophyll fluorescence parameters

Chlorophyll fluorescence devices like the PAM fluorometer and the parameters that can be determined from them can be used to monitor plant responses to various abiotic and biotic stresses (Lichtenthaler and Miehé 1997; Baker 2008). The numerous chlorophyll fluorescence parameters that can be calculated, therefore, allow for an in depth study of photosynthetic performance in plants exposed to these stresses. These parameters can be divided into two main groups, photosynthetic parameters monitoring PSII photochemistry of plants in a dark-adapted state and photosynthetic parameters monitoring PSII photochemistry in plants that are in a light-adapted state (Baker 2008). Dark adaptation of plants allows for PSII reaction centres to become maximally oxidized, a state in which the reaction center is referred to as 'open' (i.e. it is capable of performing photochemical reduction). This allows for the monitoring of the maximum photochemical efficiency of PSII (Fv/Fm) which, is the maximum efficiency at which light absorbed by PSII can be used for photochemistry (Baker 2008; Rolfe and Scholes 2010). Meanwhile, chlorophyll fluorescence measurements of plants

under actinic illumination or in the light adapted state, allows for the monitoring of how excitation energy absorbed by PSII is partitioned (Genty et. al 1996; Kramer et al. 2004; Klughammer and Schreiber 2008).

1.5.3. Imaging plant fungal interactions

The accurate detection of the early onset of disease in various crops *in situ* is vital in the context of disease prevention and precision agriculture. Chlorophyll fluorescence imaging (CFI) provides a sensitive, non-invasive and non-destructive method that can be used to provide insight into the mechanisms underlying plant pathogen interactions (Baker et al. 2001; Chaerle and Van Der Straeten 2001; Rolfe and Scholes 2010). This can be done because CFI allows for the monitoring of alterations to the photosynthetic apparatus of host plants caused by biotic and abiotic stresses that cannot otherwise be monitored visually and which can be used for early, pre-symptomatic diagnosis of infection in host plants (Rolfe and Scholes 2010).

Biotic stress, through viral, bacterial or fungal pathogen infection has been shown to negatively affect photosynthetic electron transport and downstream metabolic reactions in plants (Baker 2001; Chaerle et al. 2007; Baker 2008; Rolfe and Scholes 2010). These effects cause feed-back reactions which subsequently, lead to changes in chlorophyll fluorescence, however, because these changes are often not homogenously distributed in the leaf/plant, CFI can be used to monitor the spatial heterogeneity of leaf photosynthetic performance in response to this stress with much more accuracy than could be attained through non-imaging fluorescence measurements (Lichtenthaler and Miehé 1997; Baker 2008). Furthermore, the imaging of different fluorescence parameters can provide a wealth of information with regards to the timing and location of pathogen infection as well as the underlying mechanisms of infection in the host plant (Baker 2008; Rolfe and Scholes 2010).

1.6. Thesis objectives

The objectives of this research project were to examine the potential roles of extracellular ginsenosidases, and the ginsenoside products they produce (i.e., ginsenoside F2) in the ginseng-*P. irregulare* pathosystem.

To accomplish this, first, it was determined whether there is a correlation between the production of extracellular ginsenosidases by different strains of *Pythium irregulare* and the ability of those strains to infect ginseng. Then, the infection rate of *P. irregulare* on ginseng

roots before and after exposure to ginsenosides was monitored *in vivo* using chlorophyll fluorescence imaging, in order to determine if ginsenosides serve as a virulence factor/chemoattractant in the ginseng - *P. irregulare* pathosystem. After which, the ability of pure ginsenoside F2 (the main ginsenoside product obtained from combined G1, G2 & G3 activity *in vitro*) to act as a signalling molecule (i.e., chemo-attractant/inhibitor) for *P. irregulare* was evaluated *in vitro.*

In conjunction with this work, amino-acid sequence data obtained by Neculai et al. (2009) from trypsin digested peptide fragments from purified ginsenosidases G1, G2 and G3 were used to clone and sequence the gene that codes for one of these enzymes in order to functionally characterize protein. Altogether, these experiments provide a better understanding of the molecular triggers that could be involved in facilitating the infection of ginseng by *Pythium irregulare*.

1.7. References

Abdelghani, E.Y., Bala, K., Paul, B., 2004. Characterization of *Pythium proecandrum* and its antagonism towards *Botrytis cinera*, the causative agent of grey mould disease of grape. FEMS Microbiol. Lett. 230, 177-183.

Anderson RC et al (1993) The ecology and biology of *Panax quinquefolium* L. (Araliaceae) in Illinois. Am. Midl. Nat. 129, 357-372.

Attard, G., Gourgues, M., Galiana, E., Panabières, F., Ponchet, M., Keller, H., 2008. Strategies of attack and defense in plant-oomycete interactions, accentuated for *Phytophthora parasitica* Dastur (syn. *P. nicotianae* Breda de Haan). J. Plant Physiol. 165, 83-94.

Attele, A.S., Wu, J.A., Yuan, C.S., 1999. Ginseng pharmacology: Multiple constituents and multiple actions. Biochem. Pharmacol. 58, 1685-1693.

Baker, N.R., 2008. Chlorophyll fluorescence: A probe of photosynthesis *in vivo*. Annu. Rev. Plant Biol. 59, 89-113.

Baker N.R., Oxborough K., Lawson T., Morison J.I.L. 2001. High resolution imaging of photosynthetic activities of tissues, cells and chloroplasts in leaves. J. Exp. Bot. 52, 615-621.

Baldauf, S.L., Roger, A.J., Wenk-Seifert, I., Doolittle, W.F., 2000. A kingdom-level phylogeny of eukaryotes based on combined protein data. Science 290, 972-977.

Baranov, A.,. 1966. Recent advances in our knowledge of morphology, cultivation and uses of ginseng (*Panax ginseng* C. A. Meyer). Econ. Bot., 20, 403-406.

Betz, J.M., Der Morderosian, A.H., Lee, T.M., 1984. Continuing studies on the ginsenoside content of commercial ginseng products by TLC and HPLC. II Proceedings of the 6th North American Ginseng Conference, Guelph, ON, pp. 65-83.

Bircher, U., Hohl, H.R., 1997. Environmental signalling during induction of appressorium formation in *Phytophthora*. Mycol. Res. 101, 395-402.

Bostock, R.M., Schaeffer, D.A., Hammerschmidt, R., 1986. Comparison of elicitor activities of arachidonic acid, fatty acids, and glucans from *Phytophthora infestans*. Physiol. Mol. Plant Pathol. 29, 349-360.

Broeckling, C.D., Broz, A.K., Bergelson, J., Manter, D.K., 2008. Root exudates regulate soil fungal community composition and diversty. App. Environ. Microbiol. 74, 738-744.

Bouwmeester, H.J., Roux, C., Lopez-Raez, J.A., Bécard, G., 2007. Rhizoshere communication of plants, parasitic plants and AM fungi. Trends Plant Sci. 12, 224-230.

Bowyer, P., Clarke, B.R., Lunness, P., Daniels, M.J., Osbourn, A.E., 1995. Host range of a plant pathogenic fungus determined by a saponin detoxifying enzyme. Science 267, 371-374.

Brunner, F., Wirtz, W., Rose, J.K.C., Darvill, A.G., Govers, F., Scheel, D., Nurnberger, T., 2002. A beta-glucosidase/xylosidase from the phytopathogenic oomycete, *Phytophthora infestans*. Phytochemistry 59, 689-696.

Chaerle, L., Leinonen, I., Jones, H.G., Van Der Straeten D., 2007. Monitoring and screening plant populations with combined thermal and chlorophyll fluorescence imaging. J. Exp. Bot. 58, 773-784.

Chaerle, L., Van Der Straeten, D., 2001. Seeing is believing: imaging techniques to monitor plant health. Biochim. Biophys. Acta Gene Struct. Expr. 1519, 153-166.

Chamswarng, C., Cook, R.J., 1985. Identification and comparative pathogenicity of *Pythium* species from wheat roots and wheat-field souls in the Pacific Northwest. Phytopathology, 75, 821-827.

Cheng, L.Q., Na, J.R., Kim, M.K., Bang, M.H., Yang, D.C., 2007. Microbial conversion of ginsenoside Rb1 to minor ginsenoside F2 and gypenoside XVII by *Intrasporangium sp*. GS603 isolated from soil. J. Microbiol. Biotechnol. 17, 1937-1943.

Christensen, L.P., 2008. Chapter 1 Ginsenosides: Chemistry, biosynthesis, analysis, and potential health effects. Adv. Food Nut. Res. 55, 1-99.

Court, W.A., Reynolds, L.B., Hendel, J.G. 1996. Influence of root age on the concentration of ginsenosides of American ginseng (*Panax quinquefolium*). Can. J. Plant Sci. 76, 853-855.

Crombie, W.M.L., Crombie, L., Green, J.B., Lucas, J.A., 1986. Pathogenicity of the take-all fungus to oats; its relationship to the concentration and detoxification of the four avenacins. Phytochemistry 25, 2075-2083.

Dewick, P.M., 1997. Medicinal natural products: a biosynthetic approach. Wiley, Chichester, UK.

Dixon, R.A., Lamb, C.J. 1990. Molecular communication in interactions between plants and microbial pathogens. Annu. Rev Plant Physiol. Plant Mol. Biol. 41, 339-367.

Donaldson, S.P., Deacon, J.W., 1993. Changes in motility of *Pythium* zoospores induced by calcium and calcium-modulating drugs. Mycol. Res. 97, 877-883.

Endo, R.M., Colt, W.M., 1974. Anatomy, cytology and physiology of infection by *Pythium*. Proc American Phytopathol. Soc. 1, 215-222.

Enerkli, K., Hahn, M.G., Mims, C.W. 1997. Ultrastructure of compatible and incompatible interactions between soybean roots infected with the plant pathogenic oomycete *Phytophthora sojae*. Can. J. Bot. 75, 1493.

Ferreira, R.B., Monteiro, S., Freitas, R., Santos, C.N., Chen, Z., Batista, L.M., Duarte, J., Borges, A., Teixeira, A.R., 2006. Fungal Pathogens: The Battle for Plant Infection. Crit. Rev. Plant Sci. 25, 505-524.

Fiebig, A.E., Proctor, J.T.A., Murr, D.P., 2005. Flower abscission and induction in North American ginseng with Ethephon. HortScience 40, 138-141.

Genty, B., Briantais, J-M., Baker, N.R., 1989. The relationship between the quantum yield of photosynthetic electron transport and quenching of chlorophyll fluorescence. Biochim. Biophys. Acta 990, 87-92.

Genty, B., Harbinson, J., Cailly, A.L., Rizza, F., 1996. Fate of excitation at PSII in leaves: the non-photochemical side. Presented at the *Third BBSRC Robert Hill Symposium on Photosynthesis*, March 31 to April 3, 1996, University of Sheffield, Department of Molecular Biology and Biotechnology, Western Bank, Sheffield UK, Abstract no. P28.

Gorbe, E., Calatayud, A. 2012. Applications of chlorophyll fluorescence imaging technique in horticultural research: A review. Scientia Hortic. - Amsterdam 138, 24-35.

Govindjee, 1995. Sixty-three years since Kautsky: chlorophyll *a* fluorescence. Aus. J. of Plant Physiol. 22, 20-29.

Gow, N.A.R., 2004. New angles in mycology: studies in directional growth and directional motility. Mycol. Res. 108, 5-13.

Grayston, S.J., Griffith, G.S., Mawdsley, J.L., Campbell, C.D., Bardgett, R.D., 2001. Accounting for variability in soil microbial communities of temperate upland grassland ecosystems. Soil Biol. Biochem. 33, 533-551.

Griffith, J.M., Davis, A.J., Grant, B.R., 1991. Target sites of fungicides to control oomycetes. In Target Sites of Fungicide Action (Koller, W., ed.), pp. 69–100, CRC Press

Gull, C., Labuschagne, N., Botha, W.J., 2004. Pythium species associated with wilt and root rot of hydroponically grown crops in South Africa. Afr. Plant Prot. 10, 109-116.

Hahn, M.G., 1996. Microbial elicitors and their receptors in plants. Annu. Rev. Phytopathol. 34, 387-412.

Hardham, A.R., 2007. Cell biology of plant-oomycete interactions. Cell. Microbiol, 9, 31-39.

Hardham, A.R., Gubler, F., 1990. Polarity of attachment of zoospores of a root pathogen and pre-alignment of the germtube. Cell Biol. Int. Rep. 14, 947-956.

Hendrix F.F., Campbell, W.A., 1973. *Pythiums* as plant pathogens. Annu. Rev. Phytopathol. 11, 77-98.

Hirsch, A.M., Dietz Bauer, W., Bird, D.M., Cullimore, J., Tyler, B., Yoder, J.I., 2003. Molecular signals and receptors: controlling rhizoshere interacting between plants and other organisms. Ecology 84, 858-868.

Horio, T., Kawabata, Y., Takayama, T., Tahara, S., Kawabata, Y., Fukushi, Y., Nishimura, H., Mizutani, J., 1992. A potent attractant of zoospores of *Aphanomyces cochlioides* isolated from its host, *Spinacia oleracea*. Experientia. 48, 410-414.

Hostettmann, K., Marston, A., 1995. Saponins. Chemistry and Pharmacology of Natural Products. Cambridge University Press, Cambridge, U.K, pp. 329-337.

Howard, R.J., Garland, J.A., Seaman, W.L., 1994. Diseases and pests of vegetable crops in Canada. Canadian Phytopathological Society and Entomological Society of Canada, Ottawa, ON, pp. 11-15.

Hu, S.Y., Rudenberg, L., Tredici, P.D., 1980. Studies of American ginseng. Rhodora, 82; 627-636.

Huet, J.C., Le Caer, J.P., Nespoulos, C., Pernollet, J.C., 1995. The relationships between the toxicity and the primary and secondary structures of elicitin-like protein elicitors secreted by the phytopathogenic fungus *Pythium vexans*. Mol. Plant Microbe Interact. 8, 302-310.

Ingram, D.M., Cook, R.J., 1990. Pathogenicity of four *Pythium* species to wheat, barley, peas and lentils. Plant Pathol. 39, 110-117.

Jarvis, M.C., Threlfall, D.R., Friend, J., 1981. Potato cell wall polysaccharides: degradation with enzymes from *Phytophthora infestans*. J. Exp. Bot. 32, 1309-1319.

Jia, L., Zhao, Y.Q., 2009. Current evaluation of the millennium phytomedicine-ginseng (I): etymology, pharmacognosy, phytochemistry, market and regulations. Curr. Med. Chem. 16, 2475-2484.

Kamoun, S., Klucher, K.M., Coffey, M.D., Tyler, B.M., 1993. A gene encoding a hostspecific elicitor protein of *Phytophthora parasitica*. Mol. Plant Microbe Interact. 6, 573-581.

Kamoun, S., Young, M., Forster, H., Coffey, M.D., Tyler, B.M., 1994. Potential role of elicitins in the interaction between *Phytophthora* species and tobacco. Appl. Environ. Microbiol. 60, 1593-1598.

Keller, H., Pamboukdjian, N., Ponchet, M., Poupet, A., Delon, R., Verrier, J.L., Roby, D., Ricci, P., 1999. Pathogen-induced elicitin production in transgenic tobacco generates a hypersensitive response and nonspecific disease resistance. Plant Cell 11, 223-235.

Kelly, G.S., 1999. Nutritional and botanical interventions to assist with the adaptation to stress. Altern. Med. Rev. 4, 249-265.

Keukens, E.A.J., de Vrije, T., vanden Boom, C., de Waard, P., Plasman, H.H., Thiel, F., Chupin, V., Jongen, W.M.F., de Kruijff, B., 1995. Molecular basis of glycoalkaloid induced membrane disruption. Biochim Biophys Acta 1240, 216-228.

Kiefer, D., Pantuso, T., 2003. Asian ginseng improves psychological and immune function. Am. Fam. Physician 68, 1539-1542.

Klughammer, C., Schreiber, U., 2008 Complimentary PSII quantum yields calculated from simple chlorophyll fluorescence parameters measured by PAM fluorometry and the Saturation Pulse method. PAM Application Notes 1, 27-35.

Kramer, R., Freytag, S., Schmelzer, E., 1997. *In vitro* formation of infection structures of *Phytophthora infestans* is associated with synthesis of stage specific polypeptides. Eur. J. Plant Pathol. 103, 43-53.

Kramer D.M., Johnson G., Kiirats O., Edwards, G.E., 2004. New fluorescence parameters for determination of QA redox state and excitation energy fluxes. Photosynth. Res. 79, 209-218.

Krupa, S.V., Dommergues, Y.R., 1979. Ecology of root pathogens, in: Developments in agricultural and managed-forest ecology. Elsevier Scientific Publishing Company, Amsterdam, pp. 14-17.

Lairini, K., Ruiz-Rubio, M., 1998. Detoxification of α-tomatine by *Fusarium solani*. Mycol. Res. 102, 1375-1380.

Latijnhouwers, M., de Wit, P.J.G.M., Govers, F., 2003. Oomycetes and fungi: similar weaponry to attack plants. Trends Microbiol. 11, 462-469.

Lewis, W.H., 1988. Ginseng: a medical enigma. In Plants in indigenous medicine and diet biobehavioral approaches. Etkin, N.L. (ed). Redgrave, New York, NY, pp. 290-305.

Lewis, W.H., Zenger, V.E., 1982. Population dynamics of the American ginseng, *Panax quinquefolium* (Araliaceae). Am. f. Bot., 69, 1483-1490.

Li, T.S.C., Mazza, G., Cottrell, A.C., Gao, L., 1996. Ginsenosides in roots and leaves of American ginseng. J. Agric. Food Chem. 44, 717-720.

Liang, Y., Zhao, S., 2008. Progress in understanding of ginsenoside biosynthesis. Plant Biology 10, 415-421.

Lichtenthaler, H.K., Buschmann, C., Knapp, M., 2005. How to correctly determine the different chlorophyll fluorescence parameters and the chlorophyll fluorescence decrease ratio RFd of leaves with the PAM fluorometer. Photosynthetica 43, 375-393.

Lichtenthaler, H.K., Miehé, J., 1997. Fluorescence imaging as a diagnostic tool for plant stress. Trends Plant Sci. 2, 316-320.

Liu, S-Y., Vaughn, E.K., 1966. Control of *Pythium* infection of table beet seedlings by antagonistic microorganisms. Phytopathology 50, 787-789.

Mai, W.F., Abawi, G.S., 1981. Controlling replant diseases of pome and stone fruits in Northeastern United States by preplant fumigation. Plant Dis. 65, 859-864.

Marschner, H., 1995. Mineral Nutrition of Higher Plants. 2nd ed. Academic Press. London. U.K.

Martin, F.N., Loper, J.E., 1999. Soilborne plant diseases caused by *Pythium* species: ecology, epidemiology, and prospects for biological control. Crit. Rev. Plant Sci. 18, 111-181.

Martin-Hernandez, A.M., Dufresne, M., Hugouvieux, V., Melton, P., Osbourn, A., 2000. Effects of targeted replacement of the tomatinase gene on the interaction of *Septoria lycopersici* with tomato plants. Mol. Plant Microbe Interact. 12, 1301-1311.

Mazzola, M., Andrews, P.K., Reganold, J.P., Lévesque, C.A., 2002. Frequency, virulence, and metalaxyl sensitivity of *Pythium* spp. isolated from apples roots under conventional and organic systems. Plant Dis. 86, 669-675.

McGraw, J.B., Lubbers, L.E., Van der Voort, M., Mooney, E.H., Furedi, M.A., Souther, S., Turner, J.B., Chandler, J., 2013. Ecology and conservation of ginseng (*Panax quinquefolius*) in a changing world. Ann. N.Y. Acad. Sci. 1286, 62-91.

Mendgen, K., Hahn, M., 2002. Plant infection and the establishment of fungal biotrophy. Trends Plant Sci. 7, 352-356.

Miethling, R., Wieland, G., Backhaus, H., Tebbe, C.C., 2000. Variation of microbial rhizosphere communities in response to crop species, soil origin, and inoculation with *Sinorhizobium meliloti* L33. Microb. Ecol. 40, 43-56.

Middleton, J.T., 1943. The taxonomy, host range and geographic distribution of the genus *Pythium*. Mem. Torrey Bot. Club 20, 1-71.

Mithoefer, A., Lottspeich, F., Ebel, J., 1996. One-step purification of the beta-glucan elicitor-binding protein from soybean (*Glycine max* L.) roots and characterization of an anti-peptide antiserum. FEBS Lett. 381, :203-207.

Money, N.P., Davis, C.M., Ravishankar, J.P., 2004. Biomechanical evidence for convergent evolution of the invasive growth process among fungi and oomycete water molds. Fungal Genet. Biol. 41, 872-876.

Moorman, G.W., Kang, S., Geiser, D.M., Kim, S.H., 2002. Identification and characterization of *Pythium* species associated with greenhouse floral crops in Pennsylvania. Plant Dis. 86, 1227-1231.

Morris, B.M., Gow, N.A.R., 1993. Mechanism of electrotaxis of zoospores of phytopathogenic fungi. Phytopathology 83, 877-82.

Morris, P.F., Bone, E., Tyler, B.M., 1998. Chemotropic and contact responses of *Phytophthora sojae* hyphae to soybean isoflavonoids and artificial substrates. Plant Physiol. 117, 1171-1178.

Morrissey, J.P., Osbourn, A., 1999. Fungal resistance to plant antibiotics as a mechanism of pathogenesis. Microbiol. Mol. Biol. R. 63, 708-724.

Musgrave, A., Ero, L., Scheffer, R., Oehlers, E., 1977. Chemotropism of *Achlya bisexualis* germ hyphae to casein hydrolysate and amino acids. J. Gen. Microbiol. 101, 65-70.

Nardi, S., Concheri, G., Pizzeghello, D., Sturaro, A., Rella, R., Parvoli, G., 2000. Soil organic matter mobilization by root exudates. Chemospehere, 41, 653-658.

Neculai, M.A., 2008. Purification and characterization of extracellular glycosidases from the ginseng root pathogen, Pythium irregulare (Thesis). Faculty of Graduate Studies. Uni. Western Ontario, London, ON, CAN.

Neculai, M.A., Ivanov, D., Bernards, M.A., 2009. Partial purification and characterization of three ginsenoside-metabolizing [beta]-glucosidases from *Pythium irregulare*. Phytochemistry 70, 1948-1957.

Nes, W.D., Le, P.H., Berg, L.R., Patterson, G.W., Kerwin, J.L., 1986. A comparison of cycloartenol and lanosterol biosynthesis and metabolism by the Oomycetes. Experientia 42, 556-558.

Nicol, R.W., Traquair, J.A., Bernards, M.A., 2002. Ginsenosides as host resistance factors in American ginseng (*Panax quinquefolius*). Can. J. Bot. 80, 557-562.

Nicol, R.W., Yousef, L., Traquair, J.A., Bernards, M.A., 2003. Ginsenosides stimulate the growth of soilborne pathogens of American ginseng. Phytochemistry 64, 257-264.

O'Hara, M.A., Kiefer, D., Farell, K., Kemper, K., 1998. A review of 12 commonly used medicinal herbs. Arch. f. Med. 7, 523-536.

Osbourn, A.E., 1996. Preformed antimicrobial compounds and plant defence against fungal attack. Plant Cell 8, 1821-1831.

Osbourn, A.E., 1999. Antimicrobial phytoprotectants and fungal pathogens: a commentary. Fungal Genet. Biol. 26, 163-168.

Osbourn, A.E., Clarke, B.R., Dow, J.M., Daniels, M.J., 1991. Partial characterization of avenacinase from *Gaeumannomyces graminis* var. *avenae*. Physiol. Mol Plant Pathol. 38, 301-312.

Osbourn, A., Bowyer, P., Lunness, P., Clarke, B., Daniels, M., 1995. Fungal pathogens of oat roots and tomato leaves employ closely related enzymes to detoxify different host plant saponins. Mol. Plant Microbe Interact. 6, 971-978.

Osbourn AE et al (2003) Dissecting plant secondary metabolism – constitutive chemical defences in cereals. New Phytol. 159, 101-108.

Oxborough, K., Baker, N.R., 1997. An instrument capable of imaging chlorophyll *a* fluorescence from intact leaves at very low irradiance and at cellular and subcellular levels of organization. Plant Cell Environ. 20, 1473-1483.

Panabieres, F., Marais, A., Le Barre, J., Penot, I., Fournier, D., Ricci, P.. 1995. Characterization of a gene cluster of *Phytophthora cryptogea* which codes for

elicitins, proteins inducing a hypersensitive-like response to tobacco. Mol. Plant Microbe Interact. 8, 996-1003.

Papadopoulou, K., Melton, R.E., Leggett, M., Daniels, M.J., Osbourn, A.E., 1999. Compromised disease resistance in saponin-deficient plants. Proc. Natl. Acad. Sci. USA 96, 12923-12928.

Proctor, J.T.A., Bailey, W.G., 1987. Ginseng, industry botany and culture. Hort. Rev. 9, 187-236.

Proctor, J.T.A., Percival, D.C., Loutitt, D., 1999. Inflorescence removal affects root yield of American ginseng. HortScience 34, 82-84.

Punja, Z.K., 1997. Fungal pathogens of American ginseng (*Panax quinquefolius*) in British Columbia. Can. J. Plant Pathol. 19; 301-306.

Qu, C., Bai, Y., Jin, X., Wnaga, Y., Zhang, K., You, J., Zhang, H., 2009. Study on ginsenosides in different parts and ages of *Panax quinquefolius*. L. Food Chem. 115, 340-346.

Quidde, T., Osbourn, A.E., Tudzynski, P., 1998. Detoxification of α-tomatine by *Botrytis cinerea*. Physiol. Mol. Plant Pathol. 52, 151-165.

Reeleder, R.D., Brammall, R.A., 1994. Pathogenicity of *Pythium* species, *Cylindrocarpon destructans* and *Rhizoctonia solani* to ginseng seedlings in Ontario. Can. J. Plant Pathol. 16, 311-316.

Robold, A.V., Hardham, A.R., 2005. During attachment *Phytophthora spores* secrete proteins containing thrombospondin type 1 repeats. Curr. Genet. 47, 307-315.

Rolfe, S.A., Scholes, J.D., 2010. Chlorophyll fluorescence imaging of plant-pathogen interactions. Protoplasma 247, 163-175.

Sandrock, R.W., Van Etten, H.D., 1998. Fungal sensitivity to and enzymatic degradation of the phytoanticipin α-lomatine. Phytopathology 88, 137-143.

Saunders, M., Kohn, L.M., 2009. Evidence for alteration of fungal endophyte community assembly by host defence compounds. New Phytol. 182, 229-238.

Schluter, C., Punja, Z.K., 2000. Floral biology and seed production in cultivated North American ginseng (*Panax quinquefolius*). J. Am. Soc. Hortic. Sci. 125, 567-575.

Schönbeck, F., Schlösser, E., 1976. Preformed substances as potential protectants. *In*: Heitefuss, R, Williams, PH (eds) Physiological plant pathology. Springer, Berlin, pp. 653–678

Schreiber, U., Schliwa, U., Bilger, W., 1986. Continuous recording of photochemical and non-photochemical chlorophyll fluorescence quenching with a new type of modulation fluorometer. Photosynth. Res. 10, 51-62.

Schwinn, F., Staub, T., 1995. Oomycetes fungicides. In Modern Selective Fungicides: properties, applications, mechanisms of action (Lyr, H., ed.), pp. 323-344, Fischer Verlag.

Simons, V., Morrissey, J.P., Latijnhouwers, M., Csukai, M., Cleaver, A., Yarrow, C., Osbourn, A., 2006. Dual effects of plant steroidal alkaloids on *Saccharomyces cerevisiae*. Antimicrob. Agents and Chemother. 50, 2732-2740.

Slusarenko, A.J., Schlaich, N.L. 2003., Downy mildew of *Arabidopsis thaliana* caused by *Hyaloperonospora parasitica* (formerly *Peronospora parasitica*). Mol. Plant Pathol. 4, 159-170.

Small, E., Catling, P.M., 1999. Canadian medicinal crops. NRC Research Press, Ottawa, ON.

Soldati, F., Tanaka, O., 1984. *Panax ginseng*: relation between age of plant and content of ginsenosides. Planta Medica 50, 351-352.

Soylu, E.M., Soylu, S., 2003. Light and electron microscopy of the compatible interaction between *Arabidopsis* and the downy mildew pathogen *Peronospora parasitica*. J Phytopathol. 151, 300-306.

Sparg, S.G., Light, M.E., van Staden, J., 2004. Biological activities and distribution of plant saponins. J. Ethnopharm. 94, 219-243.

Steel, C.C., Drysdale, R.B., 1988. Electrolyte leakage from plant and fungal tissues and disruption of liposome membranes by α-tomatine. Phytochemistry 27, 1025-1030.

Stine, K.J., Hercules, R.K., Duff, J.D., Walker, B.W., 2006. Interaction of the glycoalkaloid tomatine with DMPC and sterol monolayers studied by surface pressure measurements and brewster angle microscopy. J. Physical. Chem. B 110, 22220-22229.

Strange, R.N., Scott, P.R., 2005. Plant Disease: Threat to global food security. Annu. Rev. Phytopathol. 43, 83-116.

Stuckenbrock, E.H., McDonald, B.A., 2009. Population genetics of fungal and oomycete effectors involved in gene-for-gene interactions. Mol. Plant Microbe Interact. 22, 371-381.

Teng, R., Li, H., Chen, J., Wang, D., He, Y., Yang, C., 2002. Complete assignment of 1H and 13C NMR data for nine protopanaxatriol glycosides. Magn. Reson. Chem. 40, 483-488.

Trujillo, E.E., Hine, R.B., 1965. The role of papaya residues in papaya root rot caused by *Pythium aphanidermatum* and *Phytophthora parasitica*. Phytopathology, 55, 1332-1338.

Tyler, B.M., 2002. Molecular basis of recognition between *Phytophthora* pathogens and their hosts. Annu. Rev. Phytopathol. 40, 137-167.

Tyler, B.M., Tripathy, S., Zhang, X.M., Dehal, P., Jiang, R.H.Y., Aerts, A., Arredondo, F.D., Baxter, l., et al., 2006. *Phytophthora* genome sequences uncover evolutionary origins and mechanisms of pathogenisis. Science 313, 1261-1266.

Teng, R., Li, H., Chen, J., Wang, D., He, Y., Yang, C., 2002. Complete assignment of 1H and 13C NMR data for nine protopanaxatriol glycosides. Magn. Reson. Chem. 40, 483-488.

Van de Peer, Y., De Wachter, R., 1997. Evolutionary relationships among the eukaryotic crown taxa taking into account site-to-site rate variation in 18S rRNA. J. Mol. Evol. 45, 619-630.

Van der Plaats-Niterink, A.J., 1981. Monograph of the Genus *Pythium*. Studies in Mycology, No. 21 Centrallbureau Voor Schimmelcultures, Baarn, Netherlands.

Wang, C.Z., Mehendale, S.R., Yuan, C.S., 2007. Commonly used antioxidant botanicals: active constituents and their potential role in cardiovascular illness. Am. J. Chin. Med. 35, 543-558.

Watanabe, M., Sumida, N., Yanai, K., Murakami, T., 2004. A novel saponin hydrolase from *Necosmosporsa vasinfecta*. Appl. Environ. Microbiol. 70, 865-872.

Watanabe, M., Sumida, N., Yanai, K., Murakami, T. 2005. Cloning and characterization of saponin hydrolases from *Aspergillus oryzae* and *Eupenicillium brefeldianum*. Biosci. Biotechnol. Biochem. 69, 2178-2185.

Weete, J.D., 1989. Structure and function of sterols in fungi. Adv. Lipid Res. 23, 115-167.

Weiland, J.E., Beck, B.R., Davis, A., 2013. Pathogenicity and virulence of *Pythium* species obtained from forest nursery soils on Douglas-fir seedlings. Plant Dis. 97, 744-748.

Wen, J., Zimmer, E.A., 1996. Phylogeny and biogeography of *Panax* L. (the ginseng genus, *araliaceae*): inferences from ITS sequences of nuclear ribosomal DNA. Mol. Phylogenet. Evol. 6, 167-177.

Westerveld, S., 2010. Factsheet: Ginseng production in Ontario. (OMAFRA) Ontario Ministry of Agriculture, Food and Rural Affairs. Order no. 10-081W. Retrieved from: http://www.omafra.gov.on.ca/english/crops/facts/10-081w.pdf.

You, J., Liu, X., Zhang, B., Xie, Z., Hou, Z., Yang, Z., 2015. Seasonal changes in soil acidity and related properties in ginseng artificial bed soils under a plastic shade. J. Ginseng Res. 39, 81-88.

Yousef, L.F., Bernards, M.A., 2006. *In vitro* metabolism of ginsenosides by the ginseng root pathogen *Pythium irregulare*. Phytochemistry 67, 1740-1749.

Chapter 2: Ginsenosidases and the Pathogenicity of *Pythium irregulare*

2.1. Introduction

American ginseng (*Panax quinquefolius* L.) is a slow growing perennial cultivated in temperate climate zones for the high medicinal value of its roots. A member of the Araliaceae, it is one of at least nine species that belong to the genus *Panax,* which also includes *P. ginseng* C.A. Mey.., *P. notoginseng* (Burkill) F.H. Chen ex C.Y. Wu K.M. Feng and *P. japonicus* C.A. Mey. all of which produce ginsenosides as biologically active compounds. To date, at least 40 ginsenosides have been identified in *Panax* species (Cheng et al. 2007), many of which are reported to have unique medicinal benefits (Shibata 2001). However, while the pharmacological properties of ginsenosides have been extensively studied, their ecological role as compounds released into the soil by ginseng plants has not been systematically investigated.

Ginsenosides are triterpenoid saponins, based on a dammarane carbon skeleton with four *trans*-oriented rings and side-chains that consist of various sugar moieties (e.g. mono- and disaccharides of glucose, rhamnose, xylose and arabinose) attached through the C-20 and either the C-3 or C-6 positions (Attele et al. 1999). Ginsenosides (Fig. 2.1) are classified as either 20 (S)-protopanaxadiols (e.g. Rb1 **1**, Rb2 **2**, Rc **3**, Rd **4**, gypenoside XVII (GXVII, **5**) and F2 **6**) or 20 (S)-protopanaxatriols (e.g. Re **7** and Rg1 **8**) depending on the hydroxylation pattern of the parent triterpenoid (Teng et al. 2002). While these two classes of ginsenoside differ in their glycosylation patterns, both diols and triols are bidesmosidic, containing two sugar chains, typically at the C-3 and C-20 positions (diols) or C-6 and C-20 positions (triols) (Hostettmann and Marston 1995).

In earlier work, it was hypothesized that ginsenosides function as host recognition factors and/or allelochemicals (Nicol et al. 2002, 2003). In addition, like other saponins, ginsenosides have been shown to possess antifungal properties since *in vitro* exposure inhibits the growth of foliar pathogens like *Alternaria panax* Whetzel and saprophytes from the genus *Trichoderma* (Nicol et al. 2002). However, the antifungal action of ginsenosides is not effective against all potential ginseng pathogens. In particular, ginsenosides have been shown to promote the *in vitro* growth of oomycotan pathogens like *Phytopthora cactorum* (Lebert & Cohn) J. Schröt. and *Pythium irregulare* Buisman. This is important as *P. irregulare* is a major threat to commercial ginseng cultivation, causing damping off in one-

to two-year old plants and post emergence root rot in older plants (Krupa and Dommergues 1979; Howard et al. 1994). The success of oomycetes in overcoming saponin defence compounds is commonly attributed to their inability to synthesize their own sterols (Olsen 1971). This limits the proposed mode of action of antifungal saponins on oomycotan pathogens, which is based on the interaction between saponins and cell membrane sterols, leading to a disruption in membrane stability (Morrissey and Osbourn 1999). Previous observations, however, have shown that the growth stimulation of *P. irregulare* by ginseng saponins may result from the ability of this pathogen to metabolically alter ginsenosides via extracellular β-glycosidases (Yousef and Bernards 2006; Neculai et al. 2009).

Production of ginsenoside metabolizing glycosidases (ginsenosidases) is induced when *P. irregulare* is exposed to ginsenosides *in vitro. Pythium irregulare* ginsenosidases appear to selectively metabolize the 20 (S)-protopanaxadiol ginsenosides Rb1 **1**, Rd **4** and GXVII **5** (and possibly Rb2 **2** and Rc **3**), leading to the formation and partial assimilation of ginsenoside F2 **6** (Yousef and Bernards 2006; Neculai et al. 2009). The metabolism of ginsenosides by these glycosidases requires both β(1→6) and β(1→2) glucosidase activities (Neculai et al. 2009).

The metabolism and/or degradation of saponins by extracellular glycosidases is a common defence strategy employed by fungal organisms against these compounds. Many plant pathogens produce "saponinases" which lead to detoxification or degradation of plant saponins and in some cases have even been shown to determine host specificity (Bowyer et al. 1995; Crombie et al. 1986; Papadopoulou et al. 1999). For example, *Gaeumanomyces graminis* var. *avenae,* a cereal-infecting fungus that produces an extracellular avenacinase, is able to detoxify the oat triterpenoid saponin, avenacin A-1, by hydrolysing the terminal β (1→2)-linked D-glucose of this molecule; mutants of *G. graminis* that do not produce avenacinase are unable to infect an avenacin-containing host (Papadopoulou et al. 1999). This mechanism may be relevant to the pathogenicity of *P. irregulare* on ginseng since isolates of *P. irregulare* have been shown to have significant differences in pathogenicity between hosts (Harvey et al. 2001). However, little is known about the role that extracellular glycosidases play in oomycete pathogenicity (e.g., Brunner et al. 2002).

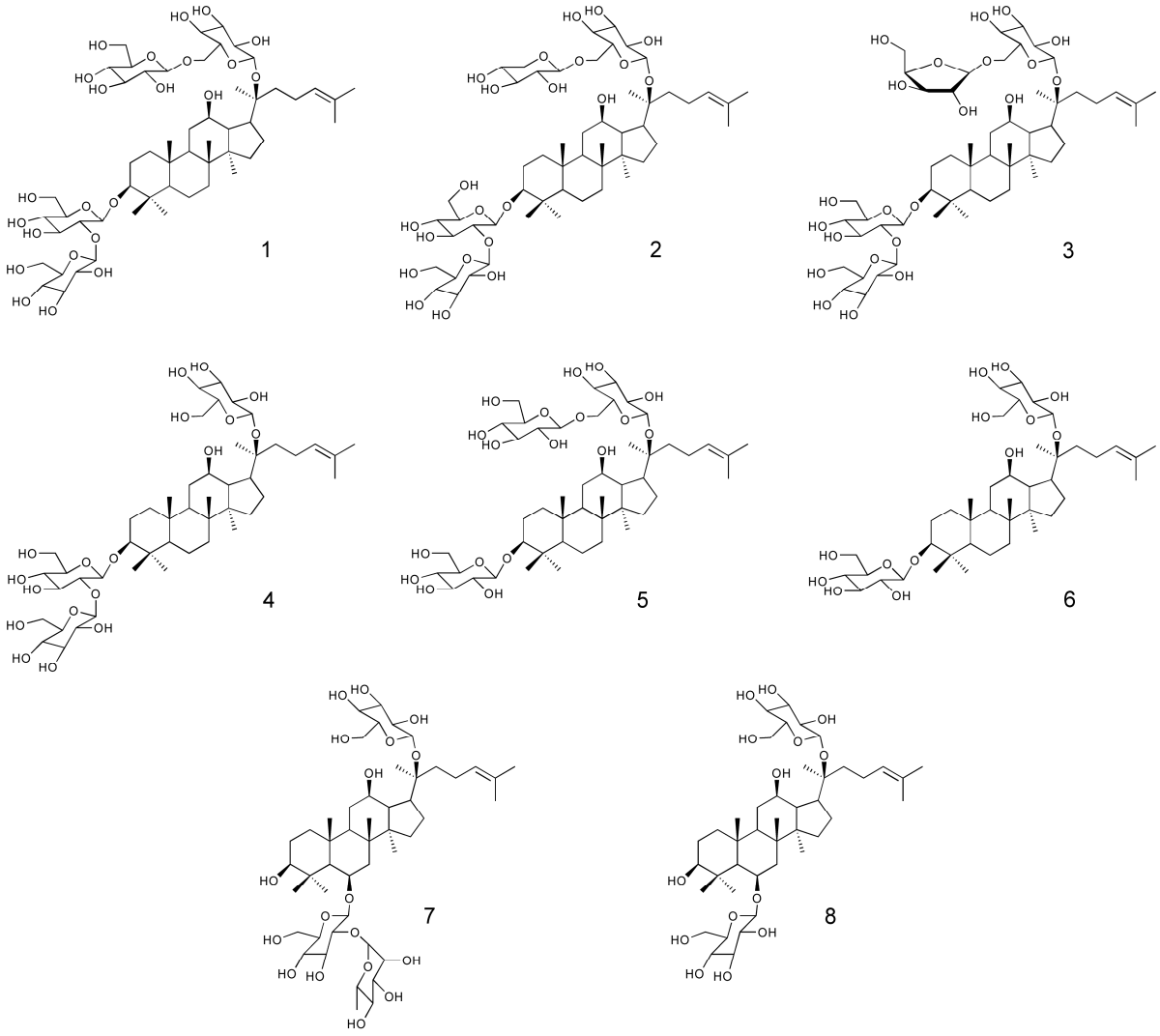

Figure 2.1. Common ginsenosides found in *Panax quinqufolius* L. Shown are 20 (S)-protopanaxadiol ginsenosides Rb1 (1), Rb2 (2), Rc (3), Rd (4), Gypenoside XVII (5) and F2 (6) as well as, 20 (S)- protopanaxatriol ginsenosides Re (7) and Rg1 (8).

In the present work, whether a correlation exists between the virulence of *P. irregulare* towards ginseng and the ability of this organism to produce ginsenosidases was examined. This was done by combining data obtained from *in vitro* ginsenoside assays and *in vivo* pathogenicity assays using *P. irregulare* strains with varying life histories.

2.2. Materials and Methods

2.2.1. Materials

Nine isolates of *Pythium irregulare* Buisman, one isolate of *Pythium ultimum* Trow, and two isolates of *Trichoderma hamatum* (Bonord.) Bainier (Table 2.1) originating from various host plants and locations were obtained from the Canadian Collection of Fungal Cultures (CCFC, Ottawa, Canada). A crude ginsenoside mixture was obtained from three-year old American ginseng (*Panax quinquefolius* L.) roots, obtained from Damaree Farms, Delhi Ontario, or provided by Dr. Dan Brown, Agriculture and Agri-food Canada. Roots were mechanically crushed, dried to a constant weight and a crude ginsenoside extract was prepared according to Nicol et al. (2002). Crude ginsenosides were further purified on C18 Extract-clean SPE (solid phase extraction) (50 μm, 60Å, 75 mL bed volume; Grace, USA) and Mega Bond Elut NH_2 (40 μm, 60Å, 60 mL bed volume; Varian, USA) columns. Crude ginsenosides (500 mg in 10 mL H_2O) were loaded on the C18 column, washed with MeOH-H_2O (25 mL, 3:7,v/v) with the ginsenosides eluted with MeOH (25mL). The C18 column eluate was loaded on the NH_2 column and eluted with MeOH (50 mL). The MeOH from the resulting eluate was evaporated *in vacuo* to yield a ginsenoside mixture (light-yellow powder). The ginsenoside composition of the mixture was confirmed by HPLC according to Nicol et al. (2002).

2.2.2. Oomycete/fungal growth and production of culture filtrates

Pythium irregulare, *P. ultimum and T. hamatum* isolates (Table 2.1) were initially grown on potato dextrose agar (PDA), at room temperature, in the dark, for 3 days or until the colonies reached the margins of a standard Petri plate. Next, liquid cultures (10 mL) were initiated by inoculating Czapek-Dox mineral broth (containing 3 g $NaNO_3$, 1 g K_2PO_4, 0.5 g $MgSO_4$, 0.5 g KCl and 0.01 g $FeSO_4$ $6H_2O$ per litre) with one plug (8 mm in diameter) taken from the edges of actively growing cultures. The liquid medium was supplemented with ginsenosides (2 mg/mL, dissolved in ddH_2O and filter-sterilized through a 0.22 μm PVDF syringe tip membrane). Liquid cultures were then incubated at room temperature for 6 days. After incubation, the medium was separated from the mycelia by vacuum filtration through a nylon membrane (0.45 μm). The filtrate, which contained the extracellular proteins secreted by the cultured organisms, was used for further analysis.

Table 2.1. ***Trichoderma*** **and** ***Pythium*** **isolates used in this study.** List of 12 isolates of pathogenic oomycetes and true fungi obtained from the Canadian Collection of Fungal Cultures at Agriculture and Agri-food Canada and used in this study. Isolates were selected based on a study of isozyme variation and morphology by Barr et al. (1997) and unpublished sequencing data from Andre Levesque (Agriculture and Agri-Food Canada).

Genus	Species	Isolate No.	Host Species	Location
Trichoderma	*hamatum*	TH 215090	*Cucumis sativus*	British Columbia, Canada
Trichoderma	*hamatum*	TH 215955	*Cucumis sativus*	British Columbia, Canada
Pythium	*irregulare*	BR 574	*Picea mariana*	Ontario, Canada
Pythium	*irregulare*	BR 901	*Cucumis sativus*	Alberta, Canada
Pythium	*irregulare*	BR 486	*Phaseolus vulgaris*	Netherlands
Pythium	*irregulare*	BR 779	*Triticum aestivum*	Transvaal, South Africa
Pythium	*irregulare*	BR 962	Soil	Wairakei, New Zealand
Pythium	*irregulare*	BR 598	*Panax quinquefolius*	Ontario, Canada
Pythium	*irregulare*	BR 1040	*Phaseolus vulgaris*	British Columbia, Canada
Pythium	*irregulare*	BR 1068	*Panax quinquefolius*	Ontario, Canada
Pythium	*irregulare*	BR 426	*Rhododendron sp.*	Alberta, Canada
Pythium	*ultimum*	BR 638	*Pisum sativum*	Alberta, Canada

2.2.3. Protein precipitation and concentration

For enzyme precipitation, 50 mL of the medium from oomycete/fungal cultures grown in the presence of pure ginsenosides (2 mg/mL) for 6 days was collected as described above. The proteins in the culture medium were acetone-precipitated with cold (-20ºC) acetone-H_2O (1:1, v/v, final concentration), at -20ºC, for at least 15 min (Deutscher 1990). After precipitation, the medium was centrifuged (4ºC) at 12,000 x g for 5 min and the protein pellet was dried under a gentle N_2 stream and re-suspended in MES buffer (10 mM, pH 6.5), to yield a crude protein preparation. Reconstitution of the enzymes was facilitated via ultrasonication with an ultra-sonic cell disruptor (VirSonic 100 from VirTis, USA) for (3 x 10 sec each, with a pause of 20 sec in between). The enzyme preparations were then centrifuged again (12,000 x g, for 5 min at 4ºC) and the supernatant was loaded onto Amicon Ultra-15 centrifugal filter devices with ultra-filtration membranes of 10 kDa MW cut off (Millipore Corporation, USA). Protein samples were concentrated down to 1 mL, by centrifugation at 3000 x g in a swinging bucket centrifuge (Allegra 6R Beckman Coulter, USA).

2.2.4. Ginsenosidase assay

The ginsenosidase activity of the concentrated protein fractions was tested by incubating the protein concentrates (800 µL) with ginsenosides (8 mg/mL), at 40ºC for 0 – 12 hours according Neculai et al. (2009). The reaction was stopped by adding an equal volume of MeOH to 100 µL of the incubated fractions at 0, 15, 30, 60, 120, 240 and 720 minutes after the addition of substrate. After centrifugation, the reaction products were subjected to HPLC analysis, according to Nicol et al. (2002). Peaks were assigned based on co-chromatography with equivalent ginsenoside preparations previously characterized by LC-MS (Nicol et al. 2003; Yousef and Bernards, 2006).

2.2.5. Plant production

One-year old ginseng plants were obtained from seeds (Delhi, Ontario) stratified in accordance with general grower practice (Oliver et al. 1990). Seeds were surface sterilized after soaking in 1% HCHO solution for 25 minutes then dried overnight at 22ºC. Seeds were then placed in muslin bags and buried under 15-45 cm of moist Pro-mix (Premier Tech Horticulture, Canada) soil and stored at 5ºC for approximately 2 – 3 months until germination occurred. Germinated seeds were transplanted into 12 cm diameter pots (3 seeds

to 1 pot) filled with moist Promix soil, such that the seeds were approximately 0.5 cm below the soil surface. Plants were grown under approx. 70% shade in a greenhouse at approx. 25ºC and watered as needed from April to June 2010. Two-year old plants were obtained by planting germinated seeds into plastic cell trays (4 cm in diameter) filled with Promix such that the seeds were 0.5 cm below the surface. Plants were grown as above until they were fully senesced and then were stored at 5ºC. Re-growth of roots from one-year old seedlings occurred between January and April 2010 and the new two-year old seedlings were transferred into 12 cm diameter pots filled with Promix and grown on a south facing windowsill from April to July 2010.

2.2.6. Pathogenicity assay

One- and two-year old ginseng seedlings were inoculated with oomycete and fungal strains (Table 2.1) according to a modified protocol from Reeleder and Brammall (1994). For each isolate, inoculum was prepared by adding one 8 mm diameter plug of 7-day old Potato Dextrose Agar (PDA) cultures to sterile V8 broth (20 mL) (Tuite 1969) contained in a plastic petri dish. The V8 cultures were incubated at 22ºC in the dark for 4 days. Mycelial mats were then removed from the petri dishes and blended at high speed for 1 min with ddH_2O (one mat per 100 mL H_2O). The resulting suspension was mixed with sterile silica sand (590 g). Ginseng seedlings were transplanted into 12 cm diameter pots, previously sterilized in 5% bleach and filled with inoculated sand (one per pot) and or with sterile sand mixed with 100 mL ddH_2O (Control treatment). Five seedlings (both one- and two-year old) were inoculated with each isolate. All plants were grown for 14 days on a south facing windowsill at 22ºC from June – July 2010 and rated for disease severity on a scale from 1-5 modified from Reeleder and Brammall (1994) (Table 2.2).

2.2.7. Fv/Fm measurement and PAM images

A pulse amplitude modulating (PAM) fluorometer (IMAGING-PAM, Heinz Walz GmbH, Efeltrich, Germany) was used to capture chlorophyll fluorescence images and to estimate the maximum quantum yield of PSII (Fv/Fm) of infected one and two-year old ginseng seedlings according to Ivanov et al. (2006). Chlorophyll fluorescence measurements were performed *in vivo* at room temperature on plants dark adapted for a minimum of 15 min. Fluorescence images were captured by a CCD camera (IMAG-K, Allied Vision Technologies, Germany) featuring 640 x 480 pixel CCD chip size and CCTV camera lens

(Cosmicar/Pentax F1.2, f=12 mm). A light emitting diode ring array (IMAG-L) consisting of 96 blue light emitting diodes (LEDs) (470 nm) provided a standard modulated excitation intensity of 0.5 μmol quanta m^{-2} s^{-1} (modulation frequency 1-8 Hz) for measuring the basal (Fo) chlorophyll fluorescence and a saturation pulse of 2400 μmol quanta m^{-2} s^{-1} PAR for measuring the maximal chlorophyll fluorescence (Fm).

2.2.8. Data handling and statistics

Three independent extracellular protein preparations were prepared for each isolate, allowing ginsenosidase assays to be performed in triplicate (N = 3). The whole experiment was repeated three times. The concentration of ginsenosides Rb1, Rd, GXVII and F2 were quantified using HPLC according to Nicol et al. (2002) and normalized using the Rg1/Re peak present in each ginsenoside elution profile. The Rg1/Re peak was used as an internal standard because it is not metabolized by the extracellular glycosidases produced by the *Pythium* and *Trichoderma* isolates used in this study (Yousef and Bernards 2006; Neculai et al. 2009). Ginsenoside metabolism was normalized by calculating the ginsenoside conversion efficiency [GCE = 1 – $((Rb1+Rd+GXVII)_{final}/(Rb1+Rd+GXVII)_{initial})$] for each isolate. This parameter normalizes the ability of each isolate to metabolize the 20 (*S*)- protopanaxadiol ginsenosides into other ginsenosides, but most notably, ginsenoside F2 (Yousef and Bernards 2006).

The pathogenicity assay for one- and two-year old ginseng seedlings was done using five replicates (N = 5), while Fv/Fm measurements were made at five independent points on the leaves of each one of those five replicates and were then averaged (N = 5). Pathogenicity scores were then determined on a relative scale of 1-5 modified from Reeleder and Brammall (1994) by three independent evaluators for each one of the five replicates. The scores of each independent evaluator were averaged for each isolate to yield the final pathogenicity score (N = 3). All values are presented as Mean ± SE.

Table 2.2. Disease severity scale from 1-5 used to evaluate disease load in one- and two-year old ginseng seedlings. Scale is modified from Reeleder and Brammall (1994).

Disease Severity		Symptoms
1	Control	- No discolouration of leaves (green), may have some small discoloured spots - Leaves turgid/firm and not wilted - Firm/turgid stem attached to root (not damped off) - Main root with no discolouration (whitish) with secondary and tertiary roots intact
2	Mild Disease	- No discolouration of leaves (green), may have some small discoloured spots - Leaves turgid/firm and not wilted - Stem not firm/turgid but not dampened off -Main root with no discolouration (whitish) with secondary and tertiary roots intact
3	Medium Disease	- Discolouration of leaves (yellowish/brown) in more than half of visible surface - Leaves turgid/firm and not wilted - Stem not firm/turgid but not dampened off - Main root with no discolouration (whitish) with secondary and tertiary roots intact
4	High Disease	- Discolouration of leaves (yellowish/brown) in more than half of visible surface -Leaves wilted -Stem not firm/turgid but not dampened off -Tap root with no discolouration (whitish) with secondary and tertiary roots intact
5	Severe Disease	- Discolouration of leaves (yellowish/brown) in more than half of visible surface - Leaves wilted - Stem dampened off or detached near main root - Main root exhibits discolouration (orange/brown)

2.3. Results and Discussion

2.3.1. Selection of *P. irregulare* strains with varying life histories

Nine isolates of *Pythium irregulare*, one isolate of *Pythium ultimum* Trow and two isolates of *Trichoderma hamatum* (Bonord.) Bainier, were obtained from the Canadian Collection of Fungal Cultures (Table 2.1). These isolates were selected to maximize the differences in their genetic diversity (Barr et al. 1997), host species (including woody and non-woody species) and place of origin. A diverse set of isolates was used because previous studies with *P. irregulare* have shown significant differences in the pathogenicity of different isolates towards various host species, indicating that different isolates of *P. irregulare* are better at infecting certain hosts more than others (Harvey et al. 2001). Similar results have also been reported for *P. ultimum* (Levesque et al. 1993). The *P. ultimum* and *T. hamatum* strains were selected as outliers to confirm whether ginsenoside metabolism differed between *Pythium* spp. (Levesque and de Cock 2004) as well as between kingdoms, as *T. hamatum* is a true fungus.

2.3.2. Ginsenoside metabolism by *Pythium* and *Trichoderma* strains

Liquid cultures of all twelve *Pythium* and *Trichoderma* isolates were initiated in Czapek Dox mineral broth supplemented with ginsenosides in order to induce the production of ginsenoside β-glucosidases (Yousef and Bernards 2006; Neculai et al. 2009). Extracellular proteins from the culture filtrates were then collected and assayed for ginsenosidase activity by incubating them with a mixture of ginsenosides and monitoring the change in ginsenoside profile over a 12 hour time period using HPLC (Fig. 2.2, 2.3).

The concentrations of four major ginsenosides (Rb1 **1**, Rd **4**, GXVII **5** and F2 **6**) remaining after 12 hours of incubation with extracellular protein concentrates was used to characterize each isolate as possessing no, partial or full ginsenoside metabolizing activities. Isolates that possessed no apparent ginsenoside metabolizing activity included the *T. hamatum* strains TH 215090 and TH 215955. These isolates showed no change in the concentration of the major ginsenosides over time (Fig. 2.3A, B) and their HPLC elution profiles (Fig. 2.2B) mimicked that of an untreated ginsenoside mixture (Fig. 2.2A).

Isolates BR 638, BR 426, BR 574, BR 779 and BR 901 all showed a decrease in the concentration of Rb1 **1** over time (Fig. 2.3C-G) with a concomitant increase in the concentration of Rd **4** (Fig. 2.2C). The concentrations of GXVII **5** and F2 **6** remained

relatively low and unchanged with only isolates BR 426, BR 779 and BR 901 showing any accumulation of ginsenoside F2 **6** over the assay period. This showed that all five of these isolates secrete extracellular enzymes with a catalytic specificity for hydrolyzing the β(1-6)-glycosidic bonds necessary for the conversion of ginsenoside Rb1 into Rd, and identified them as partial ginsenoside converters. This ginsenosidase activity is analogous to that of glycosidase G1 isolated by Neculai et al. (2009). The absence of ginsenoside F2 accumulation over time, however, shows that the extracellular enzymes produced by these isolates do not include significant amounts of the β(1-2)-glycosidase activity found in glycosidases G2 and G3 (Neculai et al. 2009), which are needed to facilitate the conversion of Rd **1** into the final F2 **6** product. Initially, isolate BR 426 appeared to be an example of a full ginsenoside converter because there was a rapid increase in the amount of F2 **6** (within 15 min) with a concomitant decline in the levels of other ginsenosides, especially Rb1 **1** (Fig. 2.3D). However, this was not sustained and levels of Rb1 **1** and Rd **4** remained higher than the amount of F2 **6** and GXVII **5** through to the end of the assay period (Fig. 2.3D).

By contrast, isolates BR 1040, BR 1068, BR 598, BR 486 and BR 962 all showed a decrease in the concentration of the major ginsenosides Rb1 **1**, Rd **4** and GXVII **5** and a concomitant increase in ginsenoside F2 **6** concentration over the assay period (Fig. 2.2D, 2.3H-L). These *P. irregulare* strains are therefore characterized as full converters. The extracellular enzymes secreted by these isolates possessed both the β(1-2) and β(1-6) glycosidic activity necessary for the full conversion of the common ginsenosides Rb1 **1**, Rd **4** and GXVII **5** into ginsenoside F2 **6**.

The BR 598 and BR 1068 strains originally isolated from *Panax quinquefolius* (American ginseng*)* and the BR 1040 strain isolated from *Phaseolus vulgaris* (bean) showed the most rapid conversion of common 20 (S)-protopanaxadiol ginsenosides into F2. Extracellular glycosidases isolated from these strains depleted the amounts of Rb1 **1** and Rd **4** *in vitro* after only 15 min of incubation and showed a corresponding increase and subsequent depletion of GXVII **5**, along with a continuous increase in F2 **6**. The accumulation of GXVII **5** results when the β(1→2) glycosidic bond between the two sugars at C-3 of Rb1 is cleaved by glycosidases G2/3 (Neculai et al. 2009), while its depletion and consequent rise in F2 levels is facilitated by the cleavage of the β(1→6) glycosidic bond between the two sugars at the C-20 position of GXVII by glycosidase G1.

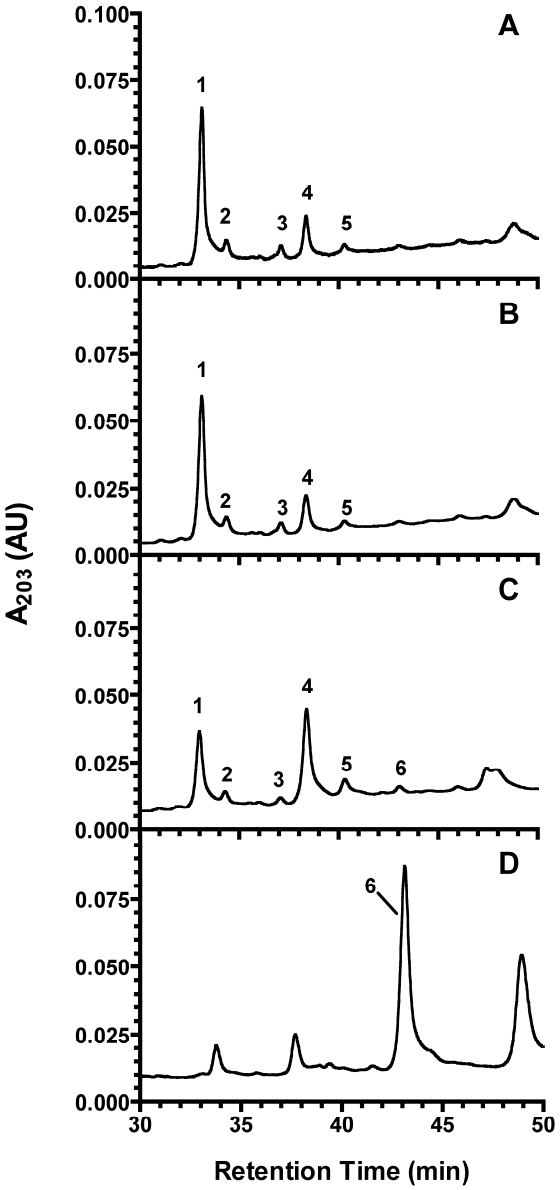

Figure 2.2. HPLC analysis of ginsenosides. Representative HPLC elution profiles of ginsenosides from ginseng root extracts, (A) before, and (B-D) after incubation with culture filtrates recovered from (B) *T. hamatum* isolate 215090 and *Pythium* isolates (C) BR 638 and (D) BR 1068. The HPLC profiles are representative of culture filtrates showing (B) no, (C) partial and (D) full ginsenoside conversion. Peak labels correspond to the compound numbers in Figure 2.1.

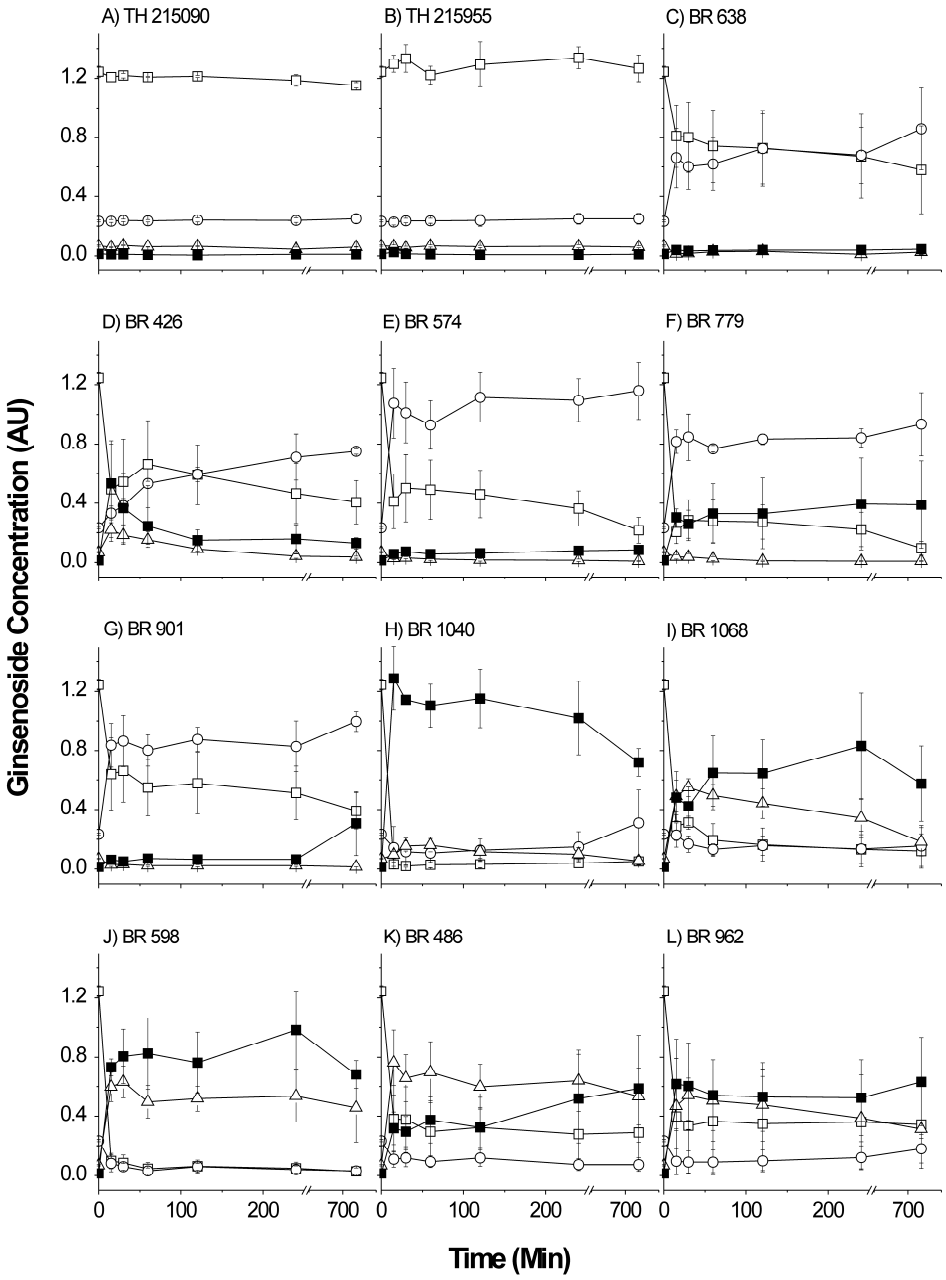

Figure 2.3. Time course of ginsenoside deglycosylation. Concentration of ginsenosides after incubation with partially purified glycosidase fractions from *Pythium* and *Trichoderma* isolates for 15, 30, 60, 120, 240 and 720 min. The amounts of the 20(S)- protopanaxadiol ginsenosides Rb1 **1** (□), Rd **4** (○), GXVII **5** (△) and F2 **6** (■) remaining after incubation were quantified by HPLC, and normalized to the amount of ginsenosides Re **7** and Rg1 **8** in the sample. Assays were performed in triplicate (N = 3). All data are mean relative amounts ± SE.

Isolates BR 486 and BR 962 also exhibited full ginsenoside conversion with the exception that Rb1 **1** levels did not decline in unison with those of Rd **4**. After a rapid initial (i.e., within 15 min) decline, the levels of Rb1 **1** remained about double those of Rd **4** throughout the 12 hour assay period (Fig. 2.3K, L). The levels of GXVII **5** also increased quickly during the first 15 min and then declined slowly for the rest of the assay period. These isolates could produce less ginsenosidases than the BR 1040, BR 598 and BR 1068 strains and as such could show a diminished overall rate of conversion during the assay period.

Overall, these data show that ginsenoside metabolism differs between isolates of *P. irregulare*. While all *Pythium* isolates, including *P. ultimum*, appear to possess β-1,6 glycosidase activity, only a subset (BR 1040, BR 1068, BR 598, BR 486, BR 962 and to a limited extent, BR426) possess sufficient β-1,2 glycosidase activity to fully convert the 20 (S)-protopanaxadiol ginsenosides into F2 **6**.

2.3.3. Normalization of ginsenoside metabolism

The efficiency with which extracellular proteins collected from each *Pythium* and *Trichoderma* isolate deglycosylated 20 (S)-protopanaxadiol ginsenosides Rb1 **1**, Rd **4** and GXVII **5** was normalized by calculating the ginsenoside conversion efficiency (GCE) for each strain (Table 2.3). GCE represents the proportion of ginsenosides Rb1 **1**, Rd **4** and GXVII **5** remaining after incubation with extracellular proteins, relative to that of the original ginsenoside mixture. This parameter normalizes the ability of each isolate to metabolize the 20 (S)-protopanaxadiol ginsenosides into other ginsenosides, but most notably ginsenoside F2 **6**, which is the primary product of extracellular glycosidase produced by *P. irregulare*, when presented with ginsenosides as substrate (Yousef and Bernards 2006). While the calculation of GCE does not account for either the further metabolism of the presumed product, ginsenoside F2 **6**, or alternative metabolism of ginsenosides Rb1 **1**, Rd **4** and GXVII **5**, it does provide a measure of the efficiency with which ginsenosides Rb1 **1**, Rd **4** and GXVII **5** are metabolized. Indeed, higher GCE values are indicative of a greater amount of ginsenoside conversion. In general, GCE values were higher for isolates showing full conversion of ginsenosides into F2 **6** (Fig. 2.3, Table 2.3).

Table 2.3. Ginsenoside conversion efficiency (GCE) of *Pythium* and *Trichoderma* isolates. The ginsenoside conversion efficiency (GCE) of *Pythium* and *Trichoderma* isolates was determined after extracellular proteins isolated from the medium of cultures pre-exposed to ginsenosides (2 mg/mL) were incubated in the presence of ginsenosides (8 mg/mL) for up to 720 minutes. Concentrations of ginsenosides Rb1 **1**, Rd **4** and GXVII **5** were determined using HPLC at each time point. GCE = 1 – $((Rb1+Rd+GXVII)_{final}$ /$(Rb1+Rd+GXVII)_{initial})$. Values are expressed as Mean ± SE. N=3.

Isolate No.	GCE					
	15min	**30min**	**60min**	**120min**	**240min**	**720min**
TH 215090	0.03 ± 0.04	0.01 ± 0.04	0.03 ± 0.03	0.02 ± 0.04	0.05 ± 0.06	0.05 ± 0.05
TH 215955	- 0.03 ± 0.06	- 0.06 ± 0.09	- 0.01 ± 0.07	- 0.04 ± 0.01	- 0.07 ± 0.08	- 0.03 ± 0.08
BR 638	0.04 ± 0.01	0.08 ± 0.06	0.10 ± 0.07	0.04 ± 0.09	0.12 ± 0.06	0.05 ± 0.02
BR 426	0.32 ± 0.19	0.28 ± 0.19	0.12 ± 0.17	0.17 ± 0.10	0.21 ± 0.06	0.23 ± 0.09
BR 574	0.02 ± 0.08	0.01 ± 0.04	0.07 ± 0.02	- 0.03 ± 0.03	0.05 ± 0.05	0.10 ± 0.08
BR 779	0.32 ± 0.03	0.25 ± 0.04	0.31 ± 0.08	0.28 ± 0.10	0.31 ± 0.11	0.33 ± 0.17
BR 901	0.03 ± 0.09	- 0.01 ± 0.01	0.11 ± 0.07	0.05 ± 0.08	0.12 ± 0.07	0.10 ± 0.03
BR 1040	0.83 ± 0.11	0.81 ± 0.05	0.81 ± 0.05	0.83 ± 0.08	0.82 ± 0.09	0.75 ± 0.16
BR 1068	0.34 ± 0.12	0.33 ± 0.02	0.47 ± 0.09	0.51 ± 0.06	0.61 ± 0.13	0.71 ± 0.17
BR 598	0.49 ± 0.11	0.50 ± 0.08	0.63 ± 0.11	0.59 ± 0.09	0.60 ± 0.14	0.66 ± 0.18
BR 486	0.19 ± 0.06	0.25 ± 0.10	0.30 ± 0.09	0.32 ± 0.10	0.36 ± 0.13	0.42 ± 0.22
BR 962	0.38 ± 0.21	0.37 ± 0.16	0.38 ± 0.18	0.40 ± 0.17	0.44 ± 0.20	0.46 ± 0.23

2.3.4. Pathogenicity of *P. irregulare* isolates on American ginseng

A pathogenicity assay was conducted to determine the virulence of *P. irregulare* strains towards American ginseng. In this study, one- and two-year old ginseng seedlings were inoculated with the various *Pythium* and *Trichoderma* isolates and the severity of symptoms evaluated on a relative scale from 1-5, 14 days after infection. Isolates were then separated into groups representing Low, Intermediate or High virulence strains, based on qualitative visual observations (Fig. 2.4). Disease load scores for one year old seedlings were overall slightly higher than for two-year old plants (Table 2.4). This may be due to higher ginsenoside production in older plants and/or their more developed/hardened root structure, which could provide a better mechanical barrier to pathogen infection.

2.3.5. Chlorophyll fluorescence imaging and *in vivo* pathogenicity detection

In addition to relative pathogenicity ranking, the maximum quantum efficiency of PSII (Fv/Fm), determined using chlorophyll fluorescence imaging, was measured in two-year old ginseng plants every 2 days until 14 days after infection with the various *Pythium* and *Trichoderma* isolates (Fig. 2.4), (Table 2.4). This chlorophyll fluorescence parameter has been used to identify plant pathogen infection, *in vivo,* in a number of different species by various viral, bacterial and fungal/oomycotic organisms (Rolfe and Scholes 2010). More specifically, chlorophyll fluorescence imaging has been used to identify disease in bean (*Phaseolus vulgaris*) infected with *Botrytis cinera* (Chaerle et al. 2007), wheat (*Triticum aestivum)* infected with *Puccinia recondita* or *Blumeria graminis* (Kuckenberg et al. 2009), lettuce (*Lactuca sativa*) infected with the oomycete *Bremia lactucae* (Prokopová et al. 2010) and grape (*Vitis vinifera*) infected with the downy mildew *Plasmopara viticola* (Cséfalvay et al. 2009). Changes, (i.e.,. decreases) in Fv/Fm values can be an excellent indicator of biotic and abiotic stress (e.g., water stress) in plants, which correlates well with the symptoms of damping off caused by nectrotrophic pathogens like *P. irregulare*. In the present study, increases in disease load in two year old ginseng plants infected with various *Pythium* isolates were shown to be correlated (R^2 = 0.79; P=0.0001) with a decrease in Fv/Fm values up to 14 days after infection (Fig. 2.5). Importantly, the decrease in Fv/Fm values in plants that had high pathogenicity scores was manifested 4 – 6 days after initial infection (Table 2.4); this is earlier than the appearance of visual symptoms of disease.

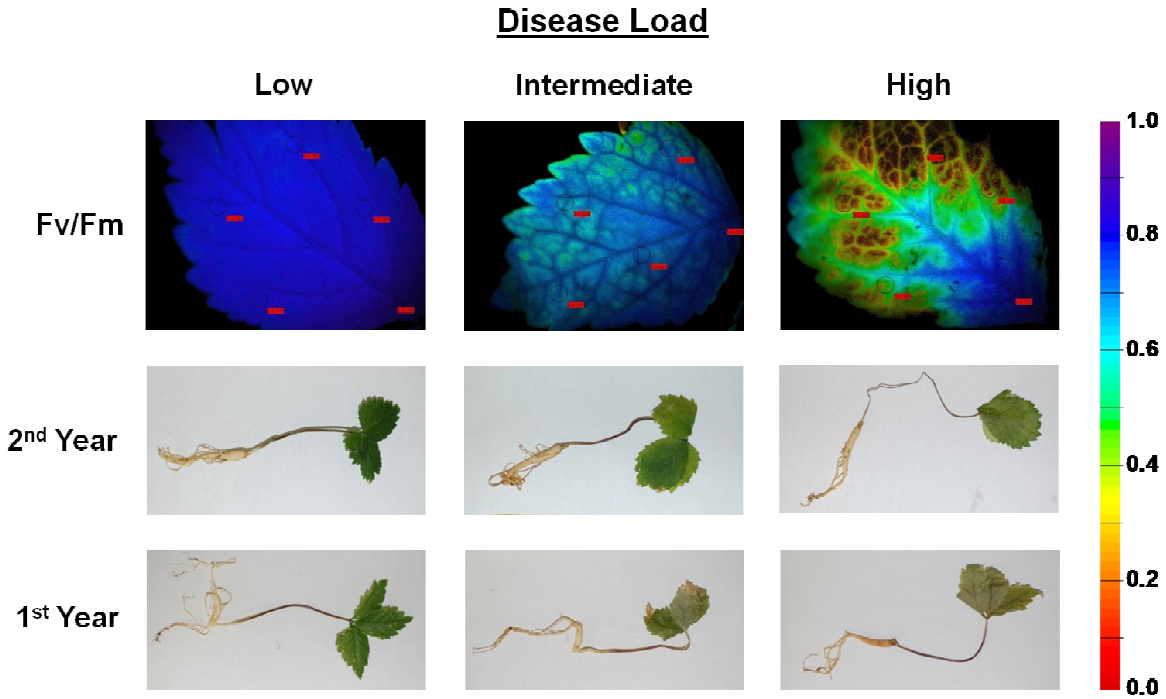

Figure 2.4. Pathogenicity of *Pythium* on ginseng. Representative images of ginseng seedlings showing low, intermediate and high disease loads after infection with various *Pythium* and *Trichoderma* isolates. Upper panels: PAM images of two-year old ginseng plants 14 days after infection (heat map scale at right). Red bars on PAM images indicate sites of individual Fv/Fm measurements. Middle and lower panels: One- and two-year old ginseng seedlings 14 days after infection, respectively.

Table 2.4. Pathogenicity of *Pythium* and *Trichoderma* isolates. Pathogenicity scores for one- and two-year old ginseng seedlings were established 14 days after infection with various *Pythium* and *Trichoderma* isolates, while values of maximum quantum efficiency of PSII (Fv/Fm) for two-year old ginseng seedlings were obtained between 0-14 days after infection with the same isolates. Pathogenicity scores were determined after plants inoculated with the various isolates were evaluated for disease severity on a relative scale from 1-5, 14 days after infection. All values are expressed as Mean ± SE. N = 3 for pathogenicity scores and N = 5 for Fv/Fm values.

	ISOLATE No.											
	TH 215090	**TH 215955**	**BR 574**	**BR 901**	**BR 486**	**BR 779**	**BR 962**	**BR 598**	**BR 1040**	**BR 1068**	**BR 426**	**BR 638**
Pathogenicity Score												
1 year old plants	2.1 ± 0.2	1.4 ± 0.2	2.3 ± 0.2	1.4 ± 0.2	2.3 ± 0.3	3.2 ± 0.1	2.9 ± 0.2	3.6 ± 0.1	3.7 ± 0.1	3.8 ± 0.2	4.3 ± 0.3	4.3 ± 0.3
2 year old plants	1.3 ± 0.1	1.7 ± 0.1	2.1 ± 0.2	2.3 ± 0.1	2.1 ± 0.1	1.7 ± 0.2	2.1 ± 0.2	2.7 ± 0.1	2.6 ± 0.1	3.2 ± 0.1	3.5 ± 0.1	3.1 ± 0.2
Fv/Fm 2 year old plants												
Day 0	0.76 ± 0.01	0.74 ± 0.01	0.73 ± 0.01	0.76 ± 0.02	0.74 ± 0.01	0.75 ± 0.01	0.75 ± 0.01	0.77 ± 0.01	0.76 ± 0.01	0.74 ± 0.01	0.76 ± 0.01	0.77 ± 0.01
Day 2	0.77 ± 0.01	0.75 ± 0.01	0.71 ± 0.02	0.76 ± 0.01	0.76 ± 0.01	0.77 ± 0.01	0.79 ± 0.01	0.74 ± 0.01	0.76 ± 0.01	0.77 ± 0.01	0.76 ± 0.01	0.77 ± 0.01
Day 4	0.75 ± 0.01	0.75 ± 0.01	0.70 ± 0.02	0.65 ± 0.01	0.70 ± 0.01	0.76 ± 0.01	0.73 ± 0.01	0.69 ± 0.01	0.72 ± 0.01	0.72 ± 0.01	0.71 ± 0.01	0.76 ± 0.01
Day 6	0.77 ± 0.01	0.76 ± 0.01	0.72 ± 0.01	0.67 ± 0.01	0.70 ± 0.01	0.75 ± 0.01	0.71 ± 0.01	0.73 ± 0.01	0.74 ± 0.01	0.71 ± 0.01	0.68 ± 0.01	0.65 ± 0.02
Day 8	0.78 ± 0.01	0.77 ± 0.01	0.75 ± 0.01	0.72 ± 0.01	0.75 ± 0.01	0.77 ± 0.01	0.77 ± 0.01	0.73 ± 0.01	0.75 ± 0.01	0.72 ± 0.01	0.73 ± 0.01	0.66 ± 0.02
Day 10	0.76 ± 0.01	0.73 ± 0.01	0.74 ± 0.01	0.69 ± 0.01	0.74 ± 0.01	0.77 ± 0.01	0.76 ± 0.01	0.74 ± 0.01	0.71 ± 0.01	0.69 ± 0.02	0.72 ± 0.01	0.63 ± 0.03
Day 12	0.75 ± 0.01	0.74 ± 0.01	0.68 ± 0.02	0.63 ± 0.01	0.73 ± 0.01	0.77 ± 0.01	0.75 ± 0.01	0.63 ± 0.02	0.62 ± 0.03	0.60 ± 0.03	0.44 ± 0.04	0.45 ± 0.06
Day 14	0.77 ± 0.01	0.76 ± 0.01	0.71 ± 0.03	0.69 ± 0.01	0.71 ± 0.02	0.76 ± 0.01	0.73 ± 0.01	0.56 ± 0.03	0.65 ± 0.03	0.53 ± 0.05	0.52 ± 0.03	0.39 ± 0.06

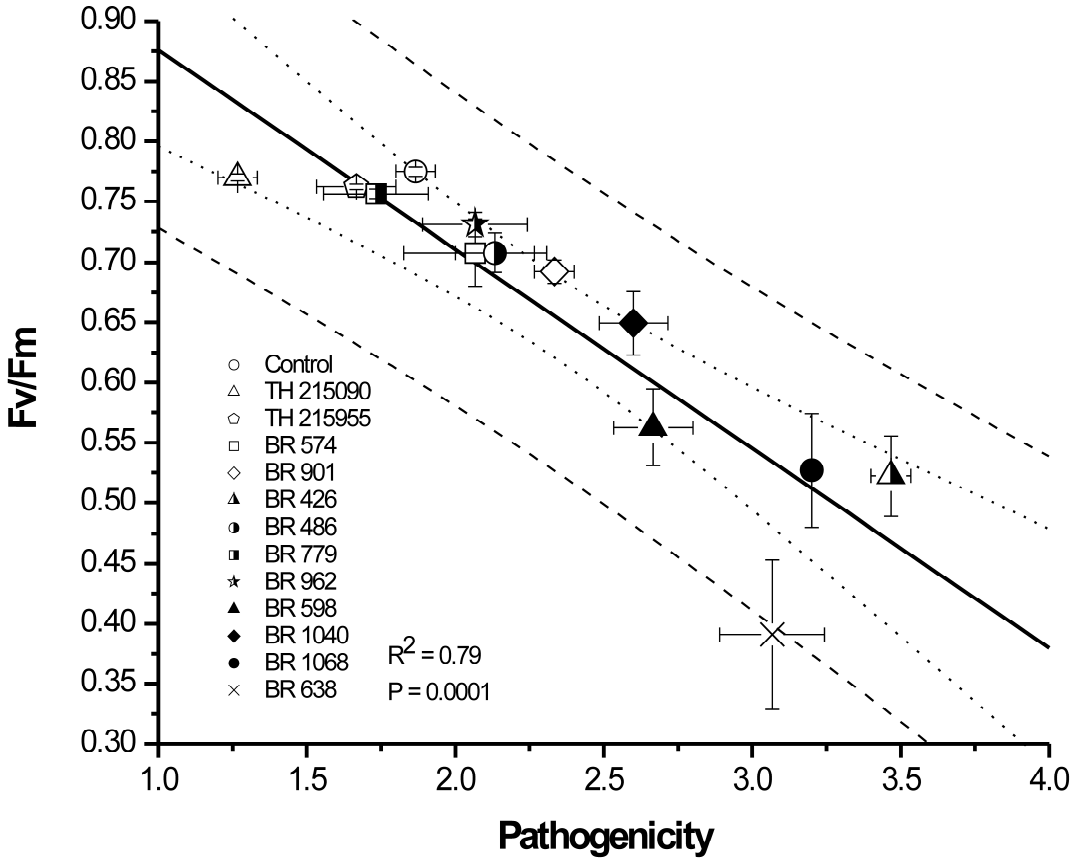

Figure 2.5. Pathogenicity and Fv/Fm. The relationship between the pathogencity scores for two-year old ginseng plants inoculated with various *Pythium* and *Trichoderma* isolates and the maximum quantum efficiency of PSII (Fv/Fm) in the same seedlings was compared. All measurements were taken 14 days after inoculation. Dashed and dotted lines represent upper and lower 95% confidence limits respectively. All values are expressed as Mean ± SE, N = 5 for Fv/Fm measurements, N = 3 for pathogenicity scores, $R^2 = 0.79$, P = 0.0001.

In the future, in addition to possibly providing an early indication of pathogen infection, chlorophyll fluorescence imaging could be used as a non-invasive, fast-screening method to determine the efficiency of various pathogen control techniques on ginseng plants. This may prove very effective as ginseng is a perennial crop, which may require different pathogen control strategies at different lifecycle stages. Fv/Fm measurements could be used as a guide to evaluate pathogen control strategies over a study period as long as the natural life cycle of the plant.

2.3.6. Relationship between ginsenoside metabolism (GCE) and the pathogenicity of *P. irregulare* towards American ginseng

The efficiency of all *P. irregulare* isolates to metabolize the 20 (S)-protopanaxadiol ginsenosides Rb1 **1**, Rd **4** and GXVII **5**, measured as GCE, was positively correlated (R^2=0.57; P=0.005) with the pathogenicity of those strains towards ginseng (Fig. 2.6). Thus, isolates of *P. irregulare* that readily infect ginseng roots also have a higher GCE, which supports a role for extracellular, ginsenoside-specific glycosidases in the process. By contrast, *P. ultimum*, which showed low GCE, was able to infect ginseng seedlings; this species was not included in the correlation. In addition to supporting our hypothesis that extracellular ginsenosidases are involved in the pathogenicity of *P. irregulare* on ginseng, these results correlate with previous observations that *P. irregulare* isolates exhibit significant differences in pathogenicity between hosts, which may be due to differing infection systems (Harvey et al. 2001).

In general, *Pythium* and *Trichoderma* isolates could be grouped according to high (BR 426, BR 598, BR 1040 and BR 1068), intermediate (BR 486, BR 779 and BR 962) and low (TH 215090, TH 215955, BR 574 and BR 901) disease load and GCE. Isolate BR 426, however, like the *P. ultimum* strain tested, showed high pathogenicity, but relatively low GCE. When BR 426 is excluded from the linear regression analysis, the correlation between disease load and GCE increases (R^2=0.85; P=0.001).

The *P. ultimum* isolate BR 638, showed high pathogenicity towards ginseng plants. However, this isolate did not appear to produce an abundance of extracellular ginsenosidases, since the extracellular protein preparation from it could only partially convert ginsenosides. This species has a different infection system than *P. irregulare* (Hendrix and Campbell 1973) and plants infected with it showed different symptoms than those infected with *P. irregulare*.

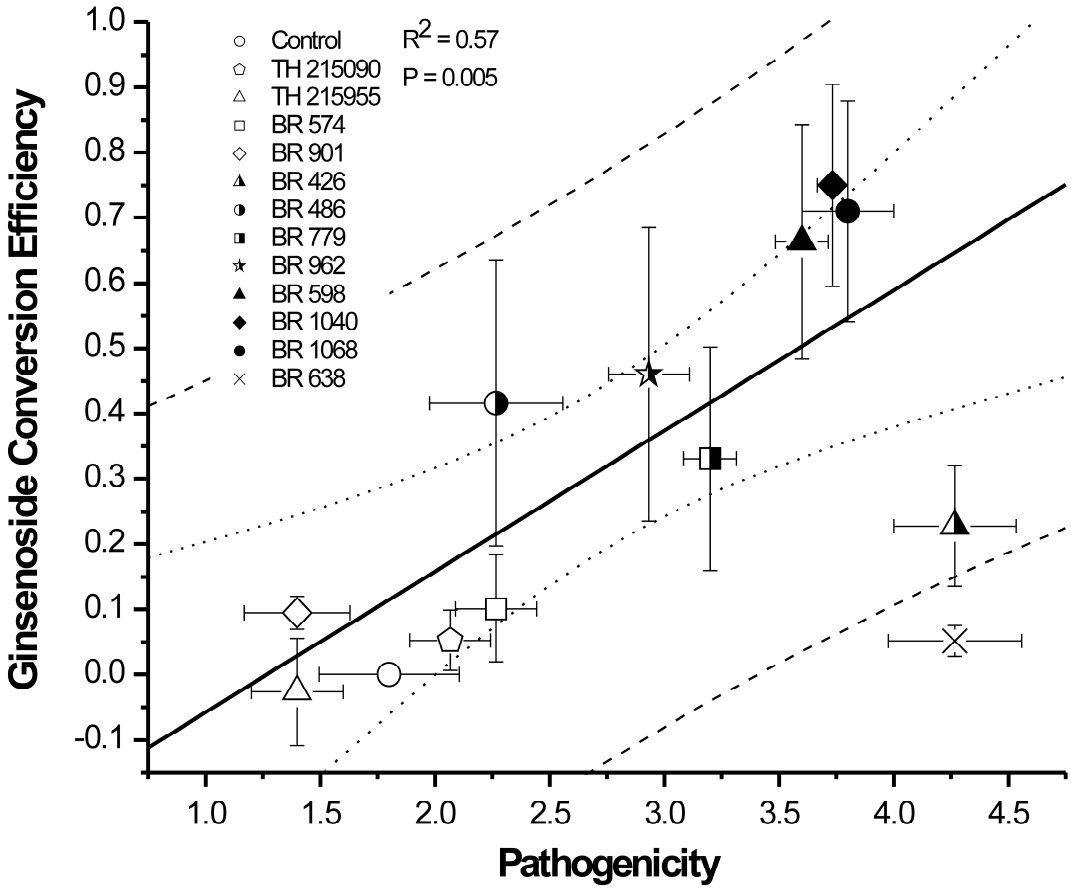

Figure 2.6. Pathogenicity and ginsenoside conversion efficiency. The relationship between the pathogencity scores for one-year old ginseng plants inoculated with various *Pythium* and *Trichoderma* isolates and the *in vitro* ginsenoside conversion efficiency of the same organisms was compared. Isolate BR 638, which is the *P. ultimum* species showing high pathogenicity but low ginsenoside conversion efficiency (see text) was not included in the linear regression analysis. Dashed and dotted lines represent upper and lower 95% confidence limits respectively. All values were calculated as Mean ± SE, N = 3 for ginsenoside conversion efficiency and pathogenicity scores, $R^2 = 0.57$, P = 0.005.

That is, BR 638 caused the leaves of infected plants to become yellow and wilt, however no damping off or root rot symptoms were observed. Thus, *P. ultimum* infects ginseng using a different mechanism than *P. irregulare* and may not rely on ginsenoside metabolism as a means of host recognition.

2.3.7. A broader role for ginsenosidases

The metabolism of common ginsenosides by extracellular β-glycosidases is not limited to isolates of *P. irregulare*. There are numerous examples of the enzymatic transformation of ginsenosides by a wide variety of organisms (Park et al. 2010). For example, human intestinal bacteria including *Bacteroides sp.* (Bae et al. 2005), *Bifidobacterium sp.* (Chi et al. 2006), *Fusobacterium sp.* (Park et al. 2001), *Lactobacillus delbrueckii* (Chi et al. 2006) and *Leuconostoc paramesenteriodis* (Chi et al. 2006) have all been shown to metabolize orally ingested ginsenosides.

In addition, microorganisms isolated from soil-cultivated ginseng, including fungi such as *Absidia coerulea* (Chen et al. 2007), *Acremonium strictum* (Chen et al. 2008), *Fusarium sacchari* (Han et al. 2007) and *Paecilomyces bainier* (Zhou et al. 2008), have been shown to be able to transform common ginsenosides, by cleaving sugar moieties from the sugar side-chains of the parent sapogenin. The ability of all of these organisms to transform the major ginsenosides (Rb1 **1**, Rb2 **2**, Rc **3**, Rd **4**, Re **7** and Rg1 **8**) into minor ginsenosides has major implications to the pharmaceutical industry, since deglycosylated ginsenosides are more readily absorbed into the blood stream and are thought to be more pharmaceutically active compounds than their glycosylated counterparts (Karikura et al. 1991). Recently, recombinant β-D-glycosidases from various thermophilic organisms have been used for ginsenoside transformation (Noh and Oh 2009; Noh et al. 2009). The transformation of ginsenosides by intestinal bacteria and other microorganisms however, has been shown to be less efficient than transformation of ginsenosides using enzymes selective to the hydrolysis of the sugar moieties of ginsenosides (Park et al. 2010).

Our study supports the hypothesis that the production of extracellular ginsenoside metabolizing β-glycosidases (ginsenosidases), and their ability to metabolize common 20 (S)-protopanaxadiol ginsenosides, plays a functional role in the pathogenicity of some organisms. That is, increased metabolism of ginsenosides by *P. irregulare* ginsenosidases, measured as GCE, correlates with the pathogenicity of this organism towards American

ginseng (Fig. 2.6). Further study of the role of ginsenosidases in the ginseng - *P. irregulare* pathosystem could lead to increased ginseng yields for producers by mitigating disease progression and infection.

2.4. Conclusion

While the pathogenicity of unique isolates of *P. irregulare* on ginseng roots correlates with their ability to deglycosylate 20 (S)-protopanaxadiol ginsenosides via extracellular ginsenosidases, this does not imply that extracellular ginsenosidases are required for infection. Indeed, *P. ultimum*, which readily infects ginseng seedlings, showed a relatively poor ability to deglycosylate ginsenosides. Nevertheless, the relationship between *P. irregulare*-derived ginsenosidases and pathogenicity supports our hypothesis that this organism uses ginsenosides as a host recognition factor (Nicol et al. 2002). Cloning of the genes of glycosidases G1, G2 and G3, analysis of their gene expression in the isolates studied herein, and selective down regulation (e.g., through RNAi technology), will be necessary to obtain a better understanding of their role in the pathogenicity of these organisms on ginseng roots. In addition, the use of Fv/Fm measurements (i.e., chlorophyll imaging) to quantify disease load in American ginseng is a promising tool for the early detection of disease, which may be incorporated into a comprehensive disease management strategy.

2.5. References

Attele, A.S., Wu, J.A., Yuan, C.S., 1999. Ginseng pharmacology: Multiple constituents and multiple actions. Biochem. Pharmacol. 58, 1685-1693.

Bae, E.A., Shin, J.E., Kim, D.H., 2005. Metabolism of ginsenoside Re by human intestinal microflora and its estrogenic effect. Biol. Pharm. Bull. 28, 1903-1908.

Barr, D.J.S, Warwick, S.I., Desaulniers, N.L., 1997. Isozyme variation, morphology, and growth response to temperature in *Pythium irregulare*. Can. J. Bot. 75, 2073-2081.

Bowyer, P., Clarke, B.R., Lunness, P., Daniels, M.J., Osbourne A.E., 1995. Host range of a plant pathogenic fungus determined by a saponin detoxifying enzyme. Science. 267, 371-374.

Brunner, F., Wirtz, W., Rose, J.K.C., Darvill, A.G., Govers, F., Scheel, D., Nurnberger, T., 2002. A [beta]-glucosidase/xylosidase from the phytopathogenic oomycete, *Phytophthora infestans*. Phytochemistry. 59, 689-696.

Chaerle, L., Hagenbeek, D., Vanrobeys, X., Van Der Straeten, D., 2007. Early detection of nutrient and biotic stress in *Phaseolus vulgaris*. Int. J. Remote Sens. 28, 3479-3492.

Chen, G., Yang, M., Lu, Z., Zhang, J., Huang, H., Liang, Y., Guan, S., Song, Y., Wu, L., Guo, D.A., 2007. Microbial transformation of 20(S)-protopanaxatriol-type saponins by *Absidia coerulea*. J. Nat. Prod. 70, 1203-1206.

Chen, G.T., Yang, M., Song, Y., Lu, Z.Q., Zhang, J.Q., Huang, H.L., Wu, L.J., Guo, D.A., 2008. Microbial transformation of ginsenoside Rb1 by *Acremonium strictum*. Appl. Microbiol. Biotechnol. 77, 1345-1350.

Cheng, L.Q., Na, J.R., Kim, M.K., Bang, M.H., Yang, D.C., 2007. Microbial conversion of ginsenoside Rb1 to minor ginsenoside F2 and gypenoside XVII by *Intrasporangium sp.* GS603 isolated from soil. J. Microbiol. Biotechnol. 17, 1937-1943.

Chi, H., Lee, B.H., You, H.J., Park, M.S., Ji, G.E., 2006. Differential transformation of ginsenosides from *Panax ginseng* by lactic acid bacteria. J. Microbiol. Biotechnol. 16, 1629-1633.

Crombie, W.M.L., Crombie, L., Green, J.B., Lucas, J.A., 1986. Pathogenicity of 'take-all' fungus to oats: Its relationship to the concentration and detoxification of the four avenacins. Phytochemistry. 25, 2075-2083.

Cséfalvay, L., Di Gaspero, G., Matouš, K., Bellin, D., Ruperti, B., Olejníčková, J., 2009. Pre-symptomatic detection of *Plasmopara viticola* infection in grapevine leaves using chlorophyll fluorescence imaging. Eur. J. Plant Pathol. 125, 291-302.

Deutscher, M.P., 1990. Guide to protein purification, in: Deutscher, M.P. (Eds.), Methods in Enzymology, vol. 182. Academic Press., London, UK.

Han, Y.I., Sun, B., Hu, X.U., Zhang, H., Jiang, B., Spranger, M.I., Zhao, Y., 2007.Transformation of bioactive compounds by *Fusarium sacchari* fungus isolated from the soil-cultivated ginseng. J. Agric. Food Chem. 55, 9373-9379.

Harvey, P.J., Butterworth, P.J., Hawke, B.G., Pankhurst, C.E., 2001. Genetic and pathogenic variation among cereal, medic and sub-clover isolates of *Pythium irregulare*. Mycol. Res. 105, 85-93.

Hendrix, F.F. Jr., Cambell, W.A., 1973. Pythiums as Plant Pathogens. Annu. Rev. Plantpathol. 11, 77-98.

Hostettmann, K., Marston, A., 1995. Saponins. Chemistry and Pharmacology of Natural Products. Cambridge University Press, Cambridge, U.K.

Howard, R.J., Garland, J.A., Seaman, W.L., 1994. Diseases and pests of vegetable crops in Canada. Canadian Phytopathological Society and Entomological Society of Canada, Ottawa, ON, pp. 11-15.

Ivanov, A.G., Hendrickson, L., Krol, M., Selstam, E., Öquist G., Hurry, V., Huner, N.P.A., 2006. Digalactosyl-diacylglycerol deficiency impairs the capacity for photosynthetic intersystem electron transport and state transitions in *Arabidopsis thaliana* due to Photosystem I acceptor-side limitations. Plant Cell Physiol. 47, 1146–1157.

Karikura, M., Miyase, T., Tanizawa, H., Taniyama, T., Takino, Y., 1991. Studies on absorption, distribution, excretion and metabolism of ginseng saponins. VII. Comparison of the decomposition modes of ginsenoside-Rb1 and -Rb2 in the digestive tract of rats. Chem. Pharm. Bull. 39, 2357-2356.

Krupa, S.V., Dommergues, Y.R., 1979. Ecology of root pathogens, in: Developments in agricultural and managed-forest ecology. Elsevier Scientific Publishing Company, Amsterdam, pp. 14-17.

Kuckenberg, J., Tartachnyk, I., Noga, G., 2009. Temporal and spatial changes of chlorophyll fluorescence as a basis for early and precise detection of leaf rust and powdery mildew infections in wheat leaves. Precision Agric. 10, 34-44.

Levesque, C.A., Beckenbach, K., Baillie, D.L., Rahe, J.E., 1993. Pathogenicity and DNA restriction fragment length polymorphisms of isolates of *Pythium spp.* from glyphosate-treated seedlings. Mycol. Res. 97, 307-312.

Levesque, C.A., De Cock, A.W.A.M., 2004. Molecular phylogeny and taxonomy of the genus *Pythium.* Mycol. Res. 108, 1363-1383.

Morrissey, J.P., Osbourn, A., 1999. Fungal resistance to plant antibiotics as a mechanism of pathogenesis. Microbiol. Mol. Biol. R. 63, 708-724.

Neculai, M.A., Ivanov, D., Bernards, M.A., 2009. Partial purification and characterization of three ginsenoside-metabolizing [beta]-glucosidases from *Pythium irregulare*. Phytochemistry. 70, 1948-1957.

Nicol, R.W., Traquair, J.A., Bernards, M.A., 2002. Ginsenosides as host resistance factors in American ginseng (*Panax quinquefolius*). Can. J. Bot. 80, 557–562.

Nicol, R.W., Yousef, L., Traquair, J.A., Bernards, M.A., 2003. Ginsenosides stimulate the growth of soilborne pathogens of American ginseng. Phytochemistry. 64, 257–264.

Noh, K.H., Oh, D.K., 2009. Production of the rare ginsenosides compound K, compound Y, and compound Mc by a thermostable [beta]-glycosidase from *Sulfolobus acidocaldarius*. Biol. Pharm. Bull. 32, 1830-1835.

Noh, K.H., Son, J.W., Kim, H.J., Oh, D.K., 2009. Ginsenoside compound K production from ginseng root extract by a thermostable [beta]-glycosidase from *Sulfolobus solfataricus*. Biosci. Biotechnol. Biochem. 73, 316-321.

Oliver, A., Van Lierop, B., Buonassisi, A., 1990. American ginseng culture in the arid climates of British Columbia. Ministry of Agriculture and Fisheries of British Columbia, Victoria, BC. Canada. pp 37.

Olsen, R.A., 1971. Triterpeneglycosides as inhibitors of fungal growth and metabolism. I. Effect on growth, endogenous respiration and leakage of UV-absorbing material from various fungi. Physiol. Plantarum. 24, 534–543.

Papadopoulou, K., Melton, R.E., Leggett, M., Daniels, M.J. and Osbourn, A.E. 1999. Compromised disease resistance in saponin-deficient plants. Proc. Natl. Acad. Sci. USA. 96, 12923-12928.

Park, S.Y., Bae, E.A., Sung, J.H., Lee, S.K., Kim, D.H., 2001. Purification and characterization of ginsenoside Rb1-metabolizing [beta]-glucosidase from *Fusobacterium* K-60, a human intestinal anaerobic bacterium. Biosci. Biotechnol. Biochem. 65, 1163-1169.

Park, C.S., Yoo, M.H., Noh, K.H., Oh, D.K., 2010. Biotransformation of ginsenosides by hydrolyzing the sugar moieties of ginsenosides using microbial glycosidases. Appl. Microbiol. Biotechnol. 87, 9-19.

Prokopová, J., Spundová, M., Sedlárová, M., Husicková, A., Novotný, R., Dolezal, K., Naus, J., Lebeda, A., 2010. Photosynthetic responses of lettuce to downy mildew infection and cytokinin treatment. Plant Physiol. Biochem. 48, 716-723.

Reeleder, R.D., Brammall, R.A., 1994. Pathogenicity of *Pythium* species, *Cylindrocarpon destructans* and *Rhizoctonia solani* to ginseng seedlings in Ontario. Can. J. Plant Pathol. 16, 311-316.

Rolfe, S.A., Scholes, J.D., 2010. Chlorophyll fluorescence imaging of plant-pathogen interactions. Protoplasma. 247, 163-175.

Shibata, S., 2001. Chemistry and cancer preventing activities of ginseng saponins and some related triterpenoid compounds. J. Korean Med. Sci. 16, S28-S37.

Teng, R., Li, H., Chen, J., Wang, D., He, Y., Yang, C., 2002. Complete assignment of ^{1}H and ^{13}C NMR data for nine protopanaxatriol glycosides. Magn. Reson. Chem. 40, 483–488.

Tuite, J., 1969. Plant Pathological Methods. Burgess Publishing Co., Minneapolis, MN., USA. pp. 233.

Yousef, L.F., Bernards, M.A., 2006. *In vitro* metabolism of ginsenosides by the ginseng root pathogen *Pythium irregulare*. Phytochemistry. 67, 1740-1749.

Zhou W., Yan Q., Li J.Y., Zhang X.C., Zhou P. 2008 Biotransformation of *Panax notoginseng* saponins into ginsenoside compound K production by *Paecilomyces bainier sp.* 229. J. Appl. Microbiol. 104, 699-706.

Chapter 3: Chlorophyll Fluorescence Imaging as a Tool to Monitor the Progress of a Root Pathogen in a Perennial Plant

3.1. Introduction

The ability to accurately detect the early onset of disease in various crops *in situ* is vital in the context of disease prevention and precision agriculture. The detection and differentiation of stress symptoms caused by various infections is therefore highly important for starting appropriate prevention measures like the application of pesticides or fungicides (Burling et al. 2010). The problem in implementing these strategies with regards to modern agriculture is that plant disease severity today is most commonly assessed visually with ordinal rating scales that allow for a qualitative but often subjective evaluation of the level of infection in the laboratory setting as well as on the field scale (Strange and Scott 2005; Bock et al. 2010; Miyake et al. 2014). This method has been, and is currently, used to rate diseases caused by a wide range of foliar and root pathogens on many different commercially grown plant species (Strange and Scott 2005; Bock et al. 2010). However, these commonly used methods are not extremely reliable in accurately gauging and predicting the severity of plant disease infections which means that the application of agricultural chemicals is often preventive and rarely targeted to a specific current infection. Therefore, one of the ways to improve on these agricultural practices is to further develop and integrate the use of non-invasive, quantitative methods for the monitoring of plant health into modern agriculture.

Chlorophyll fluorescence imaging (CFI) provides a sensitive, non-invasive and non-destructive method that can be used to provide insight into the mechanisms underlying plant pathogen interactions (Baker et al. 2001; Chaerle and Van Der Straeten 2001; Rolfe and Scholes 2010). This can be done because CFI allows for the monitoring of alterations to the photosynthetic apparatus of host plants caused by biotic and abiotic stresses that cannot otherwise be monitored visually and which can be used for early, pre-symptomatic diagnosis of infection in host plants (Rolfe and Scholes 2010). This is made even easier today due to the assortment of commercially available fluorometers, the most widely used of which is the Pulse Amplitude Modulated (PAM) fluorometer (Gorbe and Calatayud 2012). This instrument uses visible light for chlorophyll (Chl) excitation, and measures Chl fluorescence in the 690-740 nm range (Schreiber et al. 1986; Lichtenthaler and Miehé 1997; Oxborough and Baker 1997; Lichtenthaler et al. 2005a). As with non-imaging PAM Chl fluorescence, a

weak pulse-modulated measuring light, continuous non-saturating actinic light and saturating light flashes are then used to derive the five key fluorescence intensity levels Fo, F'o, Fm, F'm and Fs (Table 3.1), which are the basis for deriving all other chlorophyll fluorescence parameters reflecting the physiological status of the plant (Schreiber et al. 1986; Genty et al. 1989; Govindjee 1995; Kramer et al. 2004; Baker 2008).

PAM fluorometry has been used to monitor plant responses to numerous abiotic and biotic stresses (Lichtenthaler and Miehé 1997; Oxborough and Baker 1997; Baker 2008; Gorbe and Calaytud 2012). However, non-imaging Chl fluorescence data on stress responses in agriculturally important plant species is more commonly available than that from studies using CFI techniques (Gorbe and Calatayud 2012). Nevertheless, CFI has been shown to be able to monitor the effects of various abiotic stresses, such as nutrient deficiency (Lichtenthaler et al. 2005b), water deficit (Calatayud et al. 2006), extreme temperatures (Schreiber and Klughammer 2008), excessive light intensity/UV exposition (Kuckenberg et al. 2007; Takayama et al. 2007) and even air pollution caused by excess ozone (O_3) (Leipner et al. 2001; Chen et al. 2009), on different plant species.

An overview of these and other studies shows that a comparison between the different types of stresses is quite difficult due to the different equipment used, the variation in parameters that can be measured by them and the different types of plants measured. Although these studies differred in the stress and its severity there are, however, certain changes seen in the photosynthetic parameters of all plants that are common features of all stress responses (Chaerle et al. 2007). For example, photochemical activity of photosystem II (PSII) as measured by Fv/Fm or ΦPSII (Table 3.1) tends to decrease with prolonged exposure to stress, whereas processes involving regulated energy dissipation quantified by ΦNPQ (Table 3.1) increase initially to protect the photosynthetic apparatus, but then decrease over time when the stress becomes too severe; ΦNO (Table 3.1) shows the inverse response to Fv/Fm (Gorbe and Calatayud 2012), but the mechanisms for these changes are not yet fully understood.

Biotic stress, through viral, bacterial or fungal pathogen infection has also been shown to negatively affect photosynthetic electron transport and downstream metabolic reactions (Baker 2001; Chaerle et al. 2007; Baker 2008; Rolfe and Scholes 2010). These effects inevitably lead to changes in chlorophyll fluorescence. However, as with the effects of abiotic stresses, these changes are often not homogenously distributed in the leaf/plant

(Lichtenthaler and Miehé 1997; Baker 2008). Since CFI can be used to screen whole leaves, plants or plant communities, it can be used to monitor the spatial heterogeneity of leaf photosynthetic performance in response to stress with much more accuracy than could be attained through non-imaging fluorescence measurements (Baker 2008). Furthermore, the imaging of different fluorescence parameters can provide a wealth of information with regards to the timing and location of pathogen infection as well as the underlying mechanisms of infection in the host plant (Baker 2008; Rolfe and Scholes 2010).

To date CFI has been used to study a wide range of plant pathogen interactions with the main applications being either diagnostic (identifying infection before visual symptoms appear) or providing information about the impact of infection on host metabolism. For example, Balachandran et al. (1994) examined the compatible interaction between tobacco (*Nicotiana tabacum* cv. Xanthi) and the foliar pathogen tobacco mosaic virus (TMV) with subsequent studies using *N. tabacum* and *N. benthimiana* as model organisms (Chaerle et al. 2004; Chaerle et al. 2006; Perez-Bueno et al. 2006; Pineda et al. 2008). Chlorophyll fluorescence imaging has since been used to study the impact of bacterial (Bonfig et al. 2006; Matous et al. 2006; Berger et al. 2007; Iqbal et al. 2012) as well as fungal/oomycete pathogens (Meyer et al. 2001; Scharte et al. 2005; Swarbick et al. 2006; Burling et al. 2010; Prokopova et al. 2010; Ivanov and Bernards 2012) on numerous host plants. These studies on biotic stresses have examined the impact various infections have on numerous photosynthetic parameters like the maximum photochemical efficiency of PSII (Fv/Fm) (Bonfig et al. 2006; Ivanov and Bernards 2012; Tung et al. 2013), quantum yield of PSII photochemistry (ΦPSII) (Aldea et al. 2005, 2006; Swarbick et al. 2006), quantum yield of regulated non-photochemical quenching (ΦNPQ) (Rodrigues-Moreno et al. 2008) and the quantum yield of non regulated quenching processes (ΦNO) (Burling et al. 2010). To date however, CFI techniques have been applied almost exclusively to study the effects of foliar pathogens on plant species.

In the present study, chlorophyll fluorescence imaging was used to monitor *in vivo* the infection of American ginseng (*Panax quinquefolius* L.) by the root pathogen *Pythium irregulare* Buisman. This follows up on the work of Ivanov and Bernards (2012), which showed a negative correlation between the pathogenicity of various strains of *P. irregulare* on American ginseng and Fv/Fm. Furthermore, the suitability of the Chl fluorescence parameters ΦPSII, ΦNPQ, ΦNO and Fv/Fm to monitor disease progression in one- and two-

year old ginseng plants was evaluated, along with the light intensity at which leaves showed the greatest separation between the parameters derived from measurements in the light-adapted state (ie. ΦPSII, ΦNPQ, ΦNO). This forms the basis of the development of a general protocol for the non-invasive, *in vivo* monitoring of the disease progression of a root pathogen using light-adapted chlorophyll fluorescence parameters in a perennial plant.

3.2. Materials and Methods

3.2.1. *Pythium irregulare* isolates

Isolates of *Pythium irregulare* (Table 3.2) originating from various hosts and locations were obtained from the Canadian Collection of Fungal Cultures (CCFC, Ottawa, Canada). Stock cultures of these isolates were maintained on potato dextrose agar (PDA) medium, via sub-culturing onto fresh PDA and incubation at 22°C in the dark for 3-days, before being stored at 5°C.

3.2.2. Plant material

Ginseng (*Panax quinquefolius*), seeds, obtained from J.C.K Farms Ltd (Brantford, ON, Canada), were stratified in accordance with general commercial grower practice (Oliver et al. 1990) in order to generate one-year old ginseng plants. Briefly, seeds were surface sterilized by soaking in a solution of 20% v/v bleach (6% w/v NaClO) and 0.05% v/v Tween-20 for 10 min. The seeds were then rinsed with 10 x equal volume of sterile ddH_2O and dried for 48 h at 22°C. Seeds were then placed in muslin bags and buried under 15-45 cm of moist acid washed sand and subjected to a cold-warm-cold stratification period (approximately 8 months at 5°C, 5 months at 22°C and 5 months at 5°C) until germination occurred. Germinated seeds were transplanted into 12 cm diameter pots (3 seeds to 1 pot) filled with moist Pro-mix (Premier Tech Horticulture, Canada) soil, so that seeds were approximately 0.5 cm below the surface of the soil. One-year old ginseng seedlings were grown in a controlled environment (Can-Trol Environmental Systems, Markham, ON, Canada), under fluorescent lighting with an approximate intensity of 50-100 μmol photons$\cdot m^{-2}\cdot sec^{-1}$ at 22°C, 50% humidity and a day/night cycle of 16/8 h. Plants were grown as above and watered (from the bottom using a watering tray) as needed. Plants not used for 1-year old experiments were allowed to fully senesce (approximately 6-8 months) after which they were stored at 5°C in the dark. Subsequently, two-year old ginseng plants emerged approximately 5-6 months after initiation of cold storage, at which point seedlings were transferred and grown under a natural light environment from June to August 2014. Fully expanded leaves were used for all experiments.

Table 3.1. Chlorophyll fluorescence parameters used in studies of photosystem II photochemistry. Equations derived by Kramer et al. (2008) from the key fluorescence intensity parameters defined by (Schreiber et al. 1986) and used for parameter calculation by ImagingWin 7.0 software (Heinz-Walz GmbH, Effeltrich, Germany).

Parameter	Definition	Equation
Fv/Fm	Maximum quantum efficiency of PSII photochemistry	$F_v F_m = \frac{F_m - F_o}{F_m}$
NPQ	Non-photochemical quenching	$NPQ = \frac{F_m - F'_m}{F'_m}$
qL	Fraction of open PSII reaction centres (Lake Model)	$qL = \frac{(F'_m - F)}{(F'_m - F'_o)} \cdot \frac{F'_o}{F} = \frac{F'_q}{F'_v} \cdot \frac{F'_o}{F}$
ΦPSII	Quantum yield of PSII photochemistry	$\Phi_{PSII} = \frac{F'_m - F}{F'_m} = \frac{F'_q}{F'_m}$
ΦNO	Quantum yield of non regulated quenching processes	$\Phi_{NO} = \frac{1}{NPQ+1+q_L \cdot \left(\frac{F_m}{F_o}-1\right)} = \frac{1}{\frac{F_m - F'_m}{F'_m}+1+\frac{F'_q}{F'_v}\cdot\frac{F'_o}{F}\cdot\left(\frac{F_m}{F_o}-1\right)}$
ΦNPQ	Quantum yield of regulated non-photochemical quenching	$\Phi_{NPQ} = 1 - \Phi_{PSII} - \frac{1}{NPQ+1+q_L \cdot \left(\frac{F_m}{F_o}-1\right)}$ $= 1 - \frac{F'_q}{F'_m} - \frac{1}{\frac{F_m - F'_m}{F'_m}+1+\frac{F'_q}{F'_v}\cdot\frac{F'_o}{F}\cdot\left(\frac{F_m}{F_o}-1\right)}$
	Sum yields for energy dissipative processes of PS II	$\Phi_{NO} + \Phi_{NPQ} + \Phi_{PSII} = 1$

Table 3.2. Isolates of *Pythium irregulare* used in this study. The four isolates of *Pythium irregulare* listed were obtained from the Canadian Collection of Fungal Cultures at Agriculture and Agri-food Canada. Isolates were selected based on previous work comparing the pathogenicity of various *Pythium* isolates conducted by Ivanov and Bernards (2012).

Genus	Species	Isolate no.	Host species	Location
Pythium	*irregulare*	BR 901	*Cucumis sativus*	Alberta, Canada
Pythium	*irregulare*	BR 486	*Phaseolus vulgaris*	Netherlands
Pythium	*irregulare*	BR 962	Soil	Wairakei, New Zealand
Pythium	*irregulare*	BR 1068	*Panax quinquefolius*	Ontario, Canada

3.2.3. Pathogenicity assay

Ginseng seedlings were inoculated with *Pythium irregulare* strains (Table 3.2) according to established protocol (Reeleder and Brammall 1994) with some modifications (Ivanov and Bernards 2012). Inoculum was prepared by adding an 8 mm diameter plug of 3-day old live culture grown on PDA to 20 mL of sterile V8 broth (Tuite 1969) contained in a 100 mm diameter plastic petri-dish. The V8 cultures were grown in the dark at 22°C for 4 days. The contents of the V8 cultures including the mycelial mats were then removed from the petri-dish and blended at high speed for 1 min with Milli-Q ddH_2O (one culture per 100 mL H_2O) to obtain a homogenous culture suspension. The resulting liquid suspension was then mixed with 590 g sterile Bomix construction sand (Daubois Inc, Saint-Léonard, QC, Canada). Ginseng seedlings were transplanted into 12 cm diameter pots (one plant per pot) that had been sterilized with a 5% v/v (6% w/v NaClO) solution and filled with sand-inoculum approximately 24 hrs earlier. Five one- and two-year old seedlings were inoculated with each isolate. One-year old plants used for light response curve measurements were then grown for 15 days in a controlled environment (Can-Trol Environmental Systems, Markham, ON, Canada) under fluorescent lighting with an approximate intensity of 50-100 μmol photons$\cdot m^{-2}\cdot s^{-1}$ at 22°C, 50% humidity and a day/night cycle of 16/8 h. Two-year old plants used to generate induction curve measurements for infected plants were grown for 15 days under a shaded natural light environment at 22°C during August of 2014. At the end of the experiment, all plants were rated for disease severity on a scale from 1-5 using the established protocol of Ivanov and Bernards (2012).

3.2.4. Chlorophyll fluorescence measurements

A pulse amplitude modulating imaging fluorometer (IMAGING-PAM, Heinz Walz GmbH, Effeltrich, Germany) was used to capture chlorophyll fluorescence images and to estimate the maximum photochemical efficiency of PSII (Fv/Fm), quantum yield of PSII photochemistry (ΦPSII), quantum yield of ΔpH- and/or xanthophyll-dependent non-photochemical quenching (ΦNPQ) and the quantum yield of constitutive (non-regulated) quenching processes (ΦNO). The chlorophyll fluorescence parameters measured were calculated according to Kramer et al. (2004) using the nomenclature of van Kooten and Snel (1990) (Table 3.1). Fluorescence images were captured by a CCD camera (IMAG-K, Allied Vision Technologies) containing a 640 x 480 pixel CCD chip size and a CCTV camera lens

(Cosmicar/Pentax F1.2, f=12 mm). A light-emitting diode (LED) ring array (IMAG-L) consisting of 96 blue LEDs (470 nm) provided the light source for fluorescence excitation and actinic illumination. Basal Chl fluorescence (Fo) was measured after exposure to a standard modulated excitation intensity of 0.5 µmol photons m^{-2} s^{-1} PAR and maximal Chl fluorescence (Fm) was determined after application of a saturating pulse of 2,400 µmol photons m^{-2} s^{-1} PAR. Leaves selected for imaging were labeled so that the same leaf could be measured at each time point. Chlorophyll fluorescence measurements were made at the same five independent areas of interest (AOIs) on marked leaves, on each of five replicate plants, which were then averaged (N = 5). AOIs were selected to ensure full leaf coverage without interference from major veins.

Leaves were dark adapted for at least 10 minutes before determination of basal (Fo) and maximum (Fm) Chl fluorescence. In the presence of actinic illumination current fluorescence yield (F) and maximum light adapted fluorescence yield (F'm) were determined (Table 3.1), which allowed for the calculation of the quantum yield of PSII photochemistry (ΦPSII). All parameters were measured every 3rd day during the 15 day treatment/growth period with initial measurements (Day 0) being conducted on the day of transplantation.

3.2.4.1. Light response curves

The light response of chlorophyll fluorescence quenching parameters at various light intensities was assessed using a pre-programmed sequence of 11 increasing irradiance steps with PAR-values (2, 14, 24, 59, 154, 264, 414, 604, 714, 964, 1104 µmol photons m^{-2} s^{-1}). The illumination time at each step was 240 s and at the end of each illumination step a saturating pulse was applied in order to determine fluorescence parameters. All measurements were made on leaves dark adapted for at least 10 min so as to determine basal (Fo) and maximum (Fm) Chl fluorescence at the start of each measuring sequence.

3.2.4.2. Induction curves

The light response of photosynthetic electron transport at a single light intensity was initiated with the determination of basal (Fo) and maximum (Fm) Chl fluorescence before the onset of actinic irradiance at 414 µmol photons m^{-2} s^{-1}. A pre-programmed sequence was used to initiate actinic illumination after a delay of 40 s, with saturating pulses being applied

every 20 s thereafter for the remainder of the total data acquisition period of 300 s in order to calculate fluorescence parameters.

Fluorescence parameters were recorded and analyzed by ImagingWin 7.0 software (Heinz-Walz GmbH, Effeltrich, Germany) for both light response and induction curves. Digital images were visually displayed using a false colour code ranging from 0.000 (black) to 1.000 (purple) and were used to interpret the results.

3.2.5. Data handling and statistics

The pathogenicity assay for both one- and two-year old ginseng plants, generating light response and induction curves, respectively, was done using five independent replicates (N=5). Pathogenicity scores, which were determined by four independent evaluators, were averaged for the various isolates to yield a final pathogenicity score (N = 4). A paired t-test was used to compare pathogenicity scores between one- and two-year old plants for every isolate studied. A series of two-way repeated measures Analysis of Variance (ANOVA) with GROUP (Control, BR 486, BR 1068) and DAY (Time After Infection: 0, 3, 6, 9, 12, 15) as factors was performed to assess differences between “control” and “infected” plants for each measured parameter (Fv/Fm, ΦPSII, ΦNPQ, ΦNO) in one and two-year old plants. The Newman-Keuls test was used for post hoc comparisons. Analyses of variance were carried out using Statistica 10.0 (Statsoft Inc., Tulsa, OK, USA). For analysis of the correlation between pathogenicity and the values of the chlorophyll fluorescence parameters 15 days after infection a fitted linear regression was run using SigmaPlot 8.0 (Systat Software Inc., San Jose, CA, USA). All values are presented as Mean ± SE. The level of significance was set at $p<0.05$.

3.3. Results

3.3.1. Pathogenicity of *P. irregulare* isolates on American ginseng

Pythium irregulare strains with various life histories were obtained from the Canadian Collection of Fungal Cultures (Table 3.2) and used to conduct a pathogenicity assay to verify the level of virulence these strains show towards American ginseng. The isolates were selected based on criteria established by Ivanov and Bernards (2012) to maximize differences in their genetic diversity, host species and place of origin. One- and two-year old ginseng plants were inoculated with the different strains of *P. irregulare* and the severity of the symptoms was evaluated on a relative scale from 1-5, 15 days after infection. Disease load scores for one-year old plants were significantly higher ($P < 0.05$) than for two-year old plants, for the Control treatment and isolates BR 901 and BR 1068 (Table 3.3), and the pathogenicity of the various isolates largely fell in line with previous observations by Ivanov and Bernards (2012). *Pythium irregulare* isolates BR 1068, and BR 962 had a high pathogenicity score whereas isolates BR 486 and BR 901 had pathogenicity scores close to those of the non-inoculated control treatment, showing that they have low pathogenicity toward ginseng.

3.3.2. Light response curves from *P. quinquefolius* plants infected with *P. irregulare*.

Chlorophyll fluorescence measurements were performed on dark-adapted leaves of one-year old *P. quinquefolius* plants transplanted into soil inoculated with various strains of *P. irregulare*. Initial measurements (Day 0) were conducted on the day of transplantation with subsequent measurements being conducted every 3rd day for 15 days. The differences in the Chl fluorescence parameters monitoring ΦPSII, ΦNPQ and ΦNO were measured for each *P. irregulare* strain (Supporting Information Table S3.1). Representative differences in ΦPSII, ΦNPQ and ΦNO for plants grown in non-inoculated soil (Control), soil inoculated with a strain of *P. irregulare* with low pathogenicity towards ginseng (BR 486) and soil inoculated with a highly pathogenic strain of *P. irregulare* (BR 1068), measured with increasing irradiance levels, are presented (Fig. 3.1). Overall, ΦPSII decreased across all three treatments with increasing irradiance (µmol photons m^{-2} s^{-1} PAR) whereas ΦNPQ increased; however there were differences between treatments in the amount of change,

Table 3.3. **Pathogenicity scores for one- and two-year old ginseng plants were established 15 days after infection with various *Pythium* isolates**. Ginseng plants inoculated with *Pythium* were evaluated for disease severity on a relative scale from 1-5, 15 days after infection based on Ivanov and Bernards (2012). All values are expressed as Mean ± SE, N = 4.

	Isolate no.				
	Control	**BR 901**	**BR 486**	**BR 962**	**BR 1068**
Pathogenicity score					
1 year old plants	1.65 ± 0.06	1.90 ± 0.07	1.10 ± 0.07	3.20 ± 0.28	3.00 ± 0.16
2 year old plants	1.05 ± 0.06*	1.30 ± 0.12*	1.30 ± 0.12	3.25 ± 0.17	2.55 ± 0.26*

* Indicates significant difference between 1 year old and 2 year old plants ($P < 0.05$)

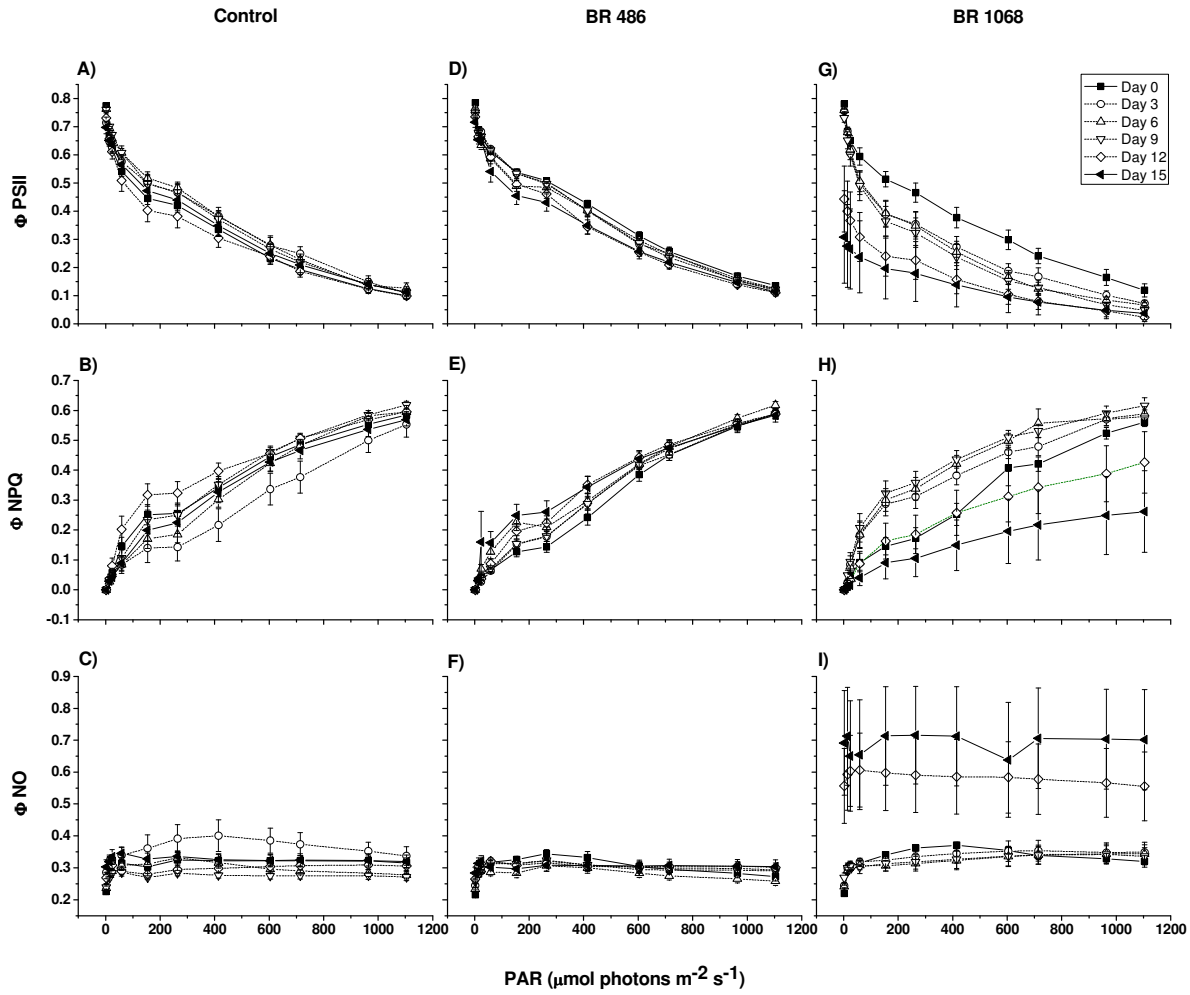

Figure 3.1. Response of one-year old ginseng to infection with *P. irregulare*. Light response curves, were repeatedly measured on the same leaf of one-year old, non-inoculated control (A, B, C) ginseng plants, one-year old ginseng plants inoculated with either a strain of *P. irregulare* with low pathogenicity toward ginseng (BR 486) (D, E, F), or a strain with high pathogenicity (BR 1068) (G, H, I). The chlorophyll fluorescence parameters ΦPSII (A, D, G), ΦNPQ (B, E, H) and ΦNO (C, F, I) were calculated (Table 3.1) from fluorescence values measured every 3 days for 15 days in total for all treatments. All values are expressed as Mean ± SE, N = 5 for ΦPSII, ΦNPQ and ΦNO measurements. On each panel values for Day 0 and Day 15 measurements are shown with filled symbols to highlight the time extremes.

depending on the day of measurement. By contrast, for any given day, ΦNO remained constant across all light exposure levels, albeit with increasing values on subsequent days.

There were no observable differences in the chlorophyll fluorescence parameters ΦNPQ, ΦPSII and ΦNO measured in plants from the control or the low infection (BR 486) group. The values of these parameters did not change over time and adhered to the broad patterns, described above, regarding changes that occur with increasing irradiance. By contrast, plants from the high infection BR 1068 group showed significant differences in ΦPSII, ΦNPQ and ΦNO, depending on the day of measurement.

ΦPSII, which is a measure of the quantum yield of PSII photochemistry, in the high infection group (BR 1068) was lower across the entire irradiance range for every day measured after Day 0. The values of ΦPSII during initial irradiance (2 µmol photons m^{-2} s^{-1} PAR) were approximately 0.75 and clustered together for the light response curves from Day 0 until Day 9 but were lower in both Day 12 (0.45) and Day 15 (0.30) compared to those initial readings. The values of ΦPSII showed the greatest difference between each day when determined at irradiance levels between 59 - 604 µmol photons m^{-2} s^{-1} PAR. At irradiance levels higher or lower than this range the difference between the measurements at different days tended to be lower than that measured within the 59 - 604 µmol photons m^{-2} s^{-1} PAR range.

In the high infection isolates, ΦNPQ, which is a measure of the quantum yield of regulated non-photochemical quenching, was higher across the entire irradiance range from Day 3 to Day 9 than it was for the initial readings at Day 0. However, Day 12 values were similar to the initial values of ΦNPQ at Day 0 when determined at irradiances between 2 - 414 µmol photons m^{-2} s^{-1} PAR and were lower than Day 0 values when determined at irradiances between 604 - 1104 µmol photons m^{-2} s^{-1} PAR. Values of ΦNPQ at Day 15 were lower than the initial readings at Day 0 for every irradiance step in the light response curves. The values of ΦNPQ showed the greatest difference between each day when determined at irradiances between 414 - 1104 µmol photons m^{-2} s^{-1} PAR, with the highest difference observed at the highest irradiance measured 1104 µmol photons m^{-2} s^{-1} PAR. At irradiance levels lower than 414 µmol photons m^{-2} s^{-1} PAR, the difference between the measurements tended to be lower than within the 414 - 1104 µmol photons m^{-2} s^{-1} PAR range.

Most notably, ΦNO, which measures the quantum yield of constitutive non-regulated quenching processes in PSII, was higher in the high infection group, across every irradiance

level measured in the light response curves, for Day 12 and Day 15 compared to initial readings at Day 0, with values for Day 15 being higher than Day 12. These differences in ΦNO values were obvious even during initial irradiance (2 µmol photons m^{-2} s^{-1} PAR) measurements, where values remained approximately 0.25 and clustered together for the light response curves from Day 0 until Day 9 but were higher in both Day 12 (0.55) and Day 15 (0.7). The values for ΦNO between Day 0 and Day 9 remained steady at approx. 0.3 across the entire irradiance range, whereas ΦNO values for Day 12 and Day 15 light response curves were approx. 0.6 and 0.7, respectively, for all irradiance steps measured.

3.3.3. Induction kinetics of chlorophyll fluorescence parameters from *P. quinquefolius* plants infected with varying strains of the root pathogen *P. irregulare*.

The fluorescence quenching parameters (ΦPSII, ΦNPQ and ΦNO) at 414 µmol photons m^{-2} s^{-1} PAR were determined for dark-adapted leaves of two-year old *P. quinquefolius* plants transplanted into soil inoculated with various strains of *P. irregulare* (Supporting Information Table S3.2). Initial measurements (Day 0) were conducted on the day of transplantation with subsequent measurements every 3 days for 15 days in total. Differences in ΦPSII, ΦNPQ and ΦNO, determined for representative treatments of plants transplanted into non-inoculated soil (Control), soil inoculated with *P. irregulare* BR 486, a strain mildly pathogenic to ginseng (Low Pathogenicity) and soil inoculated with *P. irregulare* BR 1068, a strain highly pathogenic toward ginseng (High Pathogenicity), are presented in Fig. 3.2.

Values of ΦPSII, ΦNPQ and ΦNO reached a steady state maximum approx. 100 s after the application of the actinic light pulse in all treatments and days measured. There were no measurable differences between ΦPSII, ΦNPQ and ΦNO measured in plants from the control and low pathogenicity (BR 486) treatments irrespective of the day of measurement. After 100 s of actinic illumination, ΦPSII reached steady state values of approximately 0.2 in both treatments, with values for ΦNPQ and ΦNO reaching approximately 0.5 and 0.3, respectively. Plants from the high infection BR 1068 group, however, showed significant differences in ΦPSII, ΦNPQ and ΦNO, depending on the day of measurement, in comparison to the low infection and control groups.

ΦPSII steady state values in the BR 1068 high pathogenicity treatment declined every day from initial Day 0 measurements (0.2) to approx. 0.1 by Day 15. The values of ΦNPQ

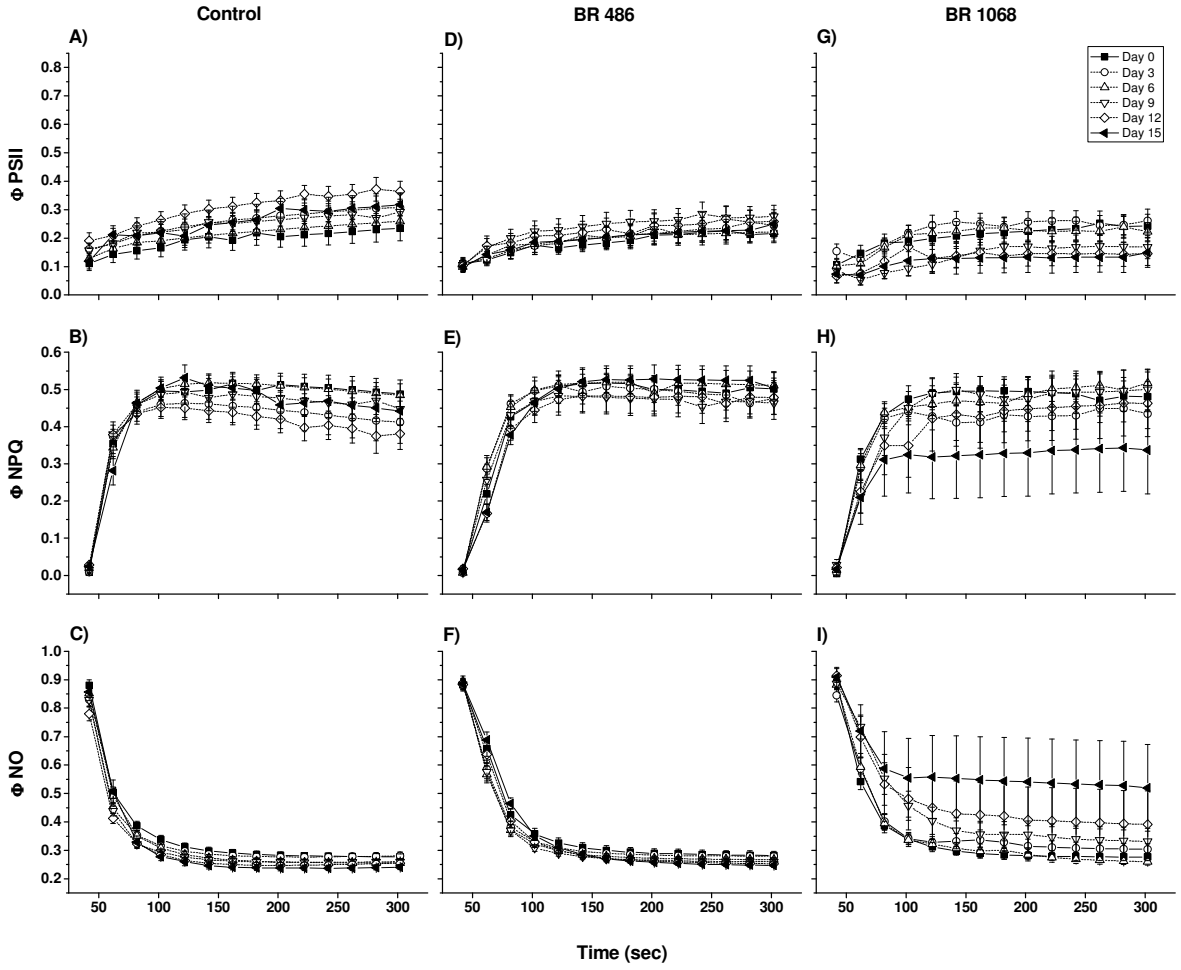

Figure 3.2. Response of two-year old ginseng to infection with *P. irregulare*. Induction curves were measured in leaves of two-year old, non-inoculated control (A, B, C) ginseng plants, and two-year old ginseng plants inoculated with either a strain of *P. irregulare* with low pathogenicity toward ginseng (BR 486) (D, E, F) or a strain with high pathogenicity (BR 1068) (G, H, I). The chlorophyll fluorescence parameters ΦPSII (A, D, G), ΦNPQ (B, E, H) and ΦNO (C, F, I) were calculated (Table 3.1) from measurements made at a single light intensity (414 µmol photons m^{-2} s^{-1} PAR) for all treatments. Measurements were taken every 3 days for 15 days in total. Data is shown from the start of actinic illumination 40s after saturating light pulse. All values are expressed as Mean ± SE, N = 5 for ΦPSII, ΦNPQ and ΦNO measurements. On each panel values for Day 0 and Day 15 measurements are shown with filled symbols to highlight the time extremes.

also declined in every day sampled with initial steady-state Day 0 values of approximately 0.5 declining to approximately 0.3 by Day 15. The decline in ΦNPQ, however, was not gradual with the biggest change occurring between Day 12 and Day 15. By contrast, ΦNO steady-state values in the high pathogenicity BR 1068 treatment increased with each successive day post infection. The value of ΦNO at Day 0 was 0.3 and increased to 0.55 by Day 15. The increases in ΦNO were not gradual, with the biggest change occurring between Day 12 and Day 15.

It is important to note that the steady-state values of ΦNO had the lowest variation between days measured in the control and low pathogenicity treatments compared to the ΦPSII and ΦNPQ parameters. By contrast, in the high pathogenicity treatment the ΦNO parameter showed the highest variation between the days measured compared to the ΦPSII and ΦNPQ parameters.

3.3.4. Change in chlorophyll fluorescence parameters over time in ginseng plants infected with different strains of *P. irregulare*.

Since the measurement of the Chl fluorescence parameters ΦPSII, ΦNPQ and ΦNO was optimal at irradiance levels of 414 µmol photons m^{-2} s^{-1} PAR and above (Fig. 3.1), as noted earlier, this level of irradiance was used for monitoring changes in these parameters over time, without having to conduct full scale light response curves. However, these data can also be extracted from light response curves as shown for one-year old plants (Fig. 3.3B, C, D). The equivalent ΦPSII, ΦNPQ and ΦNO data was generated from the 414 µmol photons m^{-2} s^{-1} PAR induction curves for the two-year old plants, using the final (300 s) data point from each curve (Fig. 3.4B, C, D). In addition, the maximum quantum efficiency of PSII (Fv/Fm; Table 3.1) was also measured in one- and two-year old ginseng plants every 3 days until 15 days after infection with various *Pythium* isolates (Fig. 3.3A and Fig. 3.4A).

In one-year old plants (Fig. 3.3) there were no significant differences in the values of Fv/Fm, ΦPSII, ΦNPQ or ΦNO between the Control and low pathogenicity (BR 486) treatments irrespective of the day of measurement. The values of Fv/Fm and ΦPSII in the Control and low pathogenicity treatments remained steady at approximately 0.75 and 0.4, respectively, for the duration of the 15 day time period, while the values of both ΦNPQ and ΦNO remained at approximately 0.3 throughout. However, values of Fv/Fm, ΦPSII, ΦNPQ or ΦNO for the high pathogenicity (BR 1068) treatment showed significant differences from

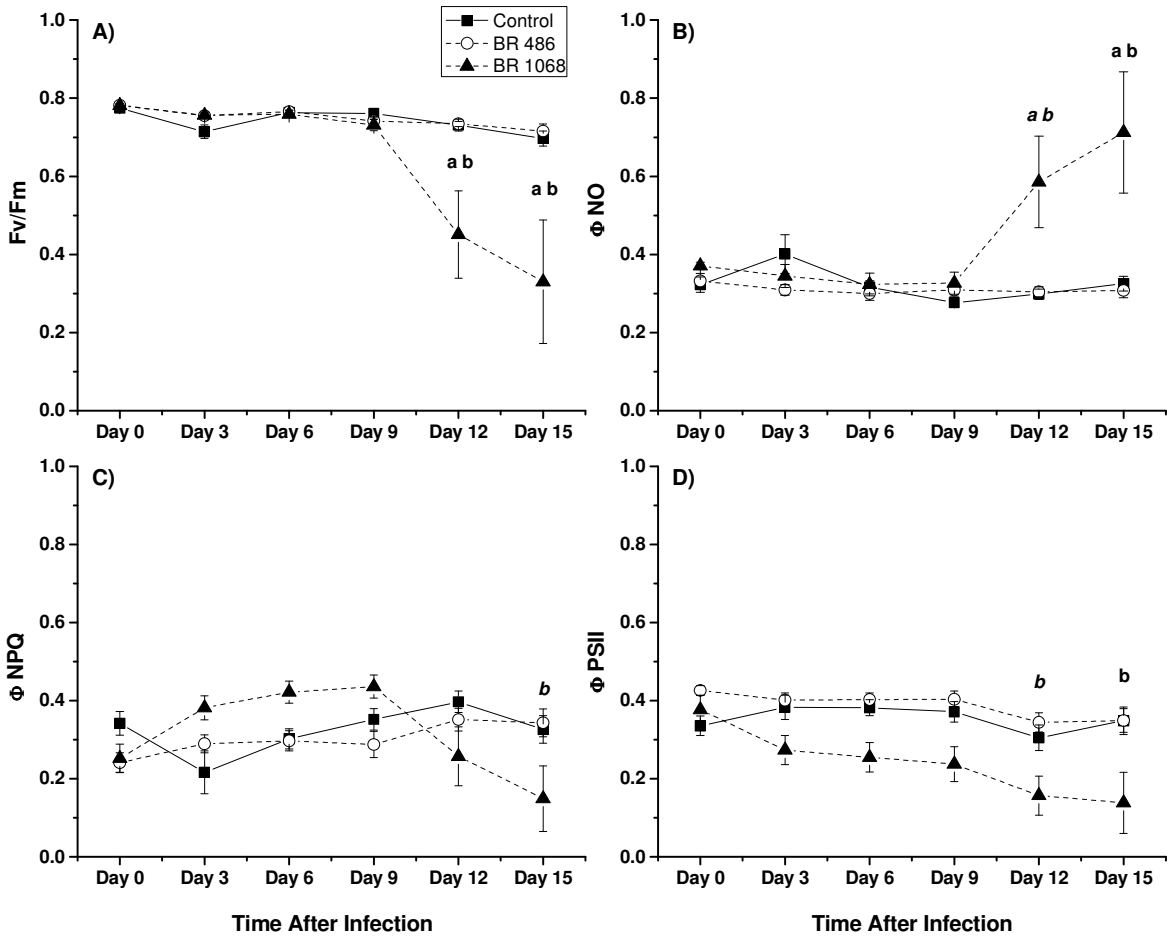

Figure 3.3. Time course of one-year old ginseng response to infection with *P. irregulare.* Changes in the chlorophyll fluorescence parameters Fv/Fm (A), ΦNO (B), ΦNPQ (C) and ΦPSII (D), were measured over time at an actinic irradiance of 414 µmol photons m^{-2} s^{-1} PAR for one-year old ginseng plants inoculated with a strain of *P. irregulare* with low pathogenicity toward ginseng (BR 486), a strain with high pathogenicity (BR 1068) as well as a non-inoculated control. Measurements were taken every 3 days for 15 days total. Fv/Fm was determined for dark-adapted leaves after initial exposure of plants to a saturating light pulse. All values are expressed as Mean ± SE, N = 5 for Fv/Fm, ΦPSII, ΦNPQ and ΦNO measurements. Statistical differences ($P < 0.05$) between treatments at each day represented by: (A) BR 1068 and Control; (B) BR 1068 and BR 486; (C) Control and BR 486. **italicized letter represents trend towards significant difference ($P < 0.1$).*

the control and low pathogenicity groups, to varying degrees, depending on the day of measurement. For example, while values for ΦPSII in the high pathogenicity (BR 1068) treatment were not significantly different from the Control treatment at Day 0, there was an observable (though also not statistically significant) decline of ΦPSII from Day 3 until Day 15, relative to the values of the Control treatment and the initial value at Day 0. At Day 12 and Day 15, however, ΦPSII values for the high pathogenicity (BR 1068) treatment were significantly lower than the low pathogenicity (BR 486) treatment. Similarly, Fv/Fm, ΦNPQ and ΦNO values for the high pathogenicity (BR 1068) treatment were not significantly different from the Control treatment at Day 0. However, ΦNPQ values increased from Day 3 to Day 9 relative to the Control followed by a continuous decline from Day 12 to Day 15 without reaching statistical significance. The same tendency was seen in the ΦNPQ values between the high (BR 1068) and low (BR 486) pathogenicity treatments with ΦNPQ in the high pathogenicity treatment showing a trend to be significantly lower ($0.05 < P < 0.1$) at Day 15. Both Fv/Fm and ΦNO values in the high pathogenicity (BR 1068) treatment meanwhile, were not significantly different from the Control and low pathogenicity (BR 486) treatments from Day 0 until Day 9. After Day 9 Fv/Fm and ΦNO parameters showed opposite behaviour with a sharp and significant increase of ΦNO by Day 12 ($P < 0.1$) and Day 15 ($P < 0.05$) and a significant decline of Fv/Fm values in Day 12 ($P < 0.05$) and Day 15 ($P < 0.05$) relative to the Control and low pathogenicity treatments.

In two-year year old plants there were no significant differences in the values of Fv/Fm, ΦPSII, ΦNPQ and ΦNO between the Control and low pathogenicity (BR 486) treatments at any of the days measured (Fig. 3.4). The values of Fv/Fm and ΦPSII remained steady at approximately 0.75 and 0.3, respectively, whereas the values of ΦNPQ and ΦNO remained at approximately 0.45 and 0.25, respectively, for all the days measured. By contrast, two-year old plants treated with the high pathogenicity *P. irregulare* strain (BR 1068) showed a significant difference from the control and low pathogenicity (BR 486) treated plants, depending on the day of measurement and which parameter was evaluated. For example, ΦPSII values for two-year old plants in the high pathogenicity (BR 1068) treatment were not significantly different from the control and the low pathogenicity treatments until they significantly decreased at Day 9 and remained lower at Day 12 and Day 15 compared to the control ($P < 0.05$ for all three comparisons). In the same time, relative to the low pathogenicity treatment, this decrease in ΦPSII of the high pathogenicity treatment

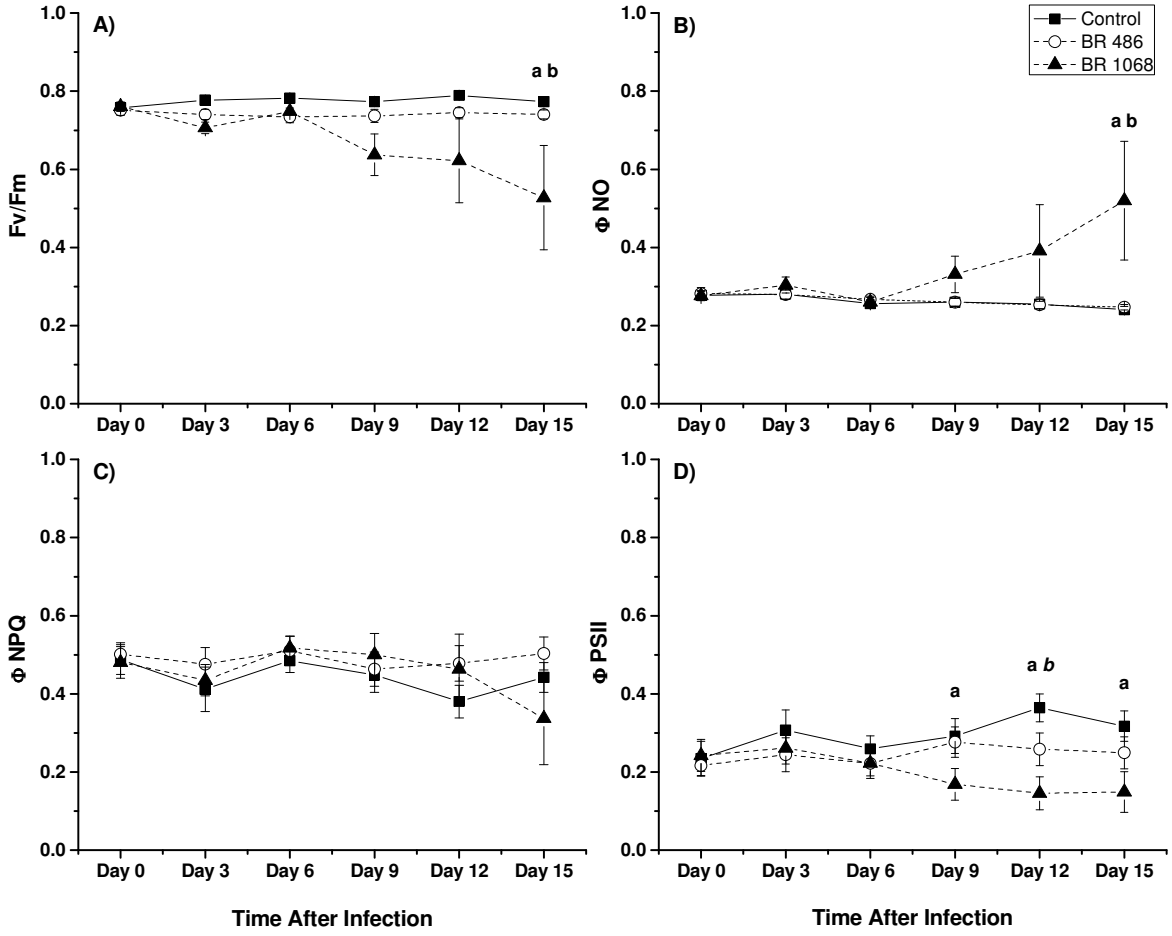

Figure 3.4. Time course of two-year old ginseng response to infection with *P. irregulare.* **C**hanges in the chlorophyll fluorescence parameters Fv/Fm (A), ΦNO (B), ΦNPQ (C) and ΦPSII (D) were measured over time at an actinic irradiance of 414 µmol photons m^{-2} s^{-1} PAR for two-year old ginseng plants inoculated with a strain of *P. irregulare* with low pathogenicity toward ginseng (BR 486), a strain with high pathogenicity (BR 1068) as well as a non-inoculated control. Measurements were taken every 3 days for 15 days total. Fv/Fm was determined for dark-adapted leaves after initial exposure of plants to a saturating light pulse. All values are expressed as Mean ± SE, N = 5 for Fv/Fm, ΦPSII, ΦNPQ and ΦNO measurements. Statistical differences ($P < 0.05$) between treatments at each day represented by: (A) BR 1068 and Control; (B) BR 1068 and BR 486; (C) Control and BR 486. **italicized letter represents trend towards significant difference ($P < 0.1$).*

was only a trend at Day 12 ($P < 0.1$) and did not reach statistical significance at Day 9 and day 15. ΦNPQ values in the high pathogenicity (BR 1068) treatment did not show a significant difference relative to the Control or low pathogenicity (BR 486) treatments on any of the days measured; however, they were slightly higher relative to the Control treatment until Day 15, when they declined below the levels of the Control treatment. Both Fv/Fm and ΦNO values in the high pathogenicity treatment, were not different from the Control or low pathogenicity treatments from Day 0 until Day 6, after which there was a gradual increase of ΦNO that became statistically significant at Day 15 from both groups ($P < 0.05$), Fv/Fm values began to gradually decrease from Day 6 and became significantly lower than the Control or low pathogenicity treatments at Day 15 ($P < 0.05$).

3.3.5. Relationship between various chlorophyll fluorescence imaging parameters and the pathogenicity of *P. irregulare* towards American ginseng.

Increases in the disease load in one- and two-year old ginseng plants infected with different *Pythium* isolates correlated with changes in the values of the chlorophyll fluorescence parameters 15 days after infection. That is, Fv/Fm, ΦPSII and ΦNPQ values decreased, whereas ΦNO values increased, with increased disease load in both one- and two-year old plants (Fig. 3.5 and Fig. 3.6). More specifically, Fv/Fm values decreased by -0.178 ($R^2 = 0.82$; $P = 0.02$) and -0.224 ($R^2 = 0.95$; $P = 0.003$) for every unit increase in disease load for one- and two-year old plants, respectively, while, ΦNPQ values decreased by -0.0815 ($R^2 = 0.51$; $P = 0.11$) and -0.116 ($R^2 = 0.91$; $P = 0.008$) and ΦPSII values by -0.098 ($R^2 = 0.81$; $P = 0.02$) and -0.106 ($R^2 = 0.93$; $P = 0.006$). This showed that Fv/Fm values declined by about double those of ΦNPQ and ΦPSII, for every unit increase in disease load. On the other hand, ΦNO values increased by 0.195 ($R^2 = 0.80$; $P = 0.03$) and 0.232 ($R^2 = 0.99$; $P = 0.0001$) per unit disease load for one- and two-year old plants respectively.

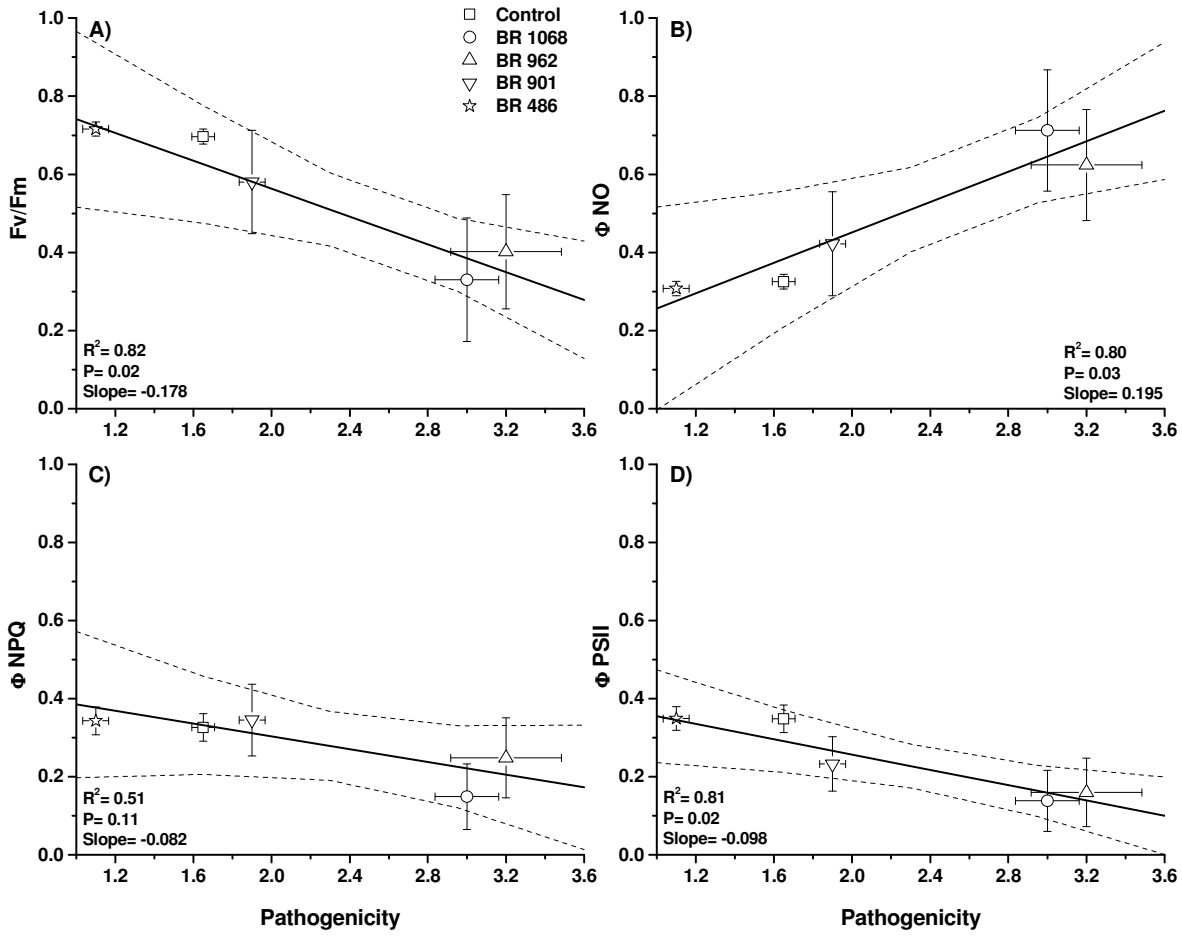

Figure 3.5. Relationship between pathogenicity and fluorescence parameters in one-year old ginseng plants. Pathogenicity scores for one-year old ginseng plants inoculated with various *Pythium* isolates (Table 3.2) are plotted against Fv/Fm (A), ΦNO (B), ΦNPQ (C), and ΦPSII (D) measured for the same plants. All measurements were taken 15 days after inoculation. Dashed lines represent upper 95% confidence limits. All values are expressed as Mean ± SE, N = 5 for Fv/Fm, ΦPSII, ΦNPQ and ΦNO measurements, N = 4 for pathogenicity scores. Fv/Fm (R^2 = 0.82; P = 0.02); ΦNO (R^2 = 0.80; P = 0.03); ΦNPQ (R^2 = 0.51; P = 0.11); ΦPSII (R^2 = 0.81; P = 0.02).

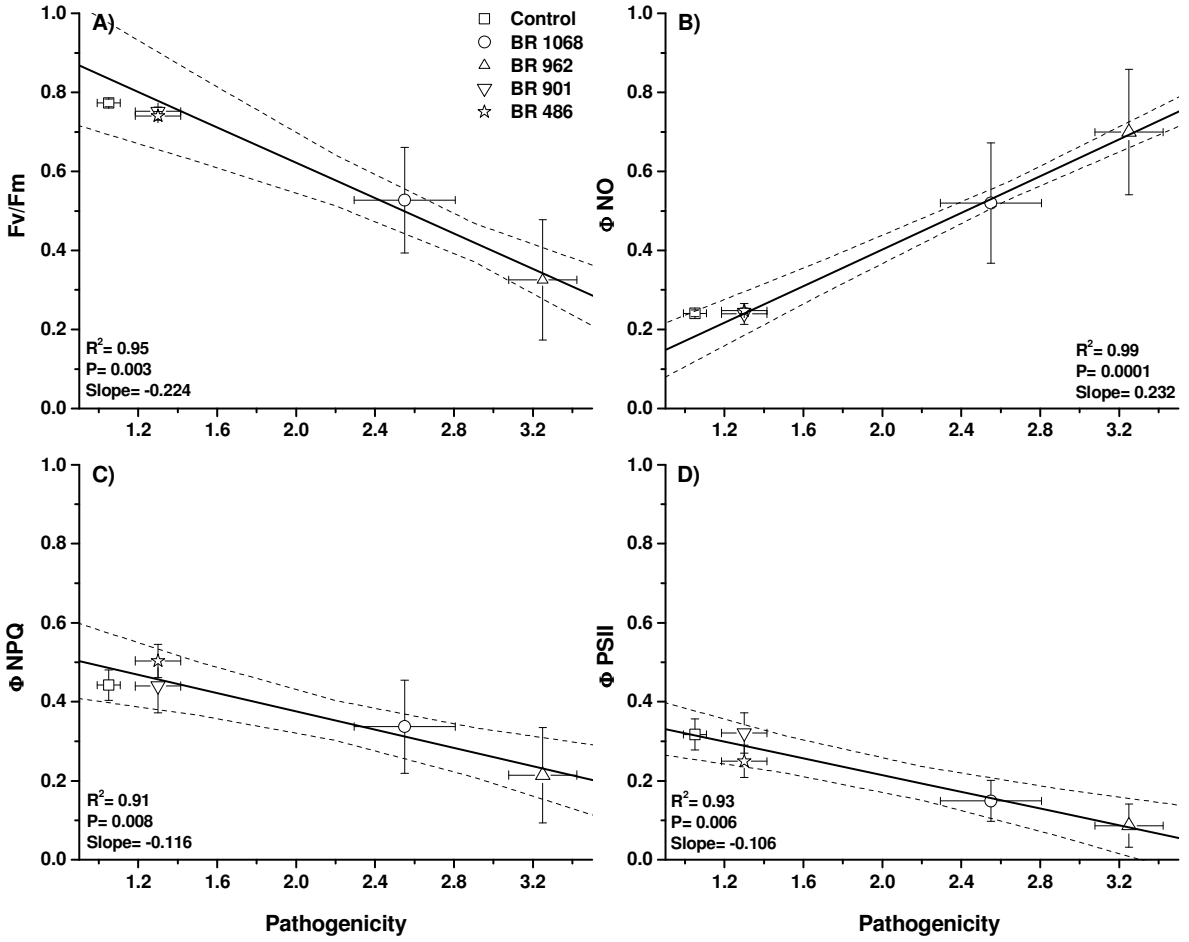

Figure 3.6. Relationship between pathogenicity and fluorescence parameters in two-year old ginseng plants. Pathogenicity scores for two-year old ginseng plants inoculated with various *Pythium* isolates (Table 3.2) are plotted against Fv/Fm (A), ΦNO (B), ΦNPQ (C), and ΦPSII (D) measured for the same plants. All measurements were taken 15 days after inoculation. Dashed lines represent upper 95% confidence limits. All values are expressed as Mean ± SE, N = 5 for Fv/Fm, ΦPSII, ΦNPQ and ΦNO measurements, N = 4 for pathogenicity scores. Fv/Fm (R^2 = 0.95; P = 0.003); ΦNO (R^2 = 0.99; P = 0.0001); ΦNPQ (R^2 = 0.91; P = 0.008); ΦPSII (R^2 = 0.93; P = 0.006).

3.4. Discussion

The accurate measurement of Fv/Fm requires dark adaptation of plant leaves, which makes it difficult to apply this parameter to monitoring plant health on a field, greenhouse or even laboratory scale (Baker 2008; Mutka and Bart 2015). In contrast the chlorophyll fluorescence parameters ΦPSII, ΦNPQ and ΦNO, measured using the saturation pulse method, can provide information during steady state illumination, or even under normal daylight conditions (Klughammer and Schreiber 2008). In this study, the pathogenicity of several *P. irregulare* strains was assessed by using the light-adapted parameters (ΦPSII, ΦNPQ and ΦNO) and their performance was compared to the established method of tracking pathogenicity in ginseng using Fv/Fm measurements in dark adapted plants (Ivanov and Bernards 2012). The optimum light conditions for reliable and reproducible measurements of ΦPSII, ΦNPQ and ΦNO were also established. This is important, because while there is extensive literature on the use of the parameters ΦPSII and ΦNPQ to monitor plant-pathogen interactions (Scholes and Rolfe 1996; Berger et al. 2007; Guidi et al. 2007; Prokopová et al. 2010), only one study has used the parameter ΦNO for this purpose (Burling et al. 2010). Furthermore, slow induction kinetic parameters have never been applied to study the effects of root pathogens on any crops. This is surprising, since it is difficult to assess root pathogen-associated damage without inspecting the roots themselves, which is a destructive process.

The parameters we evaluated are complimentary and describe the partitioning of absorbed excitation energy in photosystem II. ΦPSII corresponds to the fraction of energy that is photochemically converted in PSII, while ΦNPQ corresponds to the fraction of energy dissipated via regulated photoprotective mechanisms and ΦNO represents the fraction of energy that is dissipated as heat and fluorescence, mainly because of closed PSII reaction centres at saturating light intensities (Genty et. al 1996; Kramer et al. 2004; Klughammer and Schreiber 2008). This gives information on the capacity of a plant to deal with stress and means that the sum of the quantum yields ΦPSII, ΦNPQ and ΦNO is always unity (1) (Demmig-Adams et al. 1996; Kramer et al. 2004) (Table 3.1).

In our experiment, strains with different life histories were used (Table 3.2), because previous studies with *P. irregulare*, showed that different isolates are better at infecting certain hosts more than others, with most showing higher virulence towards their original host (Harvey et al. 2001; Bernards and Ivanov 2012). This study confirmed the earlier observation with isolates BR 1068, previously isolated from American ginseng and BR 962,

a non-specific isolate gathered from soil, showing high pathogenicity and isolates BR 901 and BR 486, isolated from cucumber and bean, respectively, showing low pathogenicity towards ginseng. Consistent with our earlier observations (Ivanov and Bernards 2012), the present study also demonstrated that one-year old plants are generally more susceptible to *P. irregulare* and other abiotic and biotic stresses (Control, BR 901 and BR 1068) compared to two-year old plants (Table 3.3). This could be due to the higher concentration of secondary metabolites in older plants or the presence of a more hardened root structure, which could provide a better, pre-formed barrier to pathogen infection and a greater ability to cope with replant stress.

Light response curves generated from one-year old ginseng plants (Fig. 3.1) showed that increasing irradiance had an effect on the energy partitioning of PSII irrespective of the pathogenicity of the strain used. At low irradiance ΦPSII was high, showing that the plants were converting a large portion of the absorbed light energy into chemical energy. As irradiance increased values of ΦNPQ increased and values of ΦPSII decreased, showing that excess incident light that could not undergo photochemical conversion was dissipated through regulated photoprotective mechanisms (ie. xanthophyll cycle.). ΦNO meanwhile remained relatively constant across all light intensities, showing that in this instance light intensity does not affect the yield of constitutive non-regulated quenching processes.

The infection of ginseng plants with *P. irregulare* isolate BR 1068, a strain with high pathogenicity towards ginseng, showed an impact on the energy partitioning of PSII as infection progressed over time (Fig. 3.1). The greatest differences in the ΦPSII parameter could be seen at light intensities below 604 µmol photons m^{-2} s^{-1} PAR, especially at longer infection times, whereas the greatest differences in the ΦNPQ parameter were observed at irradiances above 414 µmol photons m^{-2} s^{-1} PAR. Therefore, when repeating this experiment with two-year old ginseng plants, infection was monitored over time using slow induction curves at a single light intensity of 414 µmol photons m^{-2} s^{-1} PAR (Fig. 3.2). This allowed for more precise resolution of the differences between ΦPSII and ΦNPQ in infected ginseng plants. In addition, using slow induction curves also allowed for a shorter measuring period of 4 min as opposed to 40 min needed for the light intensity experimental protocol (including a dark adaptation period). The parameter ΦNO did not change with increased irradiance, but did increase with the infection of ginseng (Fig. 3.1 and Fig. 3.2). Therefore it appears that

this parameter is best suited to monitor changes in chlorophyll fluorescence of infected plants at any irradiance level.

The tracking of fluorescence parameters at a single irradiance over a 15 day period after our experiment was initiated, revealed some effects that virulent strains of *P. irregulare* had on the functional performance of the photosynthetic apparatus of ginseng plants as a result of infection (Fig. 3.3 and Fig. 3.4). For example, in one-year old plants there was an immediate decrease in ΦPSII in plants exposed to the pathogenic BR 1068 strain. This showed that infection impacts the downstream photosynthetic apparatus, or carbon metabolism, in the plants and reduces the fraction of light energy photochemically converted by PSII compared with Control plants or those infected with the low pathogenicity strains. As a result, excess absorbed light energy was dissipated through regulated non-photochemical quenching processes for the first 9 days after the start of the experiment with one year-old plants, as evident by increased values of ΦNPQ for those 9 days. However, after 12 days pathogen damage appears to limit the effectiveness of non-photochemical processes to dissipate excess absorbed energy causing host plants to resort to alternative non-regulated pathways of energy quenching. This was evident in decreases in both ΦPSII and ΦNPQ after 12 and 15 days and a concomitant rise in ΦNO on both of these days compared to the two control groups. Therefore, it seems that as infection progressed, pathogen damage led to a decreased ability of the plant to use light energy for photochemistry, with the excess absorbed light energy being dissipated through non-regulated quenching processes (as heat or fluorescence). Furthermore, as a result of infection, these same processes were observed in two-year old plants (Fig. 3.4), however, changes in the fluorescence parameters were delayed when compared to one-year-old plants. This was most likely caused by the greater resistance of two-year old plants to infection by *P. irregulare*.

In our experiments, we also observed that the increase in ΦNO in both one- and two year old plants infected with the pathogenic strain of *P. irregulare,* mirrored the equivalent decline in the values of Fv/Fm measured for the same plants (Fig. 3.3 and Fig. 3.4). This means that measuring ΦNO could serve as a useful equivalent to measuring Fv/Fm when monitoring various plant stresses, without the need for dark adaptation. Importantly, while we did in fact dark adapt leaves for all fluorescence measurements, this was only necessary because we wanted to measure Fv/Fm for comparison; it is not *required* in order to measure ΦPSII, ΦNPQ or ΦNO.

The suitability of ΦNO to sensitively estimate disease progression was confirmed when the relative pathogenicity scores of the different *P. irregulare* isolates studied in one- and two-year old ginseng plants were compared to the values of the slow induction parameters ΦPSII, ΦNPQ and ΦNO as well as to the value of Fv/Fm 15 days after infection (Fig. 3.5 and Fig. 3.6). In this case we saw that the magnitude of increase in the values of ΦNO per unit disease score was about the same as the corresponding decline in the values of Fv/Fm (i.e., similar slopes with opposite sign) when correlated to increasing disease load. Moreover, ΦNO measured in the light-adapted state was a more sensitive parameter for distinguishing increased disease load of *Pythium* in ginseng plants, than either ΦNPQ or ΦPSII.

Overall, this study provides the basis for the development of a general protocol for the non-invasive, *in vivo* monitoring of the disease progression of a root pathogen using Chl fluorescence parameters in a perennial plant (Fig. 3.7). Briefly, after identifying a leaf from the plant of interest, and identifying 5 areas of interest (AOI's) in a set pattern along leaf surface, light response curves are generated to select the appropriate light intensity for the optimal response of the slow induction Chl fluorescence parameters. Values from induction curves measured at a single, optimal light intensity, post treatment, are then plotted for each day of study to compare changes in the values of the chlorophyll fluorescence parameters monitored.

This protocol could be adapted to a wide range of root pathogens and host plants, because many show similar symptoms and have infection strategies analogous to those of *P. irregulare*. These include true fungi, such as pathogens from the genus *Rhizoctonia* and *Cylindrocarpon*, as well as oomycetes from the family *Pythiaceae* of which pathogens from the genus *Phytophthora* or *Pythium* are the most well known (Reeleder and Brammall 1994). All of these pathogens are known to cause root-rot and damping-off in a wide range of plant species and in field conditions can often function in unison (Hendrix and Campbell 1973, Reeleder and Brammall 1994, Mazzola 1998). Similar to true fungi, infection of plant hosts by oomycetes is facilitated by germ tubes arising from oospores, sporangia, and zoospore cysts or is directly initiated from hyphae (Martin and Loper 1999). Appressoria, which comprise different types of adhesion and penetration structures that form at the apex of germtubes and infectious hyphae, are essential to gaining access to the host plant and utilize a

Figure 3.7. Schematic of general protocol for the non-invasive, *in vivo* monitoring of the disease progression of a root pathogen using chlorophyll fluorescence parameters:

Step (1) - Identify leaf from plant of interest to monitor on a consistent basis for the length of the time-course. The images shows representative 2-year old American ginseng plants in non-inoculated (Control) treatment and (Disease) treatment inoculated with the pathogenic BR 962 strain of *P. irregulare*, after 15 Days.

Step (2) - Define 5 areas of interest (AOI's) in a set pattern along leaf surface, so that approximately the same areas of the leaf are monitored using CFI throughout the course of study, so that all parameters can be compared between days studied. The image shows the Fv/Fm false colour representations of the same treatments shown in Step 1.

Step (3) - Generate light response curves to monitor at what light intensity the response of the slow induction chlorophyll fluorescence parameters monitored is greatest as a result of biotic stress. Figure shown, is representative of ΦNO measured in the (Disease) treatment, every 3 days for 15 days after infection in 2-year old ginseng plants.

Step (4) - Generate induction curves to monitor chlorophyll fluorescence parameters at a single light intensity. This can be done once optimal light intensity to do so has been determined using light response curves. Allows for quick monitoring of the same parameters, time for measurement is reduced from 40 min to 4 min. Figure shown, is representative of ΦNO measured in the (Disease) treatment, every 3 days for 15 days after infection in 2-year old ginseng plants.

Step (5) - Use last value generated from induction curves as steady state value of the chlorophyll fluorescence parameter monitored. Values can be plotted for each day of study to compare changes in the values of the chlorophyll fluorescence parameters monitored. Figure shown, shows values of ΦNO measured in the (Disease) treatment, every 3 days for 15 days after infection in 2-year old ginseng plants compared to values of ΦNO in non-inoculated (Control) treatment.

* Values in all Figures shown are Mean ± SE; N=5.

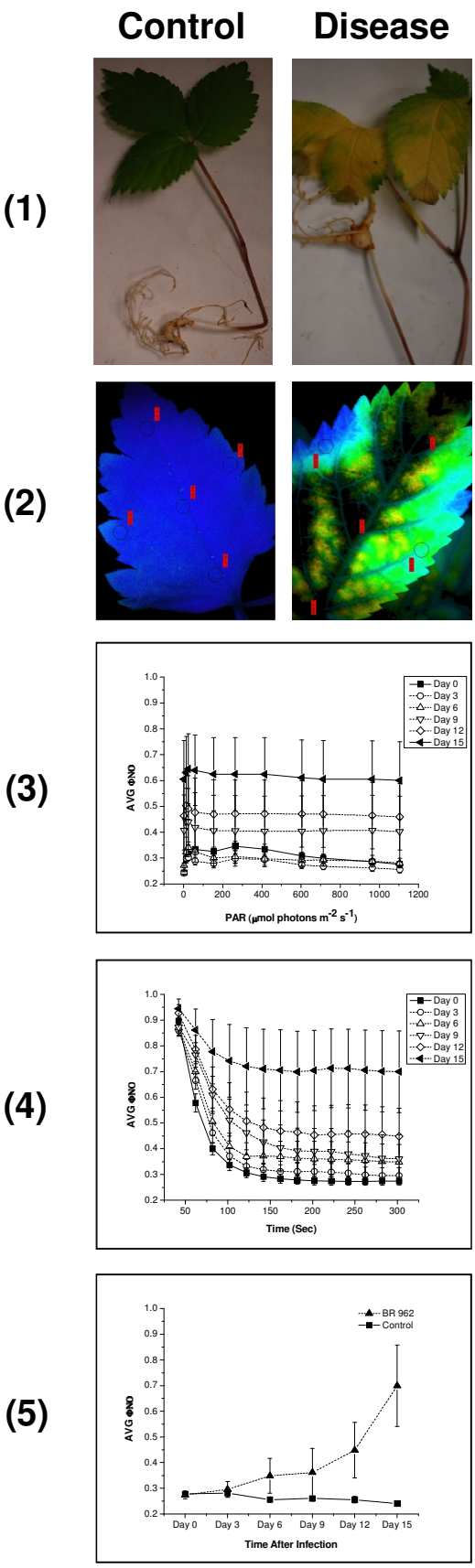
Control
Disease
(1)
(2)
(3)
(4)
(5)
Day 0
Day 3
Day 6
Day 9
Day 12
Day 15
AVG ΦNO
PAR (µmol photons m-2 s-1)
Time (Sec)
BR 962
Control
Time After Infection

combination of enzymatic degradation of the epidermal cell wall and mechanical pressure, to do so (Emmett and Parbery 1975).

After necrotrophic root pathogens, like those listed above, enter the root, enzymatic degradation destroys root host cells. These pathogens target young or succulent tissue and destroy feeder roots in older plants and also cause damping-off (stem wilt), which results from hyphal growth reaching the xylem and phloem and migrating up through the plant (Hendrix and Campbell 1973, Halleen et al. 2007). As a result of damping-off and damage to the feeder roots of the plant, it has been suggested that water transport through infected plants can be severely disrupted (Ivanov and Bernards 2012). Consequently the physiological effects of *P. irregulare* infection can mimic water stress, at least at the outset of the infection cycle. Indeed, the response of ginseng leaves to *P. irregulare* infection measured by the slow induction chlorophyll fluorescence parameters ΦPSII, ΦNPQ and ΦNO is similar, if not identical to the effects of water stress on rose leaves monitored using those same parameters (Calatayud et al. 2006). Initial decreases in ΦPSII in infected leaves, indicating a down regulation of linear photosynthetic electron transport, could be due to stomatal closure caused by water stress (Grieu et al. 1995). This could have resulted in the initial small increase in ΦNPQ, which would have been necessary for dissipation of the excess light energy that could not be utilized by electron transport (Horton et al. 1996). Finally when the damage from water stress was too high, both electron transport and regulated quenching processes in PSII were inhibited, which led to decreases in ΦPSII and ΦNPQ and a sharp increase ΦNO indicating a rise in the amount of energy dissipated through non-regulated energy quenching in PSII (Calatayud et al. 2006).

To our knowledge this study is the first to use slow induction Chl fluorescence parameters to monitor the infection progress of a root pathogen on a perennial plant. A similar approach, monitoring esca disease in grape vine (*Vitis vinifera*) utilizing fast fluorescence transients to monitor plant vitality, has been reported (Christen et al. 2007); however, the protocol reported therein required the dark adaptation of the plants. Our demonstration of the use of Chl fluorescence parameters, based on steady state, light adapted conditions, opens the possibility of larger scale (i.e, field level) monitoring of plant health as an aid in planning intervention strategies in a targeted manner.

3.5. Conclusion

Our results show that the slow induction chlorophyll fluorescence parameter ΦNO can be as sensitive in monitoring biotic stress as the measurement of Fv/Fm. However, the absence of the need to dark adapt plants to measure ΦNO, as well as the ability to monitor this parameter at a wide range of light intensities, including under natural light, means that it has the potential for wide ranging applications in monitoring plant health at the laboratory as well as the field scale. In the future, monitoring ΦNO could be used as an alternative non-invasive, fast-screening method for the *in vivo* precise and pre-symptomatic detection of diseases, as well as a way to monitor plant health without dark-adaptation in breeding programs and/or during environmental monitoring. The monitoring of this parameter under field conditions would require the modification of existing protocols to enable high throughput measurement and remote sensing. However, the work of Genty et al. (1996) and Klughammer and Schreiber (2008) on simplifying the mathematical algorithms used in the calculation of ΦNO could have major implications for the potential wide scale applications of measuring this parameter within the scope of precision agriculture.

3.6. References

Aldea, M., Hamilton, J.G., Resti, J.P., Zanger, A.R., Berenbaum, M.R., DeLucia, E.H., 2005. Indirect effects of insect herbivory on leaf gas exchange in soybean. Plant Cell Environ. 28, 402-411.

Aldea, M., Frank, T.D., DeLucia, E.H., 2006. A method for quantitative analysis of spatially variable physiological processes across leaf surfaces. Photosynth. Res. 90, 161-172.

Baker, N.R., 2008. Chlorophyll fluorescence: A probe of photosynthesis *in vivo*. Annu. Rev. Plant Biol. 59, 89-113.

Baker, N.R., Oxborough, K., Lawson, T., Morison, J.I.L., 2001. High resolution imaging of photosynthetic activities of tissues, cells and chloroplasts in leaves. J. Exp. Bot. 52, 615-621.

Balachandran, S., Osmond, C.B., Daley, P.F., 1994. Diagnosis of the earliest strain-specific interactions between tobacco mosaic virus and chloroplasts of tobacco leaves *in vivo* by means of chlorophyll fluorescence imaging. Plant Physiol. 104, 1059-1065.

Berger, S., Benediktyová, Z., Matouš, K., Bonfig, K., Mueller, M.J, Nedbal, L., Roitsch, T., 2007. Visualization of dynamics of plant-pathogen interaction by novel combination of chlorophyll fluorescence imaging and statistical analysis: differential effects of virulent and avirulent strains of *P. syringae* and of oxylipins on *A. thaliana*. J. Exp. Bot. 58, 797-806.

Bock, C.H., Poole, G.H., Parker, P.E., Gottwald, T.R., 2010. Plant disease severity estimated visually, by digital photography and image analysis, and by hyperspectral imaging. Crit. Rev. Plant Sci. 29, 59-107.

Bonfig, K.B., Schreiber, U., Gabler, A., Roitsch, T., Berger, S., 2006. Infection with virulent and avirulent *P. syringae* strains differentially affects photosynthesis and sink metabolism in *Arabidopsis* leaves. Planta 225, 1-12.

Bürling, K., Hunsche, M., Noga, G., 2010. Quantum yield of non-regulated energy dissipation in PSII (Y(NO)) for early detection of leaf rust (*Puccina triticina*) infection in susceptible and resistant wheat (*Triticum aestivum* L.) cultivars. Prec. Agr. 11, 703-716.

Calatayud, A., Roca, D., Martínez, P.F., 2006.Spatial-temporal variations in rose leaves under water stress conditions studied by chlorophyll fluorescence imaging. Plant Physiol. Biochem. 44, 564-573.

Chaerle, L., Pineda, M., Romero-Aranda, R., Van Der Straeten, D., Baron, M., 2006. Robotized thermal and chlorophyll fluorescence imaging of pepper mild mottle virus infection in *Nicotiana benthamiana*. Plant Cell Physiol. 47, 1323-1336.

Chaerle, L., Hagenbeek, D., De Bruyne, E., Valcke, R., Van Der Straeten, D., 2004. Thermal and chlorophyll-fluorescence imaging distinguish plant–pathogen interactions at an early stage. Plant Cell Physiol. 45, 887-896.

Chaerle, L., Leinonen, I., Jones, H.G., Van Der Straeten, D., 2007. Monitoring and screening plant populations with combined thermal and chlorophyll fluorescence imaging. J. Exp. Bot. 58, 773-784.

Chaerle, L., Van Der Straeten, D., 2001. Seeing is believing: imaging techniques to monitor plant health. Biochim. Biophys. Acta 1519, 153-166.

Chen, P., Frank, T.D., Long, S.P., 2009. Is a short, sharp shock equivalent to long-term punishment? Contrasting the spatial patter of acute and chronic ozone damage to soybean leaves via chlorophyll fluorescence imaging. Plant Cell Environ. 32, 327-335.

Demmig-Adams, B., Adams, W.W. III., Barker, D.H., Logan, B.A., Bowling, R.D., Verhoeven, A.S., 1996. Using chlorophyll fluorescence to assess the fraction of absorbed light allocated to thermal dissipation of excess excitation. Physiol. Plant. 98, 253-264.

Emmett, R.W., Parbery, D.G., 1975. Appressoria. Annu. Rev. Phytopathol. 13, 147-165.

Genty, B., Briantais, J-M., Baker, N.R., 1989. The relationship between the quantum yield of photosynthetic electron transport and quenching of chlorophyll fluorescence. Biochim. Biophys. Acta 990, 87-92.

Genty, B., Harbinson, J., Cailly, A.L., Rizza, F., 1996. Fate of excitation at PSII in leaves: the non-photochemical side. Presented at the *Third BBSRC Robert Hill Symposium on Photosynthesis*, March 31 to April 3, 1996, University of Sheffield, Department of Molecular Biology and Biotechnology, Western Bank, Sheffield UK, Abstract no. P28.

Gorbe, E., Calatayud, A., 2012. Applications of chlorophyll fluorescence imaging technique in horticultural research: A review. Scientia Hort. 138, 24-35.

Govindjee, 1995. Sixty-three years since Kautsky: chlorophyll *a* fluorescence. Aust. J. Plant Physiol. 22, 20-29.

Grieu, P., Rubin, C., Guckert, A., 1995. Effect of drought on photosynthesis in *Trifolium repens*: maintenance of photosystem II efficiency and of measured photosynthesis. Plant Physiol. Biochem. 33, 19-24.

Guidi, L., Mori, S., Degl'Innocenti, E., Pecchia, S., 2007. Effects of ozone exposure or fungal pathogen on white lupin leaves as determined by imaging of chlorophyll a fluorescence. Plant Physiol. Biochem.45, 851-857.

Halleen, F., Fourie, P.H., Crous, P.W., 2007. Control of black foot disease in grapevine nurseries. Plant Pathol. 56, 637-645.

Harvey, P.J., Butterworth, P.J., Hawke, B.G., Pankhurst, C.E., 2001.enetic and pathogenic variation among cereal, medic and sub-clover isolates of *Pythium irregulare*. Mycol. Res. 105, 85-93.

Hendrix, F.F., Campbell, W.A., 1973. Pythiums as plant pathogens. Annu. Rev. Phytopathol. 11, 77-98.

Horton, P., Ruban, A., Walters, R.G., 1996. Regulation of light harvesting in green plants. Annu. Rev. Plant Physiol. Plant Mol. Biol. 47, 655-684.

Iqbal, M.J., Goodwin, P.H., Leonardos, E.D., Grodzinski, B., 2012. Spatial and temporal changes in chlorophyll fluorescence images of *Nicotiana benthamiana* leaves following inoculation with *Pseudomonas syringae pv. tabaci*. Plant Pathol. 61, 1052-1062.

Ivanov, D.A., Bernards, M.A., 2012. Ginsenosidases and the pathogenicity of *Pythium irregulare*. Phytochemistry 78, 44-53.

Klughammer, C., Schreiber, U., 2008. Complimentary PSII quantum yields calculated from simple chlorophyll fluorescence parameters measured by PAM fluorometry and the Saturation Pulse method. PAM Application Notes 1, 27-35.

Kramer, D.M., Johnson, G., Kiirats ,O., Edwards, G.E., 2004. New fluorescence parameters for determination of QA redox state and excitation energy fluxes. Photosynth. Res. 79, 209-218.

Kuckenberg, J., Tartachnyk, I., Schmitz-Eiberger, M., Noga, G.J., 2007. UV-B induced damage and recovery processes in apple leaves as assessed by LIF and PAM fluorescence techniques. J. Appl. Bot. Food Quality 81, 77-85.

Leipner, J., Oxborough, K., Baker, N.R., 2001. Primary sites of ozone-induced perturbations of photosynthesis in leaves: identification and characterization in *Phaseolus vulgaris* using high resolution chlorophyll fluorescence imaging. J. Exp. Bot. 52, 1689-1696.

Lichtenthaler, H.K., Buschmann, C., Knapp, M., 2005a. How to correctly determine the different chlorophyll fluorescence parameters and the chlorophyll fluorescence decrease ratio RFd of leaves with the PAM fluorometer. Photosynthetica 43, 375-393.

Lichtenthaler, H.K., Langsdorf, G., Lenk, S., Buschmann, C., 2005b. Chlorophyll fluorescence imaging of photosynthetic activity with the flash-lamp fluorescence imaging system. Photosynthetica 43, 355-369.

Lichtenthaler, H.K., Miehé, J., 1997. Fluorescence imaging as a diagnostic tool for plant stress. Trends Plant Sci. 2, 316-320.

Martin, F.N., Loper, J.E., 1999. Soilborne plant diseases caused by *Pythium* spp.: Ecology, epidemiology, and prospects for biological control. Crit. Rev. Plant Sci. 18, 111-181.

Matouš, K., Benediktyová, Z., Berger, S., Roitsch, T., Nedbal, L., 2006. Case study of combinatorial imaging: what protocol and what chlorophyll fluorescence image to use when visualizing infection of *Arabidopsis thaliana* by *Pseudomonas syringae*. Photosynth. Res. 90, 243-253.

Meyer, S., Saccardy-Adji, K., Rizza, F., Genty, B., 2001. Inhibition of photosynthesis by *Colletotrichum lindemuthianum* in bean leaves determined by chlorophyll fluorescence imaging. Plant Cell Environ. 24, 947-955.

Miyake, N., Nagai, H., Kageyama, K., 2014. Wilt and root rot of poinsettia caused by three high-temperature-tolerant *Pythium* species in ebb-and-flow irrigation systems. J. Gen. Plant Pathol. 80, 479-489.

Mutka, M.A., Bart, R.S., 2015. Image-based phenotyping of plant disease symptoms. Front. Plant Sci. 5, 734. doi: 10.3389/fpls.2014.00734.

Mazzola, M., 1998. Elucidation of the microbial complex having a causal role in the development of apple replant disease in Washington. Phytopathology 88, 930-938.

Oliver, A., Van Lierop, B., Buonassisi, A., 1990. American ginseng culture in the arid climates of British Columbia. In Ministry of Agriculture and Fisheries of British Columbia, pp. 37.Victoria, BC, Canada.

Oxborough, K., Baker, N.R., 1997. An instrument capable of imaging chlorophyll *a* fluorescence from intact leaves at very low irradiance and at cellular and subcellular levels of organization. Plant Cell Environ. 20, 1473-1483.

Pérez-Bueno, M.L., Ciscato, M., vandeVen, M., García-Luque, I., Valcke, R., Barón, M., 2006. Imaging viral infection: studies on *Nicotiana benthamiana* plants infected with the pepper mild mottle tobamovirus. Photosynth. Res. 90, 111-123.

Pineda, M., Soukupová, J., Matouš, K., Nedbal, L., Barón, M., 2008. Conventional and combinatorial chlorophyll fluorescence imaging of tobamovirus-infected plants. Photosynthetica 46, 441-451.

Prokopová, J., Špundová, M., Sedlářová, M., Husičková, A., Novotný, R., Doležal, K., Lebeda, A., 2010. Photosynthetic responses of lettuce to downy mildew infection and cytokinin treatment. Plant Physiol. Biochem. 48, 716-723.

Reeleder, R.D., Brammall, R.A., 1994. Pathogenicity of *Pythium* species, *Cylindrocarpon destructans* and *Rhizoctonia solani* to ginseng seedlings in Ontario. Can. J. Plant Pathol. 16, 311-316.

Rodriguez-Moreno, L., Pineda, M., Soukupova, J., Macho, A.P., Beuzon, C. R., Baron, M., Ramos, C., 2008. Early detection of bean infection by *Pseudomonas syringae* in asymptomatic leaf areas using chlorophyll fluorescence imaging. Photosynth. Res. 96, 27-35.

Rolfe, S.A., Scholes, J.D., 2010. Chlorophyll fluorescence imaging of plant-pathogen interactions. Protoplasma 247, 163-175.

Scharte, J., Schön, H., Weis, E., 2005. Photosynthesis and carbohydrate metabolism in tobacco leaves during an incompatible interaction with *Phytophthora nicotianae*. Plant Cell Environ. 28, 1421-1435.

Scholes, J.D., Rolfe, S.A., 1996. Photosynthesis in localised regions of oat leaves infected with crown rust (*Puccinia coronata*): quantitative imaging of chlorophyll fluorescence. Planta 199, 573-582.

Schreiber, U., Klughammer, C., 2008. Non-photochemical fluorescence quenching and quantum yields in PSI and PSII: Analysis of heat-induced limitations using Maxi-Imaging-PAM and Dual-PAM-100. PAM Application Notes 1, 15-18.

Schreiber, U., Schliwa, U., Bilger, W., 1986. Continuous recording of photochemical and non-photochemical chlorophyll fluorescence quenching with a new type of modulation fluorometer. Photosynth. Res. 10, 51-62.

Strange, R.N., Scott, P.R., 2005. Plant disease: a threat to global food security. Annu. Rev. Phytopathol. 43, 83-116.

Swarbrick, P.J., Schulze-Lefert, P., Scholes, J.D., 2006. Metabolic consequences of susceptibility and resistance (race-specific and broad-spectrum) in barley leaves challenged with powdery mildew. Plant Cell Environ. 29, 1061-1076.

Takayama, K., Sakai, Y., Nishina, H., Omasa, K., 2007. Chlorophyll fluorescence imaging at 77K for assessing the heterogeneously distributed light stress over a leaf surface. Environ. Contr. Biol. 45, 39-46.

Tuite, J., 1969. Plant Pathological Methods. pp. 233. Burgess Publishing Co., Minneapolis. MN, USA.

Tung, J., Goodwin, P.H., Hsiang, T., 2013. Chlorophyll fluorescence for quantification of fungal foliar infection and assessment of the effectiveness of an induced systemic resistance activator. Eur. J. Plant Pathol. 136, 301-315.

van Kooten, O., Snel, J., 1990. The use of chlorophyll fluorescence nomenclature in plant stress physiology. Photosynth. Res. 25, 147-150.

Chapter 4: Chemoattractant Potential of Ginsenosides in the Ginseng - *P. irregulare* Pathosystem

4.1. Introduction

American ginseng (*Panax quinquefolius* L.) is a slow growing perennial, cultivated for the high medicinal value of its root. A native North American member of the *Araliaceae*, it is one of 17 species that belong to the genus *Panax*, which also includes *P. ginseng* C.A. Mey., *P. notoginseng* (Burkill) F.H. Chen ex C.Y. Wu K.M. Feng and *P. japonicus* C.A. Mey., all of which are recognized as medicinal plants and produce ginsenosides as the main bioactive ingredient (Wen and Zimmer 1996; Small and Catling 1999). *Panax quinquefolius* is most commonly found in rich, moist, mature deciduous forests (Anderson et al. 1993). However, due to industrial scale harvesting beginning in the 1800s, wild populations of ginseng today are extremely rare and the modern ginseng supply relies on intensive field cultivation under artificial shade structures (McGraw et al. 2013; You et al. 2015). Ginseng roots are commonly harvested after 3–5 years and ginsenosides constitute approximately 3 to 8% of the root dry weight (Court et al. 1996).

Ginsenosides are triterpenoid saponins, that can be classified into two groups; dammarane type or oleanane type triterpenes (Liang and Zhao 2008). Of the >40 different ginsenosides that have been identified in *Panax* species (Cheng et al. 2007), the most common are based on a dammarane carbon skeleton, which is unique to the genus *Panax.* This core structure is comprised of four trans-oriented rings and contains side-chains of mono- and disaccharide sugar moieties (eg. glucose, rhamnose, xylose and arabinose) (Attele et al. 1999). Based on the hydroxylation pattern of this parent triterpenoid, these common ginsenosides (Fig. 4.1) can be further classified as either 20 (S)-protopanaxadiols (e.g., Rb1, Rd, Gypenoside GXVII, F2) or 20 (S)-protopanaxatriols (e.g., Rg, Re) (Teng et al. 2002). These two classes of ginsenosides differ in their glycosylation patterns but are both considered bidesmosidic, since they each contain two saccharide side-chains, at the C-3 and C-20 positions (diols) or C-6 and C-20 positions (triols) (Hostettmann and Marston, 1995).

The growing demand for cultivated American ginseng (Pritts, 2010) means that it is becoming increasingly important to establish methods of disease prevention in order to maximize crop yield. Since saponins as a class of compounds demonstrate antifungal properties (e.g., Osbourn 1996) and possess allelopathic potential (Nicol et al. 2003), it is

important to evaluate the ecological role of ginsenosides as compounds released into the soil, and not merely examine their pharmacological properties. Indeed, ginsenosides have been shown to act as resistance factors against various foliar and root fungal pathogens (Nicol et al. 2002; Zhao et al. 2012). However, exposure of the ginseng root pathogen *Pythium irregulare* Buisman to ginsenosides has been shown to enhance its growth in a dose dependent manner, leading to speculation that ginsenosides may function as chemoattractants and/or growth regulators in the context of the ginseng - *P. irregulare* pathosystem (Nicol et al. 2002; Nicol et al. 2003). Furthermore, the same level of growth stimulation was observed when *P. irregulare* was exposed to equivalent doses of ergosterol, a common sterol component of fungal membranes (Nicol et al. 2003). Therefore, it has been hypothesized that ginsenosides, which are derived from the same cytosolic mevalonate pathway as phytosterols (Chappell 2002), may function to enhance growth in this organism, just like phytosterols do in other oomycetes and fungi (Nicol et al. 2003). This may occur because oomycetes, like *P. irregulare,* are unable to synthesize sterols and therefore, must acquire them from the environment or host organisms (Marshall et al. 2001; Gaulin et al. 2010).

The ability of *P. irregulare* to utilize ginsenosides for growth is important because this organism poses a major threat to commercial ginseng cultivation, causing damping off and post emergence root rot in ginseng plants (Krupa and Dommergues 1979; Howard et al. 1994). The insensitivity of *P. irregulare* and other oomycetes to saponin defence compounds is not uncommon, and is attributed again, to the inability of these organisms to synthesize their own sterols (Olsen 1971). This is because the toxic action of saponins in fungi involves their ability to complex with membrane sterols and cause pore formation, leading to a loss of membrane integrity (Fenwick et al. 1992). Oomycetes from the genus *Pythium* and *Phytophthora*, which contain little to no sterol in their membranes are therefore rendered resistant to saponin bioactivity (Ameson and Durbin 1968; Keukens et al. 1995). However, while most oomycetes (*Peronosporales*) lack the ability to produce sterols, they can acquire them from the environment. *Phytophthora cactorum* has been shown to incorporate some steroidal alkaloids into its membranes and to discriminate and even biotransform certain sterols *in vitro* into forms it can use for growth and reproduction (Nes et al. 1983; Nes and Stafford 1983). Triterpene molecules fall within this group as the biosynthetic pathway for

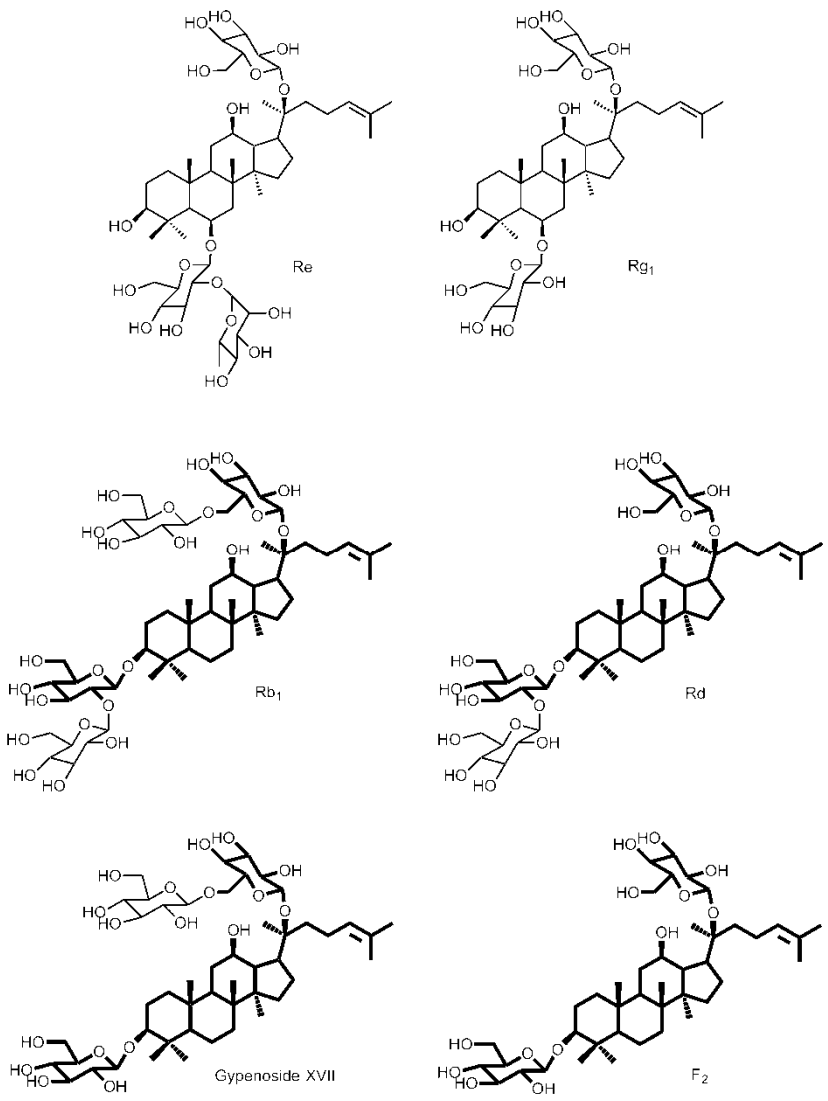

Figure 4.1. Common ginsenosides found in *Panax quinquefolius* L. Ginsenosides Re and Rg1 are 20 (S)-protopanaxatriols. Ginsenosides Rb1, Rd, Gypenoside XVII (GXVII) and F2 are common 20 (S)-protopanaxadiol. The core structure of ginsenoside F2 is shown in **BOLD**, emphasizing that selective ß (1-6) and ß (1-2) glucosidase metabolism of sugar residues from 20 (S)-protopanaxadiol ginsenosides can lead to formation of F2.

sterol and triterpenes is identical until the formation of 2,3-oxidosqualene (Abe et al. 1993).

In this context, the ability of *P. irregulare* to metabolize ginsenoside saponins via extracellular β-glycosidases has been correlated to pathogenicity (Chapter 2; Ivanov and Bernards 2012). The production of these glycosidases is induced in the presence of ginsenosides and catalyzes the structural transformation of 20 (S)-protopanaxadiol ginsenosides to ginsenoside F2 by shortening sugar side chains at the C-3 and C-20 positions (Yousef and Bernards 2005; Neculai et al. 2009). *Pythium irregulare* has been shown to internalize ginsenoside F2, suggesting that it may serve to stimulate growth of the pathogen as if a host root was nearby, or it may be mimic a general growth hormone (Nes 1987). Furthermore, the production of extracellular enzymes metabolizing β-glycosidases (ginsenosidases), and their ability to metabolize common 20 (S)-protopanaxadiol ginsenosides into ginsenoside F2 plays a functional role in the pathogenicity of *P. irregulare* towards American ginseng (Chapter 2; Ivanov and Bernards 2012).

As a working hypothesis, the theoretical framework for the ginsenosides-mediated interaction between American ginseng and *P. irregulare* is as follows (Bernards et al. 2011): American ginseng produces ginsenosides and releases these biologically active compounds into the rhizosphere. Nicol et al. (2003) demonstrated that ginsenosides are released in biologically relevant concentrations from American ginseng roots and make up approximately 0.06% of rhizosphere soil dry weight. *Pythium irregulare,* meanwhile, secretes broad specificity glycosidases into its surroundings, which are able to metabolize ginsenosides into products like ginsenoside F2. The subsequent F2 gradient and potential internalization of F2 may lead to the expression of more specific ginsenosidases and ultimately may lead to enhanced and directed pathogen growth *in vivo* towards ginseng plants. However, there is no certainty if de-glycosylation of ginsenosides and the formation of ginsenoside F2 are necessary to stimulate the growth of *P. irregulare* or if simply the detection of ginsenosides may be sufficient to lead the pathogen to the plant.

If rhizosphere secreted ginsenosides stimulate *P. irregulare* growth, and in turn facilitate pathogen infection, this may be one of the factors contributing to replant failure in commercial ginseng cultivation. Replant failure results in yield reductions and crop failure when attempting to re-use ginseng fields for successive crops, and is characterized by low germination, poor seedling growth and severe disease (Yang et al. 2015). This problem is generally attributed to an accumulation of disease inoculum in soil and persists for decades

after the cultivation of ginseng (Reeleder and Brammal 1994; Reeleder et al. 2002; Kernaghan et al. 2007) as well as perennial tree crops like apple, olive and some stone fruits (Mai and Abawi 1981; Braun 1995; Mercado-Blanco et al. 2003). To date, no single pathogen has been identified as the leading cause of replant failure and the problem is commonly attributed to the presence of a pathogen complex of fungi/oomycetes of the genera *Rhizoctonia*, *Cylindrocarpon*, and *Pythium* (Braun 1991; Reeleder and Brammal 1994; Mazolla 1998; Mazolla and Brown 2010). All three genera contain common pathogens to American ginseng, with growth of *Cylindrocarpon* and *Pythium* stimulated by the presence of ginsenosides (Nicol et al. 2003; Zhao et al. 2012)

In the present study, the chemoattractant potential of ginsenosides in the interaction through which *P. irregulare* finds its host and/or promotes infection is evaluated. The effects of selected pure protopanaxadiol and -triol ginsenosides (Rb1, Re and F2) on the growth of the pathogen were examined by *in vitro* assays and compared to the effect of a purified total ginsenoside extract. Meanwhile, an *in vivo* assay was used to monitor the pathogenicity of *P. irregulare* toward ginsenoside-treated and -untreated one- and two-year old ginseng seedlings using a chlorophyll fluorescence imaging technique (Chapter 3; Ivanov and Bernards *submitted*). These studies will allow us to better understand the ginseng-*Pythium* interrelationship, which will provide insight into how ginsenosides secreted into the soil by *Panax* species affect pathogenic orgainsms in the rhizospere. This may well have important positive implications in understanding the biological mechanisms causing replant failure and to the establishment of better methods for disease prevention.

4.2. Materials and Methods

4.2.1. *Pythium irregulare* cultures

Pythium irregulare (BR 1068) as strain pathogenic to American ginseng (*Panax quinquefolius*) was obtained from the Canadian Collection of Fungal Cultures (CCFC, Ottawa, Canada). *S*tock cultures were maintained on potato dextrose agar (PDA) medium at 22°C in the dark.

4.2.2. Plant production

American ginseng seeds, obtained from J.C.K Farms Ltd (Brantford, ON, Canada), were stratified in accordance with general commercial grower practice (Oliver et al. 1990) in order to generate one- and subsequently, two-year old ginseng plants (Chapter 3; Ivanov and Bernards *submitted*). Briefly, seeds were surface sterilized by soaking in a solution of 20% v/v bleach (6% w/v NaClO) and 0.05% v/v Tween-20 for 10 min. The seeds were then rinsed with 10 x equal volume of sterile ddH_2O and dried for 48 h at 22°C. Seeds were placed in muslin bags and buried under 15-45 cm of moist acid washed sand and subjected to a cold-warm-cold stratification period (approximately 8 months at 5°C, 5 months at 22°C and 5 months at 5°C) until germination occurred. Germinated seeds were transplanted into 12 cm diameter pots (3 seeds to 1 pot) filled with moist Pro-mix (Premier Tech Horticulture, Canada) soil, so that seeds were approximately 0.5 cm below the surface of the soil. One-year old ginseng seedlings were grown in a controlled environment (Can-Trol Environmental Systems, Markham, ON, Canada), under fluorescent lighting with an approximate intensity of 50-100 μmol photons$\cdot m^{-2}\cdot s^{-1}$ at 22°C, 50% humidity and a day/night cycle of 16/8 h. Plants were grown as above and watered (from the bottom, using a watering tray) as needed. Plants not used for one-year old experiments were allowed to fully senesce (approximately 6-8 months) after which they were stored at 5°C in the dark. Subsequently, two-year old ginseng plants emerged approximately 5-6 months after initiation of cold storage, at which point seedlings were transferred and grown under a natural light environment from June to August 2014. Fully expanded leaves were used for all experiments.

4.2.3. Ginsenoside extraction

A crude ginsenoside mixture was prepared from three-year old roots of American ginseng obtained from Damaree Farms (Delhi, ON, Canada) according to a protocol initially

outlined by Nicol et al. (2002). Roots were mechanically crushed, dried for 20 hours at 38°C until a constant weight, and extracted for 24 hours with 80% (MeOH) (aq) (10 mL/g dry weight) under constant mixing. The resulting extract was vacuum filtered using No. 40 Ashless filter paper (Whatman International Ltd. Maidstone, England). MeOH was removed under reduced pressure and the remaining aqueous extract was defatted 3x with an equal volume of $CHCl_3$ and partitioned 2x with an equal volume water-saturated n-BuOH to yield a crude ginsenoside mixture. Crude ginsenosides were further purified using C18 Extract-clean SPE (solid phase extraction) (50 μm, 60Å, 75 mL bed volume; Grace, USA) and Mega Bond Elut NH_2 (40 μm, 60 Å, 60 mL bed volume; Varian, USA) columns, according to the protocol of Ivanov and Bernards (2012), to yield a purified ginsenoside mixture (GSF). Ginsenoside composition of the subsequent purified extract was determined using high-pressure liquid chromatography (HPLC) (Ivanov and Bernards 2012). Pure ginsenoside F2, Rb1 and Re were obtained from Chengdu Biopurify Phytochemicals Ltd., China, and the purity was verified by liquid chromatography-mass spectrometry (LC-MS). Briefly, samples (10 μL) were injected onto a Zorbax Extend C-18 column (2.1 x 100 mm, 1.8 μm, Agilent Technologies), and eluted with a gradient of acetonitrile (Solvent B: 90% acetonitrile containing 0.1% formic acid and 1 mg/L NaAcetate) in H_2O (Solvent A: containing 0.1% formic acid and 1 mg/L NaAcetate) as follows: Initial conditions 25% B in A, held for 1 min, followed by a linear gradient to 35% B over 2 min, 60% B over 4.5 min and 95% B over 2.5 min, and held at 95% for 2 min before returning to the initial conditions . The flow rate was set to 0.4 mL/min, and the eluent monitored at 203 nm before infusion into an Agilent 6320 TOF mass spectrometer through a Dual Spray ESI source with gas temperature of 325^{o}C flowing at 12 L/min, and a nebulizer pressure of 45 psi. The fragmentor voltage was set to 120V with a Vcap of 4,500V. Automated internal calibration was done using reference ions 121.0508 and 922.0096. The column was conditioned at 25% B for 10 min between samples. Ginsenosides were detected as their Na^+ adducts, in positive ion mode $(M+Na]^+$.

4.2.4. Fluorescence measurements and PAM images

A pulse amplitude modulating imaging fluorometer (IMAGING-PAM, Heinz Walz GmbH, Effeltrich, Germany) was used to capture chlorophyll fluorescence images and to estimate the quantum yield of constitutive (non-regulated) quenching processes in PSII (ΦNO) at a single light intensity. Measurements were initiated with the determination of

basal (Fo) and maximum (Fm) Chl fluorescence before the onset of actinic irradiance at 104 µmol photons m^{-2} s^{-1} (for one-year old plants) and at 414 µmol photons m^{-2} s^{-1} (for two-year old plants). Fluorescence parameters in one-year old plants, were evaluated at 104 µmol photons m^{-2} s^{-1} PAR, because that was the maximum light intensity recorded at leaf level in the controlled environment growth chamber where they were grown. Meanwhile, an actinic irradiance at 414 µmol photons m^{-2} s^{-1} PAR, was used in assessing fluorescence parameters in two-year old plants, because that was the optimum light intensity determined for measurement of slow induction chlorophyll fluorescence parameters in ginseng plants infected with *P. irregulare* (Chapter 3; Ivanov and Bernards 2015 *submitted*). A pre-programmed sequence was used to initiate actinic illumination after a delay of 40 s, with saturating pulses being applied every 20 s thereafter for the remainder of the total data acquisition period of 300 s in order to calculate ΦNO. The chlorophyll fluorescence parameters measured were calculated according to Kramer et al. (2004) using the nomenclature of van Kooten and Snel (1990). Fluorescence images were captured by a CCD camera (IMAG-K, Allied Vision Technologies) containing a 640 x 480 pixel CCD chip size and a CCTV camera lens (Cosmicar/Pentax F1.2, f=12mm). A light-emitting diode (LED) ring array (IMAG-L) consisting of 96 blue LEDs (470 nm) provided the light source for fluorescence excitation and actinic illumination. Basal Chl fluorescence (Fo) was measured after exposure to a standard modulated excitation intensity of 0.5 µmol photons m^{-2} s^{-1} PAR and maximal Chl fluorescence (Fm) was determined after application of a saturating pulse of 2400 µmol photons m^{-2} s^{-1} PAR. Measurements were taken every day for 15 days of the treatment/growth period with initial measurements (Day 0) being conducted on the day of transplantation.

4.2.5. Migration of purified total ginsenoside extract (GSF) through sand

Pots (15 cm in diameter) sterilized in a 5% v/v (6% w/v NaClO) solution for at least 24 hours, were filled with 1000 g sterile Bomix construction sand. A column of sand 11 mm in diameter was removed 3.5 cm away from the pot edges. No. 1 Ashless filter papers (Whatman International Ltd. Maidstone, England), rolled up into cylinders, were infused with 6.5 mL of 1 mg·mL^{-1} purified ginsenoside extract (dissolved in ddH_2O) and placed in the empty sand columns to create a point source of ginsenosides. For recovery of ginsenosides, 11 mm columns of sand were removed 2, 4, 6 and 8 cm away from the

ginsenoside infused filter papers in pots left at 22°C for 2, 4, 6 and 8 days. Recovered sand was extracted for 24 hours with 8.5 mL MeOH (aq) under constant mixing on a gyratory shaker. Samples were centrifuged at 1700 x g for 2 min, the resulting MeOH suspension was evaporated under reduced pressure and the resulting ginsenoside residue was re-suspended in 1.5 mL MeOH. The amount of ginsenoside Rb1 was quantified by LC-MS as above for each sample distance and was adjusted for the mass of sand (g) used in the extraction..

4.2.6. Effects of purified ginsenoside extract and pure ginsenosides on *in vitro* growth of *P. irregulare*

An 8 mm diameter plug of a 3-day old Potato Dextrose Agar (PDA) culture was placed in the center of each 90 mm petri dish containing 25 mL Czapek Dox Mineral Agar (containing 3 g $NaNO_3$, 1 g K_2PO_4, 0.5 g $MgSO_4$, 0.5 g KCl, 0.01 g $FeSO_4 \cdot 6H_2O$ and 15 g granulated agar per liter ddH_2O). Sterilized, 6 mm antibiotic-assay discs (Schleicher & Schuell, Germany) were placed at equal distance on either side of the *P. irregulare* (BR 1068) plug (approx. 2.5 cm from centre). Discs on the left were infused with 100 µL of 10 $mg \cdot mL^{-1}$ purified ginsenoside extract (GSF), 5 mg mL^{-1} ginsenoside Re, 5 mg mL^{-1} ginsenoside Rb1 or 5 mg mL^{-1} ginsenoside F2 (all extracts dissolved in MeOH). Discs on the right were infused with 100 µL MeOH, and served as a control. The MeOH was allowed to evaporate (~ 10 min) after which the plates were incubated at 22°C in the dark. Mycelial growth was photographed, while plates were illuminated from below by two angled specular light sources, every 24 hrs for 120 hrs using a Nikon D50 digital camera equipped with a 60 mm AF Micro Nikkor lens (Nikon Corp., Tokyo, Japan). Images were taken using auto white balance, aperture set at -1 and a shutter speed of 200 ISO. Images were modified using Photoshop v.14.2.1 (Adobe Systems Inc., San Jose, CA, USA) by applying a Black & White Adjustment layer followed by a Curves Adjustment layer to enhance the contrast of the mycelia against the medium, making the structures more visible.

4.2.7. Monitoring *in vivo* infection of *P. irregulare* on ginsenoside-treated and untreated American ginseng

Pythium irregulare (BR 1068) inoculum was prepared by placing one 8 mm diameter plug of 3-day old PDA culture into 20 mL sterile V8 broth (Tuite, 1969) contained in a 90 mm petri dish. The V8 cultures were incubated at 22°C in the dark for 4 days. One- and two-

year old ginseng plants were uprooted from their growth pots, rinsed with ddH_2O and either soaked in 10 $mg \cdot mL^{-1}$ purified ginsenoside extract (in ddH_2O) for 15 minutes or ddH_2O alone for 15 minutes. One plant from each treatment group was planted on opposite sides (8 cm away from each other) of 15 cm diameter pots, previously sterilized with a 5% v/v (6% w/v NaClO) solution (for at least 24 hours) and filled with 1000 g of sterile Bomix construction sand (Daubois Inc., Saint- Léonard, QC, Canada). Columns of sand (13 mm diameter) were then removed from the middle of each pot (4 cm away from the base of each plant) and filled with an entire mycelial mat from previously made V8 culture (homogenized in the sand removed from the center of the pot) or sterile sand (Control). One-year old plants were grown for 15 days in a controlled environment chamber (Can-Trol Environmental Systems, Markham, ON, Canada) under fluorescent lighting with an approximate intensity of 50-100 µmol photons$\cdot m^{-2} \cdot s^{-1}$ at 22°C, 50% humidity and a day/night cycle of 16/8 h. Two-year old plants were grown for 20 days under a shaded natural light environment at 22°C during August of 2014. Time to infection and disease progression was monitored every 24 hours using a pulse amplitude modulating (PAM) fluorometer.

4.2.8. Data handling and statistics

The *in vivo* ginsenoside treatment assays were done using six independent replicates (N=6) for the ddH_2O and 10 mg mL^{-1} purified ginsenoside treatments in the presence of *P. irregulare* for one-year old plants and using eight independent replicates (N=8) for the assays done using two-year old plants. Controls, where plants were exposed to 10 mg mL^{-1} purified ginsenosides but there was no *P. irregulare* inoculum present, were measured using four independent replicates (N=4) for one-year old plants and eight independent replicates (N=8) for two-year old plants. Chlorophyll fluorescence measurements were made at the same five independent areas of interest (AOIs) on marked leaves, on each one of the replicates above, which were averaged to yield a single measurement (N=1) of that replicate. AOIs were selected to ensure full leaf coverage without interference from major veins. A two-way repeated measures Analysis of Variance (ANOVA) with GROUP (Control: Ginsenoside + No Pathogen, Treatment: Ginsenoside + Pathogen, Control treatment: ddH_2O + Pathogen) and DAY (Time After Pathogen Exposure: 0 - 15 days for year-one plants; 0 - 20 days for year-two plants) as factors was performed to assess differences between “control” and “infected” plants for the parameter ΦNO in one- and two-year old plants (Fig. 4.4). The

Newman-Keuls test was used for post hoc comparisons. Analyses of variance were carried out using Statistica 10.0 (Statsoft Inc., Tulsa, OK, USA). All values are presented as Mean ± SE. The level of significance was set at $p<0.05$.

Concentrations of ginsenoside Rb1 were determined using three independent replicates (N=3) for every day and distance from the ginsenoside point source that was sampled in the ginsenoside migration experiment. The *in vitro* effects on the growth of *P. irregulare* (BR 1068) of purified ginsenosides extract (GSF) as well as pure ginsenosides Re, Rb1 and F2 was also monitored in triplicate (N=3) with the same plate for each treatment imaged every 24 hours (1 day) for 120 hours (5 days). For all measurements the average of the 3 repetitions was calculated.

4.3. Results

4.3.1. Ginsenosides migration experiment

In order to assess the mobility of ginsenosides in sandy soil, a ginsenoside migration experiment was conducted in which a point source containing 6.5 mL of a 1 mg mL^{-1} (dissolved in ddH_20) purified total ginsenoside extract was inserted into a 15 cm diameter pot containing sand (Fig. 4.2). The amount of ginsenoside Rb1 (ng/g soil) was then determined at a distance of 2, 4, 6 and 8 cm away from the ginsenoside point source every 2 days for a total of 8 days. Two days after the addition of the ginsenosides into the soil, more than 70 ng ginsenoside Rb1 per gram of soil was detected 2 cm away from the ginsenoside point source (Fig. 4.3). Lower concentrations were also detected up to 6 cm away as early as Day 2. These levels persisted through to Day 4, where a slightly higher amount of ginsenoside Rb1 (100 ng/g soil) was detected 2 cm away from the point source but the amounts at 4 and 6 cm away were similar to that measured at Day 2 for the same distances. By Day 6, ginsenoside Rb1 was detected at 2, 4, 6 and 8 cm away from the ginsenoside point source and by Day 8 the amount of ginsenoside Rb 1 detected at every distance was the highest compared to all other days measured.

4.3.2. *In vivo* experiment monitoring infection of *P. irregulare* on ginsenoside-treated and -untreated American ginseng

One- and two-year old American ginseng plants soaked in either ddH_2O or a 10 mg mL^{-1} solution of purified ginsenoside extract (dissolved in ddH_2O) were planted an equal distance apart (8 cm) in a 15 cm diameter pot. A V8 culture of *Pythium irregulare* (BR 1068), known to be highly pathogenic towards American ginseng, was then added in between the two plants, at a fixed point as a source of inoculum. Meanwhile, control plants were soaked in 10 mg mL^{-1} solution of purified ginsenoside extract (dissolved in ddH_2O), and planted in pots free of inoculum. The time to infection of each plant was then monitored by chlorophyll fluorescence imaging by measuring the quantum yield of non-regulated energy dissipation of PSII (ΦNO) in dark adapted leaves of both one- and two- year old plants every day for 15 days in younger plants and 20 days in the older plants (Chapter 3; Ivanov and Bernards *submitted*).

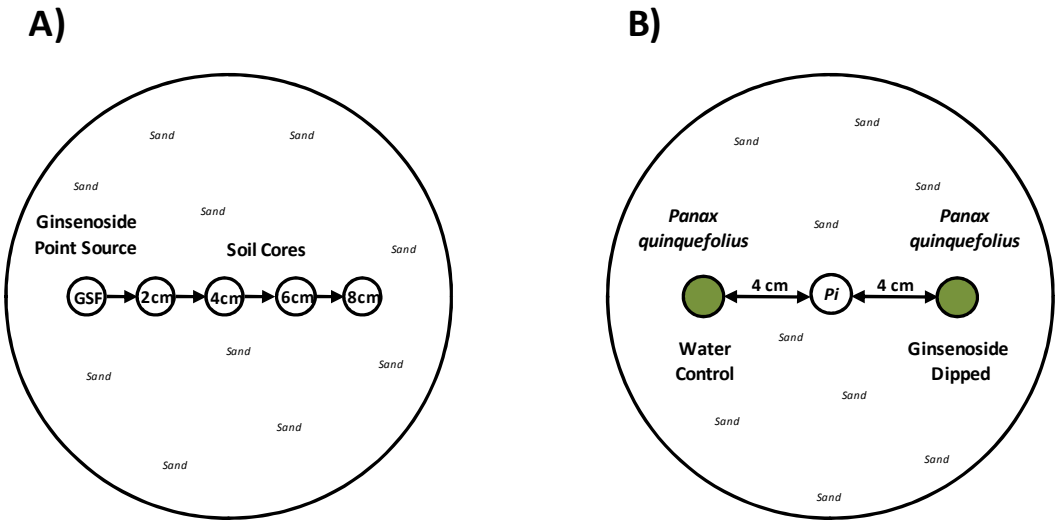

Figure 4.2. Schematic of experimental design. A) Diagram of experimental set-up to determine if ginsenoside (Rb1) migrates through a soil matrix in a 15 cm diameter pot. Cores of sand were taken 2, 4, 6, 8 cm away from a ginsenoside point source (GSF) and analyzed using LC-MS to determine presence of ginsenosides. B) Diagram of experimental set-up to determine level of infection caused by *Pythium irregulare* BR1068 on one- and two-year old ginsenoside-treated and untreated ginseng plants 4-cm away from *P. irregulare* inoculum point source.

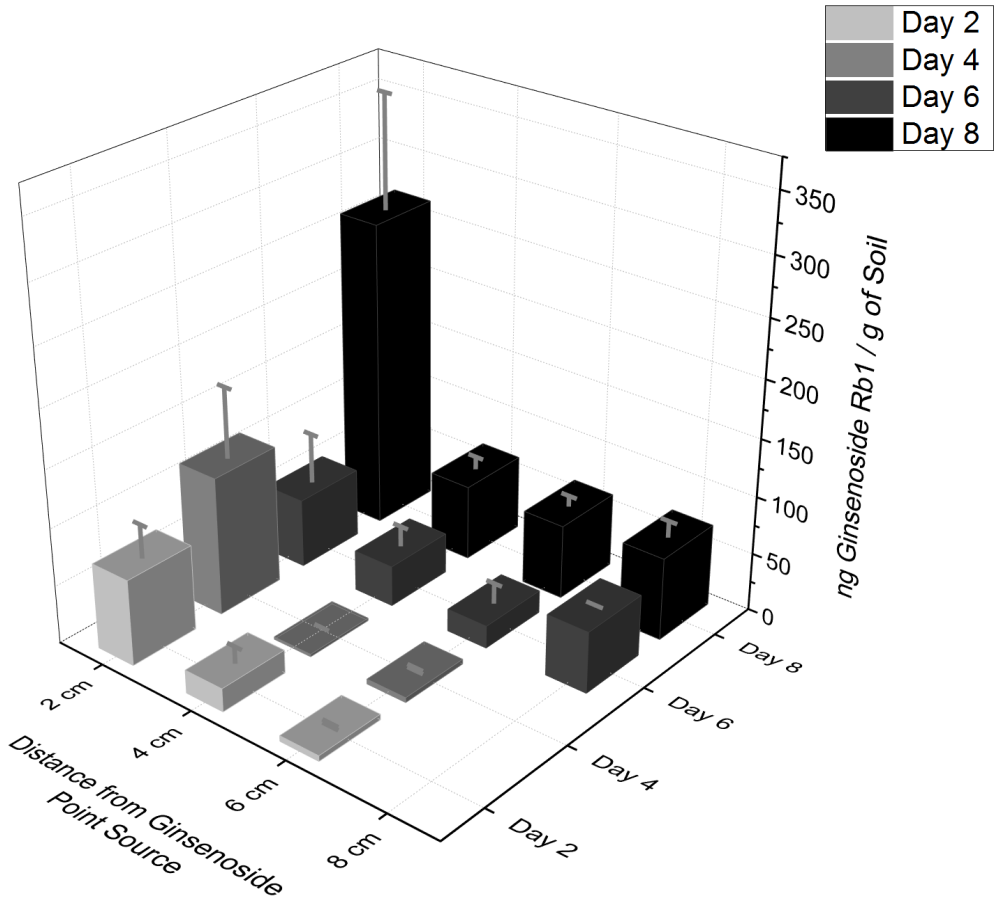

Figure 4.3. Time course of ginsenoside migration. A column of sand 11 mm in diameter was removed and filled with a rolled up Whatman filter paper infused with 6.5 mL of 1 mg mL^{-1} (dissolved in ddH_20) purified ginsenoside extract. Columns of sand were then removed 2, 4, 6, and 8 cm away from the ginsenosides infused filter paper every 2 days for 8 days total. Removed sand columns were weighed and suspended in 8.5 mL MeOH for 24 hrs and subsequently, concentrated to 1.5 mL MeOH, The amount of ginsenoside Rb1 was quantified using LC-MS and adjusted for weight of soil used in extraction. All values are expressed as Mean ± SE (N=3).

Statistical analysis revealed that overall ΦNO values differed significantly between the tested groups of plants and between days (GROUP: $P < 0.001$; DAY: $P < 0.001$, for both one- and two-year old plants). More specifically, the ΦNO values determined for ddH_2O soaked inoculated treatment plants (Control Treatment) were significantly higher than for ginsenoside soaked (Control) ($P < 0.01$) and ginsenoside soaked (Treatment) ($P < 0.001$) plants from both years. In the same time, there was an overall progressive increase in the ΦNO values for all groups of plants from Day 0 throughout the monitored period that became significant at Day 11 (one-year old; $P < 0.05$) and Day 17 (two-year old; $P < 0.05$).

Described in more detail, the values of ΦNO determined for ginsenoside soaked control plants showed a slight but constant increase throughout the monitored period in both one- and two- year old plants (Fig. 4.4A, B; black squares). ΦNO changed from approx. 0.3 at Day 0 to approx. 0.5 at Day 15 in one- year old plants, and from approx. 0.25 at Day 0 to 0.45 at Day 20 in two- year old plants without reaching statistical significance. Meanwhile, ΦNO values in ddH_2O soaked treatment plants (Control treatment), remained constant until Day 4 and Day 6, for one- and two- year old plants respectively, relative to values measured at Day 0 and values in the control plants (Fig. 4.4A, B; open circles). ΦNO values then increased rapidly from 0.3 to 0.7 at Day 10 ($P < 0.05$) in one- year old plants and remained elevated to the Day 0 and Control plant values at approximately the same level. In two-year plants a ΦNO increase of the same magnitude was observed from Day 6 until Day 13 ($P < 0.05$), after which values of ΦNO stabilized until the end of the monitoring period.

Similarly the values of ΦNO in one-year old ginsenoside soaked treatment plants (Treatment) increased in response to inoculation; however, response times were delayed relative to the ddH_2O soaked treatment. That is, ΦNO remained constant (approx. 0.3) until Day 9 relative to values at Day 0 and in the Control plants, after which there was a rapid increase in ΦNO from approx. 0.3 to 0.6 between Day 9 and Day 12 ($P < 0.05$), with a subsequent stabilization in ΦNO at the higher value until the end of the 15 Day monitoring period (Fig. 4.4A; open triangles). ΦNO values for two- year old plants in the ginsenoside soaked treatment, meanwhile, remained constant until Day 8, relative to values at Day 0 and in the Control plants, after which there was a gradual increase in ΦNO from approx. 0.25 to 0.45 at the end of the 20 day monitoring period (Fig. 4.4B). No statistically significant difference was found between the treatment groups on any of the measurement days.

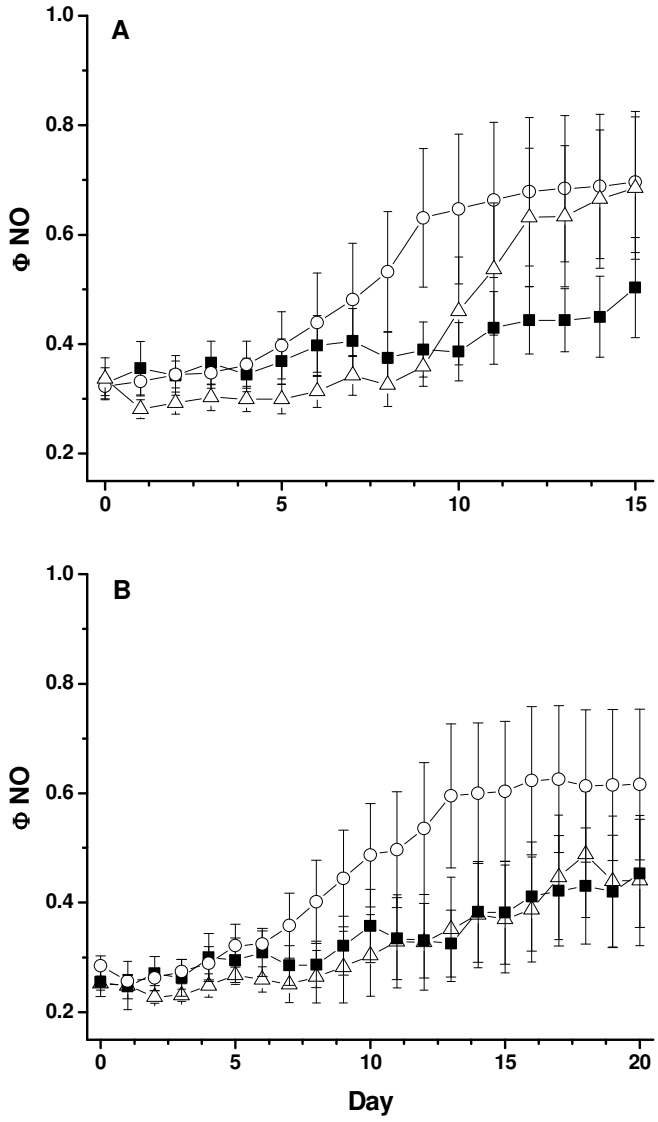

Figure 4.4. Time course of ginseng infection by *Pythium irregulare*. Ginseng plants were soaked in either ddH_2O or 10 mg mL^{-1} (ddH_2O) purified ginsenoside extract and planted 8 cm apart. Uninoculated plants: ΦNO values for (A) one- and (B) two year old plants treated with 10 mg mL^{-1} (dissolved in ddH_2O) purified ginsenosides extract (■) were collected every day for 15 days (one-year old) and for 20 days (two-year old). Inoculated plants: A 13 mm column of sand was removed 4 cm away from the base of each plant, in the middle of the pot, and filled with a *Pythium irregulare* (BR 1068)-sand mix inoculum. ΦNO values for (A) one- and (B) two-year old plants treated with ddH_2O (○) or 10 mg mL^{-1} (dissolved in ddH_2O) purified ginsenosides extract (△) were collected every day for 15 days (one-year old) and for 20 days (two-year old). All ΦNO values are expressed as Mean ± SE. N = 6 for one-year old plant treatments; N = 4 for one-year old control; N = 8 for two-year old plant treatments and control.

4.3.3. *In vitro* exposure of *P. irregulare* to purified ginsenoside extract and pure ginsenosides

Petri dishes containing Czapek-Dox Mineral Agar were prepared and the differential growth of mycelia from *P. irregulare* BR 1068, an isolate highly pathogenic toward ginseng, was monitored as it progressed toward treated and non-treated discs placed equal distances from a plug of the pathogen (Fig. 4.5). The assay disks on the left in each column carried different ginsenoside treatments and were infused with 100 µL of either: 10 mg mL^{-1} purified total ginsenoside extract (GSF, Fig. 4.5A), 5 mg mL^{-1} ginsenoside Re (Fig. 4.5B), 5 mg mL^{-1} ginsenoside Rb1 (Fig. 4.5C), or 5 mg mL^{-1} ginsenoside F2 (Fig. 4.5D), all dissolved in MeOH, while the corresponding assay discs on the right in each column were infused with 100 µL MeOH. Growth of mycelia from the inoculum plug in the center toward the assay discs was monitored every day for five days. Since it took approximately two days for mycelial growth to reach the discs and show visible differences between treatments, therefore, images of the various treatments are only shown after this time point (Fig. 4.5).

Mycelial growth appeared to be unaffected by the presence of the control discs infused with MeOH as well as discs infused with 5 mg mL^{-1} of the 20 (S)-protopanaxatriol ginsenoside Re (Fig. 4.5B). Mycelia grew directly through those discs, showing no visible alteration in growth habit up to five days after initiation of growth (Fig. 4.5).

Meanwhile, exposure of *P. irregulare* BR 1068 to 10 mg mL^{-1} purified total ginsenoside extract (GSF), resulted in enhanced aerial mycelial growth (Fig. 4.5A). After two days of growth, there was a distinct accumulation of mycelia around discs infused with total ginsenosides, albeit a short distance away from the filter disc. After three days, the accumulation of mycelia had increased even further, with a clear ring of enhanced aerial mycelial growth. Simultaneously, there was visible accumulation of mycelia forming directly around the disc. After four days, the accumulation of mycelia a short distance away persisted, forming a visible ring around the filter disc. Mycelia continued to project out from this ring and accumulate directly around the assay filter disc until the end of the monitoring period of five days.

Exposure of *P. irregulare* BR 1068 to 5 mg mL^{-1} 20 (S)-protopanaxadiol ginsenoside Rb1 (Fig. 4.5B), had a similar, although slightly reduced effect on the growth of mycelia, compared to exposure to total ginsenoside extract (GSF). Two days after initiation of growth there was a slight accumulation of mycelia around the Rb1 infused disc. After three days

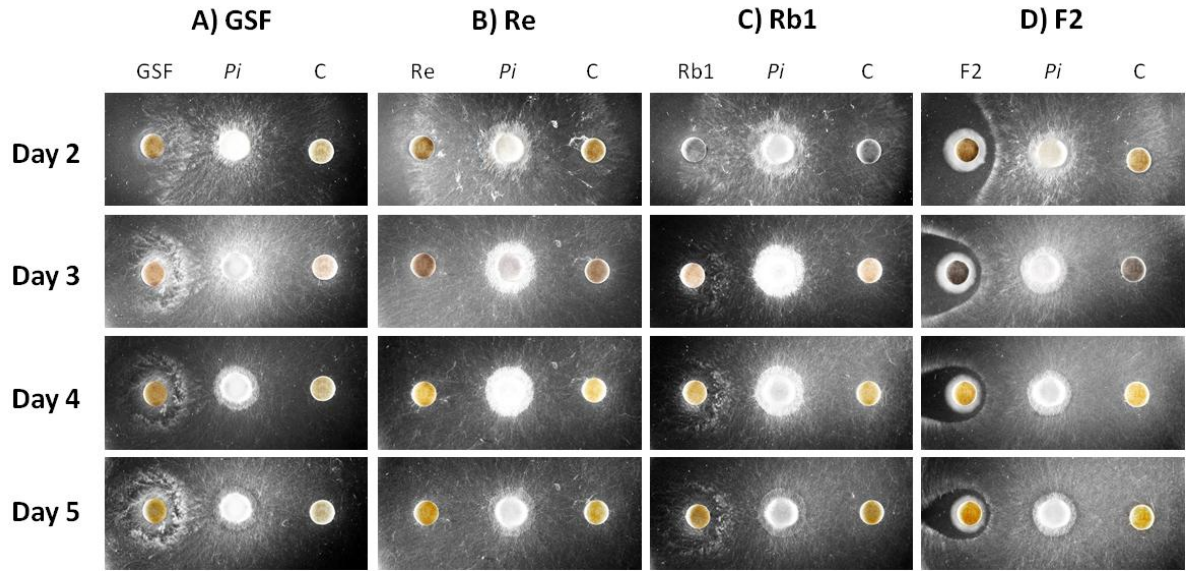

Figure 4.5. Effect of ginsenosides on *Pythium irregulare* BR 1068 growth *in vitro*. Representative images of 90 mm petri dishes filled with Czapek Dox Mineral Agar containing 6 mm antibiotic-assay discs placed an equal distance from an 8 mm diameter plug of *P. irregulare* BR 1068 are portrayed. Discs on the left in each column are infused with 100 µL, A) 10 mg mL^{-1} purified ginsenoside extract [GSF (G)], B) 5 mg mL^{-1} ginsenoside Re, C) 5 mg mL^{-1} ginsenoside Rb1 or D) 5 mg mL^{-1} ginsenoside F2. All discs on the right in each column are controls infused with 10 0 µL MeOH. Experiment was performed in triplicate (N = 3). Images shown are representative of a single plate, for each treatment, monitored every 24 hours for 120 hours. Earlier (24 hour) images are not included because mycelia had not reached filters and no effects were seen in any treatments. All ginsenosides were dissolved in MeOH.

there was a half-ring of enhanced mycelial growth around the disc and the beginning of aerial hyphal growth. Then after four days, there was accumulation of mycelia a short distance away from the filter and almost a complete ring of mycelia around the filter disc. After five days of growth, the ring of mycelia around the filter was complete and mycelial growth projected beyond it.

In contrast to the patterns of mycelial growth observed after exposure to the above ginsenosides, the growth of mycelia was clearly inhibited around the assay disc infused with 5 mg mL^{-1} of the 20 (S)-protopanaxadiol ginsenoside F2 (Fig. 4.5D). Even after two days of growth, inhibition of mycelial growth towards the F2 infused assay disc was visually evident. This zone of inhibition a short distance away from the F2 infused disc became more prominent after three days as the mycelia visibly grew around and away from the disc. While the inhibitory effect of F2 persisted throughout the five day time course, it did appear to diminish, as mycelia began to grow around the filter disk, almost completely surrounding it by the end of the experiment. However, mycelia were never seen to grow through the filter; neither was any aerial growth observed and no growth enhancement was evident at any time during the time course. Importantly, the apparent discolouration observed in the medium around the F2 infused discs is attributed to ginsenoside that has leached into the agar medium from the disc after evaporation of the MeOH solvent. This effect is present in all other ginsenoside infused filters to varying degrees, and arises from manipulation of the lighting used to provide contrast between the mycelia and background medium.

It should also be noted, that the effects on mycelial growth of all ginsenoside treatments, except ginsenoside Re, have been shown to be dose dependent (see Supporting Information Fig. S4.1-S4.4). That is, enhanced mycelial growth increased with ginsenoside concentration around filters treated with purified total ginsenosides (GSF) and ginsenoside Rb1, while the zone of inhibition around discs infused with ginsenoside F2 increased with concentration.

4.4. Discussion

The potential role of ginsenosides to act as chemoattractants for ginseng root pathogens like *Pythium irregulare*, when secreted into the rhizosphere, and facilitate the infection of American ginseng (*Panax quinquefolius*), has been suggested but never thoroughly studied (Bernards et al. 2011; Ivanov and Bernards 2012). In this report we examined this interrelationship *in vivo* by monitoring the disease severity of *P. irregulare* infection, using a chlorophyll fluorescence imaging technique (Chapter 3; Ivanov and Bernards *submitted*), on ginsenoside-treated and -untreated seedlings (both one- and two-year old), in a pot-based experiment.

Before this experiment was conducted it was confirmed that ginsenosides can diffuse through a moist soil matrix, identical to the one employed for the *in vivo* assay (Fig. 4.3). The accumulation of the most abundant 20 (S)-protopanaxadiol ginsenoside (Rb1) was monitored over time at various distances from a point source of ginsenoside spiked sand using LC-MS. Two days after initiation of the experiment, ginsenoside Rb1 was detected 2 and 4 cm away from the point source. It then took until Day 6 for ginsenoside Rb1 to be detected 8 cm from the point source. There was also an accumulation of ginsenosides over time as the amount of ginsenosides at every distance sampled was highest by Day 8, the last day of the time course. In the *in vivo* assay, it was assumed that ginsenosides exogenously applied to the roots of ginseng plants would similarly move into the sand, and therefore be encountered by the mycelia of *P. irregulare* before the pathogen could grow to the root, as ginsenosides would migrate towards the pathogen point source.

Previously, *in vitro* exposure of *P. irregulare* and other ginseng root pathogens to ginsenosides was shown to stimulate their growth in the absence of a sugar source (Nicol et al. 2003; Yousef and Bernards 2005, Zhao et al. 2012). Furthermore, the metabolism of terminal sugar moieties from the common 20 (S)-protopanaxadiol ginsenosides via extracellular ginsenosidases secreted by *P. irregulare*, which facilitates the formation of ginsenoside F2, has been correlated to increased pathogenicity of this organism toward ginseng. Therefore, we hypothesized that ginsenosides may act as chemoattractents for *P. irregulare,* and that early exposure to ginsenosides may facilitate quicker infection of ginseng by this organism (Bernards et al. 2011). However, in the present study, monitoring *in vivo* disease progression in ginseng plants treated and untreated with exogenous purified total

ginsenoside extract (GSF) revealed a protective role for ginsenosides in young plants, when treated with relatively high doses.

Disease severity and time to infection (TTI) of *P. irregulare* in ddH_2O soaked and ginsenosides soaked one- and two- year old ginseng plants was monitored by measuring the quantum yield of non-regulated quenching processes (ΦNO) using chlorophyll fluorescence imaging. This chlorophyll fluorescence parameter is the most sensitive of the slow induction chlorophyll fluorescence parameters at detecting biotic stress, *in vivo*, and has been used as a non-invasive method to identify and track over time the infection of ginseng by *P. irregulare* (Chapter 3; Ivanov and Bernards *submitted*). Furthermore, determination of ΦNO has been shown to be as effective in monitoring disease progression in ginseng as the measurement of the maximum quantum efficiency of PSII (Fv/Fm) (Chapter 3; Ivanov and Bernards *submitted*). The parameter Fv/Fm has previously been used to study fungal/oomycete plant pathogen infections *in vivo* in a number of different species like bean (*Phaseolus vulgaris*) (Chaerle et al. 2007), wheat (*Triticum aestivum*) (Kuckenberg et al. 2009), lettuce (*Lactuca sativa*) (Prokopová et al. 2010) and even American ginseng where a decrease in Fv/Fm has been correlated to increasing disease load (Ivanov and Bernards 2012). However, ΦNO was selected in our study because there is no need for dark adaptation of plants before measuring ΦNO and because this parameter can be monitored during steady state illumination at a wide range of light intensities (Klughammer and Schreiber 2008).

Our experiment showed that ΦNO values gradually increased for the duration of the infection period in one- and two-year old control plants that had been soaked in ginsenoside extract (GSF) but not exposed to *P. irregulare* (Fig. 4.4A, B). This gradual change in ΦNO can be attributed to non-pathogen related stress in the plants monitored as a result of transplantation and manipulation during the experiment. This can be further supported by the lack of visible symptoms of *P. irregulare* infection on the plants in the control group at any point during the time course. Values of ΦNO for the control treatment (ddH_2O soaked) plants exposed to *P. irregulare* inoculum showed that infection, monitored by a sharp rise in ΦNO in one-year old plants began approximately 2 days earlier compared to two-year old plants (Fig 4.4A, B). Furthermore, the infection period in two-year old plants, which is measured by the time it took ΦNO values to stabilize at a higher magnitude, was 2 days longer than in one-year old plants. This falls in line with previous studies, which show that mature ginseng plants are more resistant to *P. irregulare* infection than one-year old seedlings (Ivanov and

Bernards 2012; Chapter 3, Ivanov and Bernards *submitted*). For this reason the monitoring period of the infection time course was five days longer for two-year old plants in our *in vivo* assay to allow extra time for infection to take place.

The values of ΦNO from plants soaked in purified total ginsenoside extract and exposed to *P. irregulare*, however, showed that infection by the pathogen was delayed by approximately five days in one-year old plants compared to the same age plants from the control treatment group (Fig. 4.4A, B). These results were surprising since Nicol et al. (2003) previously demonstrated that *in vitro* exposure to ginsenosides increased *P. irregulare* growth, and by extension, we predicted that the pathogen would grow faster in the presence of increased concentrations of ginsenosides, consequently locating and infecting the ginsenoside soaked plants sooner than the water soaked plants. Instead, ginsenosides present in the rhizosphere around ginsenoside-treated one-year old plants at the dosage applied, may have provided temporary protection, ultimately delaying infection. This conclusion is supported by data from two-year old plants, where increases in the values of ΦNO in ginsenoside treated plants were gradual and in line with those observed in control ginsenoside treated plants which were not exposed to *P. irregulare* inoculum. This suggests that ginsenosides may have mitigated or delayed infection of more mature plants to a greater extent than in one-year old plants.

Alternatively, the presence of relatively large doses of ginsenosides in the rhizosphere may have simply altered the growth pattern of the pathogen in the soil, as seen when *P. irregulare* is grown in medium supplemented with ginsenosides (Nicol et al. 2002; 2003; see also below). Moreover, *P. irregulare* has been shown to directly interact with ginsenosides *in vitro*, by deglycosylating them into ginsenoside F2 (Yousef and Bernards 2005, Neculai et al. 2009; Ivanov and Bernards, 2012). It is possible, therefore, that this interaction results in altered patterns of growth in the soil, which may have the secondary effect of delaying infection. Unfortunately, our attempts to directly assess the extent of *P. irregulare* growth in the pots, using ITS region nuclear ribosomal DNA markers (Okubara et al. 2006; Schroeder et al. 2006, Kernaghan et al. 2007, 2008) were unsuccessful, and further studies are necessary to explore the hypothesis that rhizosphere ginsenosides alter *P. irregulare* growth in advance of infection.

The effects of a purified total ginsenoside extract and selected pure protopanaxadiol and -triol ginsenosides (Rb1, Re and Ginsenoside F2) on the growth of *P. irregulare, in vitro*,

allowed us to gain a more complete understanding of what effect a point source of ginsenosides has on the growth pattern of the pathogen. Specifically, there was an accumulation of mycelia around assay discs infused with 10 mg mL^{-1} purified total ginsensides extract (GSF) or 5 mg mL^{-1} ginsenoside Rb1, within 2 days, compared to control filter discs (Fig 4.5). The concentration of Rb1 used is half of the concentration of total ginsenoside extract because it coincides with the approximate amount of Rb1 in the total ginsenoside extract. The mycelia were observed a short distance away from the treatment discs and in time created a ring of enhanced growth around the discs. Presumably this is the primary point of contact between the pathogen and the ginsenosides because otherwise *P. irregulare* mycelia grew thinly and in all directions until within close proximity to the treated discs. In the subsequent days, there was extensive mycelial growth and hyphal branching observed around the GSF and Rb1 treated discs. However, after close inspection hyphal growth was not inhibited by this accumulation and spread directly through the treated filter discs the same way it did through the controls. By contrast, the common protopanaxatriol ginsenoside Re had no effect, positive or negative, on the growth of *P. irregulare in vitro*. This suggests that the protopanaxadiol ginsenosides, which are the only ginsenosides shown to be enzymatically altered by *P. irregulare* (Yousef and Bernards 2005; Neculai et al. 2009; Ivanov and Bernards 2012), are also the more bioactive towards the pathogen and it lends support to the hypothesis that enzymatic alteration of ginsenosides is involved in the alteration of growth and the potential infection strategy of *P. irregulare*.

It is not clear from this *in vitro* data if the enhanced growth of *P. irregulare* in the presence of protopanaxadiols was due to ginsenosides acting as chemoattractants or simply serving as a growth factor. Furthermore, while ginsenoside Rb1 appeared to stimulate pathogen growth on its own, the effect of the ginsenoside mixture was greater and correlated to the increased concentration of ginenosides applied. Ginsenoside Rb1 applied in the same concentration as the ginsenoside mixture showed an equivalent level of growth stimulation (Supporting Information Fig. S4.1, S4.2, S4.3 and S4.4). Therefore, we can see that ginsenoside Rb1 is involved in growth stimulation of *P. irregulare* but is not the only ginsenoside that has this effect. One hypothesis, mentioned previously, is that the ginsenosides act as a source of sterols for *P. irregulare*. Oomycetes, such as *P. irregulare*, are unable to synthesize sterols (Wood and Gottlieb, 1978) and therefore deploy sterol-carrying proteins, known as elicitins, in order to acquire sterols from their environment

(Mikes *et al*., 1997). Ginsenosides are structurally and biosynthetically similar to sterols (Liang and Zhao 2007). However, their bidesmosidic nature suggests that most likely they are not incorporated into *P. irregulare* membranes (Yousef and Bernards 2005). Instead, *P. irregulare,* which metabolizes protopanaxadiol ginseng saponins via extracellular glycosidases to form ginsenoside F2, may internalize this product resulting in the altered growth pattern and growth stimulation observed (Yousef and Bernards 2005, Bernards et al. 2011). Ginsenoside F2 may thus act as a growth hormone in *Pythium* species as has been shown for other sterols (Nes 1987).

This possibility was also tested, but contrary to our expectations, our *in vitro* assay clearly indicated that ginsenoside F2 caused a well-defined zone of inhibition and limited *P. irregulare* growth (Fig. 4.5D). However, this inhibitory effect began to diminish after 3 days and hyphal growth almost surrounded the filter disc but did not go through it 5 days after initiation of the experiment.

It remains unclear why *P. irregulare* invests the energy to convert ginsenosides into ginsenoside F2, when in fact the growth of this organism is visibly inhibited when it encounters the pure compound. It is possible that *P. irregulare* adjusts its metabolism in the presence of ginsenosides, and its reaction to the compound F2 requires this metabolic shift in order to circumvent the potential deleterious effects that it can have on growth. This metabolic shift may be part of a physiological change in the pathogen that facilitates the infection of ginseng, as suggested by the strong correlation between the ability of *P. irregulare* to convert ginsenosides into ginsenoside F2 and its pathogenicity (Ivanov and Bernards 2012).

4.5. Conclusion

In conclusion, we have demonstrated that the treatment of ginseng plants with a relatively high dose of ginsenosides by dipping their roots into a solution of ginsenosides prior to planting results in a delay of infection by *P. irregulare* in pot experiments, as monitored by non-invasive Chl fluorescence imaging. It remains unclear whether this observation results from a protective effect of the ginsenosides, or from a modification of *P. irregulare* growth, as observed in our *in vitro* assays, that delays hyphal progression while enhancing hyphal build-up. While we set out to test the hypothesis that ginsenosides act as chemoattractants for *P. irregulare in vivo*, our results suggest that instead, ginsenosides serve to alter the growth and metabolism of this organism, which may serve to facilitate infection.

4.6. References

Abe, I., Rohmer, M., Prestwich, G.D., 1993. Enzymatic cyclization of squalene and oxidosqualene to sterols and triterpenes. Chem. Reviews 93, 2189-2206.

Anderson, R.C., Fralish, J.S., Armstrong, J.E., Benjamin, P.K., 1993. The ecology and biology of *Panax quinquefolium* L. (*Araliaceae*) in Illinois. Am. Midl. Nat. 129, 357-372.

Ameson, P.A., Durbin, R.D., 1968. The sensitivity of fungi to *a*-tomatine. Phytopathology 58, 536-537.

Attele, A.S., Wu, J.A., Yuan, C.S., 1999. Ginseng pharmacology: Multiple constituents and multiple actions. Biochem. Pharmacol. 58, 1685-1693.

Bernards, M.A., Ivanov, D.A., Neculai, A.M., Nicol, R.W., (2010) Ginsenosides: Phytoanticipins or host recognition factors? Recent Advances in Phytochemistry 41, 13-32.

Braun, P.G., 1991. The combination of *Cylindrocarpon lucidum* and *Pythium irregulare* as a possible cause of apple replant disease in Nova Scotia. Can. J. Plant Pathol. 13, 291-297.

Braun, P.G., 1995. Effects of *Cylindrocarpon* and *Pythium* species on apple seedlings and potential role in apple replant disease. Can. J. Plant Pathol. 17, 336-41.

Chaerle, L., Hagenbeek, D., Vanrobeys, X., Van Der Straeten, D., 2007. Early detection of nutrient and biotic stress in *Phaseolus vulgaris*. Int. J. Remote Sens. 28, 3479-3492.

Chappell, J., 2002. The genetics and molecular genetics of sterol and terpene origami. Curr. Op. Plant Biol. 5, 151-157.

Cheng, L.Q., Na, J.R., Kim, M.K., Bang, M.H., Yang, D.C., 2007. Microbial conversion of ginsenoside Rb1 to minor ginsenoside F2 and gypenoside XVII by *Intrasporangium sp*. GS603 isolated from soil. J. Microbiol. Biotechnol. 17, 1937-1943.

Court, W.A., Reynolds, L.B., Hendel, J.G. 1996. Influence of root age on the concentration of ginsenosides of American ginseng (*Panax quinquefolium*). Can. J. Plant Sci. 76, 853-855.

Fenwick, G.R., Price, K.R., Tsukamota, C., Okubo, K., 1992. Saponins. *In* Toxic Substances in Crop Plants, J.P. DMello, C.M., Duffus, and J.H. Duffus, eds (Cambridge, UK: Royal Society of Chemistry), pp. 285-327.

Gaulin, E., Bottin, A. Bernard, D., 2010. Sterol biosynthesis in oomycete pathogens. Plant Signal Behav. 5, 258-260.

Hostettmann, K., Marston, A., 1995. Saponins. Chemistry and Pharmacology of Natural Products. Cambridge University Press, Cambridge, U.K, pp. 329-337.

Howard, R.J., Garland, J.A., Seaman, W.L., 1994. Diseases and pests of vegetable crops in Canada. Canadian Phytopathological Society and Entomological Society of Canada, Ottawa, ON, pp. 11-15.

Ivanov, D.A., Bernards, M. A., 2012. Ginsenosidases and the pathogenicity of *Pythium irregulare*. Phytochemistry 78, 44-53.

Kernaghan, G., Reeleder, R.D., Hoke, S.M.T., 2007. Quantification of *Cylindrocarpon destructans* f. sp. *panacis* in soils by real-time PCR. Plant Pathol. 56, 508–516.

Kernaghan, G., Reeleder, R.D., Hoke, S.M.T., 2008. Quantification of Pythium populations in ginseng soils by culture dependent and real-time PCR methods. Appl. Soil Ecol. 40, 447-455.

Keukens, E.A.J., de Vrije, T., van den Boom, C., de Waard, P., Plasma, H.H., Thiel, F., Chupin, V., Jongen, W.M.F., de Kruijff, B., 1995. Molecular basis of glycoalkaloid induced membrane disruption. Biochim. Biophys. Acta 1240, 216-228.

Klughammer, C., Schreiber, U., 2008. Complimentary PSII quantum yields calculated from simple chlorophyll fluorescence parameters measured by PAM fluorometry and the Saturation Pulse method. PAM Application Notes 1, 27-35.

Kramer D.M., Johnson G., Kiirats O. Edwards G.E., 2004. New fluorescence parameters for determination of QA redox state and excitation energy fluxes. Photosynth. Res. 79, 209-218.

Krupa, S.V., Dommergues, Y.R., 1979. Ecology of root pathogens, in: Developments in agricultural and managed-forest ecology. Elsevier Scientific Publishing Company, Amsterdam, pp. 14-17.

Kuckenberg, J., Tartachnyk, I., Noga, G., 2009. Temporal and spatial changes of chlorophyll fluorescence as a basis for early and precise detection of leaf rust and powdery mildew infections in wheat leaves. Precision Agric. 10, 34–44.

Liang, Y., Zhao, S., 2007. Progress in understanding of ginsenoside biosynthesis. Plant Biology 10, 415-421.

Mai, W.F., Abawi, G.S., 1981. Controlling replant diseases of pome and stone fruits in Northeastern United States by preplant fumigation. Plant Disease 65, 859-864.

Marshall, J.A., Dennis, A.L., Kumazawa, T., Haynes, A.M., Nes, W.D., 2001. Soybean sterol composition and utilization by *Phytophthora sojae*. Phytochemistry 58, 423-428.

Mazzola, M., 1998. Elucidation of the microbial complex having a causal role in the development of apple replant disease in Washington. Phytopathology 88, 930-938.

Mazzola, M., Brown, J., 2010. Efficacy of brassicaceous seed meal formulations for the control of apple replant disease in conventional and organic production systems. Plant Dis. 94, 835-842.

Mercado-Blanco, J., Collado-Romero, M., Parrilla-Araujo, S., Rodriguez-Jurado, D., Jimenez-Diaz, R.M., 2003. Quantitative monitoring of colonization of olive genotypes by *Verticillium dahliae* pathotypes with real-time polymerase chain reaction. Physiol. Mol. Plant Pathol. 63, 91-105.

Mikes, V., Milat, M.L., Ponchet, M., Ricci, P., Blein, J.P., 1997. The fungal elicitor cryptogein is a sterol carrier protein. FEBS Lett. 416, 190-192.

McGraw, J.B., Lubbers, L.E., Van der Voort, M., Mooney, E.H., Furedi, M.A., Souther, S., Turner, J.B., Chandler, J., 2013. Ecology and conservation of ginseng (*Panax quinquefolius*) in a changing world. Ann. N.Y. Acad. Sci. 1286, 62-91.

Neculai, M.A., Ivanov, D., Bernards, M.A., 2009. Partial purification and characterization of three ginsenoside-metabolizing [beta]-glucosidases from *Pythium irregulare*. Phytochemistry 70, 1948-1957.

Nes, W.D., Stafford, A.E., 1983. Evidence for metabolic and functional discrimination of sterols by *Phytophthora cactorum*. Proc. Natl. Acad. Sci. 80, 3227-3231.

Nes, W.D., 1987. Biosynthesis and requirement for sterols in the growth and reproduction of Oomycetes. In: Fuller, G., Nes, W.D. (Eds.), Ecology and Metabolism of Plant Lipids. American Chemical Society, Washington, DC, pp. 304-328.

Nes, W.D., Saunders, G.A., Heftmann, E., 1983. A reassessment of the role of steroidal alkaloids in the physiology of *Phytophthora*. Phytochemistry 22, 75-78.

Nicol, R.W., Traquair, J.A., Bernards, M.A., 2002. Ginsenosides as host resistance factors in American ginseng (*Panax quinquefolius*). Can. J. Bot. 80, 557-562.

Nicol, R.W., Yousef, L., Traquair, J.A., Bernards, M.A., 2003. Ginsenosides stimulate the growth of soilborne pathogens of American ginseng. Phytochemistry 64, 257-264.

Okubara, P.A, Schroeder, K.L, Paulitz, T.C., 2005. Real-time polymerase chain reaction: applications to studies on soilborne pathogens. Can. J. Plant Pathol. 27, 300–313

Olsen, R.A., 1971. Triterpeneglycosides as inhibitors of fungal growth and metabolism. I. Effect on growth, endogenous respiration and leakage of UV absorbing material from various fungi. Physiol. Plantarum. 24, 534-543.

Osbourn, A.E., 1996. Preformed antimicrobial compounds and plant defense against fungal attack. Plant Cell. 8, 1821–1831.

Pritts, K.D., 2010. Ginseng: how to find, grow, and use America's forest gold. Stackpole Books.

Prokopová, J., Spundova, M., Sedlarova, M., Husickova, A., Novotny´ , R., Dolezal, K., Naus, J., Lebeda, A., 2010. Photosynthetic responses of lettuce to downy mildew infection and cytokinin treatment. Plant Physiol. Biochem. 48, 716–723.

Reeleder, R.D., Brammall, R.A., 1994. Pathogenicity of *Pythium* species, *Cylindrocarpon destructans* and *Rhizoctonia solani* to ginseng seedlings in Ontario. Can. J. Plant Pathol. 16, 311-316.

Reeleder, R.D., Roy, R., Capell, B., 2002. Seed and root rots of ginseng (*Panax quinquefolius*) caused by *Cylindrocarpon destructans* and *Fusarium* spp. J. Ginseng Res. 26, 151-158.

Schroeder, K.L., Okubara, P.A., Tambong, J.T., Lévesque, C.A., Paulitz, T.C., 2006. Identification and quantification of pathogenic *Pythium* spp. from soils in Eastern Washington using real-time polymerase chain reaction. Ecol Epidemiol. 96, 637-647.

Small, E., Catling, P.M., 1999. Canadian medicinal crops. NRC Research Press, Ottawa, ON, pp. 7-12.

Teng, R., Li, H., Chen, J., Wang, D., He, Y., Yang, C., 2002. Complete assignment of 1H and 13C NMR data for nine protopanaxatriol glycosides. Magn. Reson. Chem. 40, 483-488.

Tuite, J., 1969. Plant Pathological Methods. pp. 233. Burgess Publishing Co., Minneapolis. MN, USA.

van Kooten, O., Snel J., 1990, The use of chlorophyll fluorescence nomenclature in plant stress physiology. Photosynth. Res. 25, 147-150.

Wen, J., Zimmer, E.A., 1996. Phylogeny and biogeography of *Panax* L. (the ginseng genus, *Araliaceae*): inferences from ITS sequences of nuclear ribosomal DNA. Mol. Phylogenet. Evol. 6, 167-177.

Wood, S.G., Gottlieb, D., 1978. Evidence from mycelial studies for differences in the sterol biosynthetic pathway of *Rhizoctonia solani* and *Phytophthora cinnamomi*. Biochem. J. 170, 343-354.

Yang, M., Zhang, X., Xu, Y., Mei, X., Jiang, B., Liao, J., Yin, Z., Zheng, J., Zhao, Z., Fan, L., He, X., Zhu, Y., 2015. Autotoxic ginsenosides in the rhizosphere contribute to the replant failure of *Panax notoginseng*. PLoS ONE 10, doi:10.1371/journal.pone.0118555.

You, J., Liu, X., Zhang, B., Xie, Z., Hou, Z., Yang, Z., 2015. Seasonal changes in soil acidity and related properties in ginseng artificial bed soils under a plastic shade. J. Ginseng Res. 39, 81-88.

Yousef, L.F., Bernards, M.A., 2006. *In vitro* metabolism of ginsenosides by the ginseng root pathogen *Pythium irregulare*. Phytochemistry 67, 1740-1749.

Zhao, X., Gao, J., Song, C., Fang, Q., Wang, N., Zhao, T., Liu, D., Zhou, Y., 2012. Fungal sensitivity to and enzymatic deglycosylation of ginsenosides. Phytochemistry 78, 65-71.

Chapter 5: Sequencing and Preliminary Bioinformatics Analysis of a Potential Ginsenoside Metabolising ß-glucosidase from *P. irregulare*

5.1. Introduction

Ginseng root has been used as an herbal medicine in many East Asian countries for thousands of years and is widely used around the world today (Attele et al. 1999; Kiefer and Pantuso 2003; Ligor et al. 2005; Wang and Yuan 2008). Ginsenosides, a class of triterpenoid saponins are considered to be the principal pharmacologically active compounds produced by ginseng plants. These ginseng saponins have been reported to have biological effects on the central nervous system (Christensen 2009), cardiovascular system (Wang et al. 2007) and have been shown to possess various antidiabetic (Attele et al. 2002), anticancer (Qi et al. 2010) and immunomodulatory properties (Predy et al. 2006).

The synthesis of these molecules is unique to the genus *Panax* (family *Araliaceae*) which includes 17 species with the most widely utilized and cultivated being American ginseng (*Panax quinquefolius* L.) and Asian ginseng (*Panax ginseng* C.A. Mey.) (Wen and Zimmer 1996, Jia and Zhao 2009). To date more than >40 different ginsenosides have been isolated from ginseng roots (Cheng et al. 2007), which is where commercially available ginseng extracts are obtained from, and more than >180 have been identified in total, depending on species and location of the plant they were isolated from (Christensen 2009; Jia and Zhao 2009).

Ginsenosides can be categorized as either oleanane-type or dammarane-type saponins based on the structure of their aglycones (Liang and Zhao 2008). Most ginsenosides, however, have a dammarane carbon skeleton, comprised of four trans-oriented rings with mono- and dissacharide carbohydrate moieties attached to carbons on the parent aglycone (Attele et al. 1999; Liang and Zhao 2008). These ginsenosides are further classified based on the hydroxylation pattern of the parent triterpenoid as either protopanaxadiol or protopanxatriol ginsenosides (Teng et al. 2002) with diols containing saccharide-side chains at the C-3 and C-20 positions and triols at the C-6 and C-20 positions (Hostettmann and Marston 1995).

The most common ginsenosides (Rb1, Rb2, Rc, Rd, Re and Rg1) are a mixture of protopanaxadiol and -triol ginsenosides and comprise more than 80% of total ginsenosides in Asian and American ginseng roots (Qu et al. 2009; Shi et al. 2007). However, the minor

ginsenosides (F1, F2, Rg3, Rh1, Rh2, compound Y, compound Mc and compound K), which are present in low concentrations in ginseng species, are believed to have superior pharmacological activities to those of the major ginsenosides (Park et al. 2010). This is because major ginsenosides are bidesmosidic (contain two carbohydrate side-chains) and absorbed poorly by the human gastrointestinal tract, in contrast to the minor ginsenosides, which are absorbed more readily because they are monodesmosidic (Tawab et al. 2003; Karikura et al. 1991).

The ability to transform major ginsenosides into minor ginsenosides therefore, has major implications for the pharmaceutical industry and there are numerous methods that have been used to facilitate these transformations including acid hydrolysis and heating, as well as microbial and enzymatic transformations (Park et al. 2010). Human intestinal bacteria including *Bifidobacterium breve* (Shin et al. 2003), *Fusobacterium* sp. (Park et al. 2001), *Lactobacillus delbrueckii* (Chi et al. 2006), and *Leuconostoc paramesenteroides* (Chi et al. 2006) all have the ability to metabolize orally ingested ginsenosides; however, this microbial transformation has low yield and poor productivity. Likewise, microorganisms isolated from field-grown ginseng plants including fungi such as *Curvularia lunata* (Dong et al. 2003), *Fusarium sacchari* (Han et al. 2007), *Paecilomyces bainier* (Zhou et al. 2008), *Cylindrocarpon destructans* (Zhao et al. 2012), oomycetes such as *Pythium irregulare* (Yousef and Bernards 2005), and bacteria such as *Bacillus megaterium* (Kim et al. 2005), *Burkholderia pyrrocinia* (Kim et al. 2005) and *Caulobacter leidyia* (Cheng et al. 2006) have also been shown to transform common ginsenosides, by cleaving sugar side-chains from the parent sapogenin. However, due to higher specificity, yield and productivity, the production of minor ginsenosides through the hydrolysis of the carbohydrate side-chains in major ginsenosides using recombinant ß-D-glycosidases has been shown to be the most efficient method for transformation (Park et al. 2010).

Many ginsenoside transforming recombinant ß-D-glycosidases from various organisms have recently been purified and used for ginsenoside transformation (Noh and Oh 2009; Noh et al. 2009; Ruan et al. 2009; An et al. 2012; Cui. et al. 2013). Purification of these enzymes can be conducted in a one-step processes and they have a relatively high yield because they can hydrolyze several ginsenosides simultaneously due to their varying substrate specificities (Park et al. 2010). This makes them better suited for large scale production than native enzymes. However, in order to hydrolyze ginsenosides even more

efficiently, novel recombinant ginsenoside hydrolyzing enzymes with high catalytic efficiencies and specificity for ginsenosides are needed.

Previous studies have indicated that the ginseng pathogen *Pythium irregulare*, is able to selectively deglycosylate the common 20 (S)-protopanaxadiol ginsenosides (Rb1, Rb2, Rc, Rd, and gypenoside XVII (GXVII) by means of extracellular glycosidases into ginsenoside F2 (Yousef and Bernards 2006, Neculai et al. 2009). It has also been shown that the production of ginsenoside metabolizing glycosidases (ginsenosidases) is induced, *in vitro,* when *P. irregulare* is exposed to ginsenosides (Yousef and Bernards 2006, Neculai et al. 2009, Ivanov and Bernards 2012) and that the ability to deglycosylate ginsenosides has an undefined functional role in increasing the pathogenicity of *P. irregulare* towards ginseng plants (Ivanov and Bernards 2012; Chapter 4)

The ginsenoside metabolizing enzymes responsible for this transformation have been purified from *P. irregulare* culture filtrates and partially characterized (Neculai et al. 2009). The three specific glycosyl hydrolases isolated were glycosidase 1 (G1), a homodimer of two 78 kDa subunits and glycosidases 2 (G2) and 3 (G3) which are monomeric enzymes of 61 and 57 kDa, respectively (Neculai et al. 2009). These glycosyl hydrolases possess different catalytic specificities towards ginseng saponins, with G1 exhibiting specific ß(1→6) glucosidase activity and the ability to convert ginsenosides Rb1 and GXVII into ginsenosides Rd and F2, respectively, and G2 and G3 showing specific ß (1→2) glucosidase activity and the ability to convert Rb1 and Rd into GXVII and F2, respectively (Neculai et al. 2009). Furthermore, partial *de-novo* sequencing of G1 peptide fragments showed it to be a protein that is novel to *P. irregulare*, while sequence analysis of G2 and G3 clearly placed these enzymes amongst the ß-glucosidases, most likely belonging to glycosyl hydrolase (GH) family 1 (Neculai et al. 2009). Glycoside hydrolases are classified into 115 families according to the Carbohydrate-Active Enzyme classification server, CAZy (Lombard et al. 2014) and ß-glucosidases that metabolize ginsenosides are most commonly classified into GH families 1 and 3 (Park et al. 2010; Cui et al. 2013).

In the present study, *de-novo* amino-acid sequence data obtained by Neculai et al (2009) from purified ginsenosidases G2 and G3 was used to design degenerate oligonucleotide primers in order to amplify the genes potentially encoding these ß(1-2)-glucosidases. This allowed us to obtain the full coding sequence for one potential ginsenoside metabolizing ß-glucosidase, denoted PiGH1-x from *P. irregulare.* Following amplification,

DNA fragments were cloned into pFLAG-CTS expression vector, which eventually will be used for the synthesis of large amounts of the protein once the constructor is transformed into *E. coli*. At this time, however, we can only distinguish what glycosyl hydrolase family the protein encoded belongs to and not whether it is G2 or G3. This is the first ever reported gene of a potential ginsenosidase isolated from *P. irregulare.*

5.2. Materials and Methods

5.2.1. *Pythium irregulare* strain and culture conditions

Pythium irregulare (BR 1068) was obtained from the Canadian Collection of Fungal Cultures (CCFC, Ottawa, Canada) and was maintained on potato dextrose agar (PDA) medium at 22°C, in the dark. For genomic DNA extraction, one 8 mm diameter plug of a 3-day old PDA culture of *P. irregulare* was placed in 25 mL sterile V8 broth (strained through 8-layers of cheesecloth, contained in a 90 mm petri dish (Tuite 1969). V8 cultures were incubated at 22°C in the dark for 5 days. After incubation, mycelium was collected by vacuum filtration using 0.45 µm nylon membranes, flash frozen in liquid N_2 and stored at -80°C. For RNA extraction, *P. irregulare* was initially grown on PDA at 22°C in the dark, for 3 days. Next, 10 mL liquid cultures were initiated by inoculating Czapek-Dox minimal salt media, supplemented with 1% sucrose (w/v), with an 8 mm diameter plug of *P. irregulare*. Liquid cultures were grown for 5 days in the dark at 22°C on a rotary shaker after which mycelia from each culture were transferred into 10 mL of Czapek-Dox minimal salt media with no sugar source, and the cultures were grown for an additional 7 days. The transferred cultures were then supplemented with 4 mg/mL purified ginsenoside extract (dissolved in ddH_2O and filter sterilized through a 0.22 µm PVDF syringe tip membrane). The ginsenoside-supplemented cultures were then incubated for a further 24 hours, after which the mycelia were collected by vacuum filtration using 0.45 µm nylon membranes, flash frozen in liquid N_2 and stored at -80°C.

5.2.2. Degenerate primers for PCR

To identify fragments of the nucleotide and amino acid sequences that encode ß(1-2)-glucosidase(s) from *P. irregulare* isolated by Neculai et al. (2009), mycelia from the organism was ground in liquid nitrogen, and genomic DNA was extracted using the DNeasy plant mini kit (Qiagen N.V., Venlo, Netherlands), according to manufacturer's instructions. Degenerate PCR primers were then designed from sequenced tryptic digest peptides of 61 kDa and 57 kDa ß-1,2 glycosidases, showing 100% confidence scores, isolated from *P. irregulare* (Neculai et al. 2009). To do this, two highly conserved regions among tryptic peptides, from both glucosidases, encoding amino acids with high homology to those sequenced in 6 proteins from *P. ultimum* BR 144 annotated as ß-glycosidases were identified

using BLASTp analysis (Altschul et al. 1990) of the Pythium Genome Database (http://pythium.plantbiology.msu.edu) (Levesque et al. 2010). These conserved regions with amino acid sequences T-P-S-L-W-D-D and P-E-F-S-T-E-E were then used to construct primers Gly2/3F4 and Gly2/3R2, respectively (Table 5.1). The subsequent PCR reaction was carried out in 50 µL total volume containing 60 mM Tris-SO_4 (pH 8.9), 18 mM ammonium sulphate, 2 mM $MgCl_2$, 0.4 mM of each dNTP, 0.3 µM of each primer, 5 units of Taq DNA polymerase (Invitrogen) and 100 ng genomic DNA isolated from *P. irregulare* as template. PCR amplification was performed under cycling conditions that included an initial denaturation step of 2 min at 94°C, followed by 30 cycles of 45 s at 94°C (melting), 45 s at 52°C (annealing), 3 min at 72°C (extension), and a final extension step of 10 min at 72°C.

5.2.3. Cloning, transformation and sequencing

PCR resulted in the amplification of fragments with the expected size of approximately 800 bp, these fragments were amplified and extracted from a 1% agarose gel after electrophoretic separation using a QIAquick Gel Extraction Kit (Qiagen N.V., Venlo, Netherlands). The fragments were then inserted into the pGEM-Teasy expression vector, according to manufacturer's instructions in the pGEM-Teasy vector kit (Promega Corp. Fitchburg, WI, USA). The resulting plasmids were transformed into *Escherichia coli* DH5α competent cells by heat shock according to manufacturer instructions (Invitrogen, Walthamm MA, USA). Recombinant plasmids were then extracted from 30 recombinant bacterial colonies using QIAprep spin Miniprep Kit (Qiagen N.V., Venlo, Netherlands) and digested with FastDigest EcoRI to verify the presence of the expected insert. The PCR products were sequenced with T7 and Sp6 primers in a 3730xl DNA Analyzer (Applied Biosystems, Waltham, MA, USA) (Sanger et al. 1977) at the London Regional Genomics Centre (Robarts Research Institute, London, ON, Canada).

5.2.4. RNA isolation, 3' and 5' RACE experiments

To determine the full sequence of the ginsenoside metabolizing ß(1-2)- glucosidase(s) from *P. irregulare* the mycelia of the organism was ground in liquid nitrogen, and total RNA was extracted using the RNeazy plant mini kit (Qiagen N.V., Venlo, Netherlands). Primers for 3'RACE (3'GSP and 3'GSP/N) and 5'RACE (5'GSP1, 5'GSP2 and 5'GSP2/N) were then designed from the partial sequence of the putative glycosidase obtained using

Table 5.1. Primers utilized for degenerate PCR, 3' RACE, 5' RACE, and cloning of the full open reading frame (ORF) of the potential ginsenoside metabolizing glycosidase (PiGH1-x) in to pFLAG-CTS expression vector. (I is inosine, N is C, A, G or T).

Primer	Sequence (5'-3')	PCR Reaction (Primer direction)
Gly2/3F4	ACNCCNAGNNTNTGGGACGAC	Degenerate (F)
Gly2/3R2	CTCCTCNGCNGTAAACTCNGG	Degenerate (R)
3'GSP	ATTGTCGACCACTTCTACTACCC	3'RACE (F)
3'GSPN	GGATTCGGCTGGTTCTTCATTCC	3'RACE (F)
3'AUAP	GGCCACGCGTCGACTAGTAC	3'RACE (R)
5'GSP1	CGAGAGGGTAGTAGAAGTGGTCGA	5'RACE (R)
5'GSP2	CTTGAGCTCACTGTGCAATTCGC	5'RACE (R)
5'GSP2N	GCAATTCGCTCGGGAGGTCC	5'RACE (R)
5'AAP	GGCCACGCGTCGACTAGTACGGGIIGGGIIGGGIIG	5'RACE (F)
5'AUAP	GGCCACGCGTCGACTAGTAC	5'RACE (F)
G2/3HindIIIF	CCCAAGCTTTAATGAAGTGTCTGC	Cloning of ORF (F)
G2/3BglIIR	TTTAGATCTCTGTCCACGCACG	Cloning of ORF (R)

*All primers are presented 5'-3', but direction is noted in ( ) (F is Forward, R is Reverse)

degenerate PCR, in order to elucidate the full-length sequences of the potential ginsenosidase(s) (Table 5.1).

3'RACE first strand cDNA synthesis was initiated at the poly(A) tail of the mRNA in 5 µg total RNA, using the adaptor primer AP and Superscript II RT provided in the 3' RACE System for Rapid Amplification of cDNA Ends (Invitrogen, Waltham, MA, USA). Single strand cDNA was then used as the template for PCR in the presence of the 3'GSP primer and the abridged universal amplification primer (AUAP) provided in the Invitrogen 3'RACE kit. The resulting PCR product was then purified using a QIAquick PCR purification kit (Qiagen NV., Venlo, Netherlands) and a nested PCR was carried out using the purified PCR product from the previous reaction as template in a reaction mixture that contained the 3'GSPN nested primer and primer AUAP. Meanwhile, 5'RACE first strand cDNA was synthesized from 5 µg of total RNA using the specific 5'GSP1 primer we designed and Superscript II RT provided in the 5' RACE System for Rapid Amplification of cDNA Ends (Invitrogen). Then a homopolymeric tail was added at the 3'-end of the cDNA using Terminal deoxynucleotidyl transferase (TdT). This modified cDNA was then used as a template for PCR in the presence of the 5'GSP2 primer and the abridged anchor primer (AAP) provided in the Invitrogen 5'RACE kit. This PCR product was then purified using a QIAquick PCR purification kit (Qiagen N.V., Venlo, Netherlands) and diluted (1:1000) in a second PCR mixture containing the nested primer 5'GSP2N and the abridged universal amplification primer contained the 5'RACE kit.

The PCR conditions utilized and reaction mixture contents for all 3' and 5' RACE amplifications that were performed were according to the manufacturer's instructions. The cDNA fragments of both the 3'- and 5'-end extensions of the original 800 bp fragment, obtained from the RACE experiments, were then purified from an agarose gel and ligated by a standard cloning procedure, described above, into pGEM-Teasy expression vector. After transformation of plasmids into *E. coli* DH5α competent cells, 10 recombinant plasmid clones, from each of the 5' and 3' RACE experiments respectively, were selected, purified and subjected to automated sequencing, as described above.

5.2.5. Sequence editing and analysis

Cloned sequences from degenerate PCR and RACE experiments were trimmed of vector sequence using VecScreen at NCBI (http://www.ncbi.nlm.nih.gov). Assembly of the

fragments from degenerate PCR and RACE experiments, to obtain the full nucleotide sequence of the putative glycosidase(s), and subsequent translation to get the predicted amino acid sequence was performed using DNAMAN v.6.0 software (Lynnon LLC, San Ramon, CA, USA). The identity of the predicted glycosidase obtained from *P. irregulare,* was then confirmed by comparisons of the full nucleotide and amino acid sequence with sequences in the NCBI non-redundant protein sequences database, the Pythium Genome Database, GenBank (http://www.ncbi.nlm.nih.gov/genbank/) (Benson et al. 2013), NCBI Conserved Domain Database (CDD) (Marchler-Bauer et al. 2015), and the UniProt (http://www.uniprot.org/blast/) (The Uniprot Consortium 2015) databases using BLASTn and BLASTp analysis. The molecular mass and isoelectric point of the predicted glycosidase was determined using DNAMAN v.6.0 (Lynnon LLC, San Ramon, CA, USA).

Determination of the conserved amino acid motifs used for degenerate PCR design was carried out after *de-novo* sequenced tryptic digest fragments from 61 kDa and 57 kDa ß(1-2) glycosidases (Neculai et al. 2008) were used to identify 6 candidate ß-glycosidases from the Pythium Genome Database using BLASTp analysis. Sequence alignments of the tryptic digest fragments with the candidate ß-glycosidases was performed using Clustal X analysis (Thompson et al. 1997) in DNAMAN v6.0 (Lynnon LLC, San Ramon, CA, USA) in order to determine orientation for primer design and to predict the fragment size to be amplified by degenerate PCR. Sequence alignments of tryptic digest fragments, using Clustal X, to the predicted amino acid sequences of 800 bp fragments, generated by degenerate PCR, were also used to determine which fragments were candidate sequences of the glycosidases isolated by Neculai et al. (2009).

5.2.6. Cloning of ginsenosidase into expression vector

The complete gene encoding the predicted glycosidase (PiGH1-x), verified through *in silico* analysis, was amplified from genomic DNA and cDNA of *P. irregulare,* in order to verify absence of introns in the gene sequence. Primers G2/3HindIIIF and G2/3BglIIR (Table 5.1) were designed for amplifying the entire sequence of glycosidase G2/3, and had HindIII and BglII restriction sites inserted at the 5' and 3'ends, respectively. The full PCR-amplified sequence of glycosidase PiGH1-x, obtained from cDNA, was then ligated into the HindIII and BglII restriction sites present in the multiple cloning site (MCS) of the pFLAG-CTS vector (Sigma-Aldrich, St. Louis, MI, USA), which allows for secreted expression of C-

terminal FLAG fusion proteins. Constructed plasmids were then transformed into *E. coli* DH5α competent cells and recombinant plasmid clones were selected, purified and subjected to automated sequencing, as described above, to verify presence of insert in plasmid.

5.2.7. Structure prediction of PiGH1-x

Secondary structure of the putative protein was predicted by DNAMAN v.6.0 software (Lynnon LLC, San Ramon, CA, USA) using the Discrimination of protein Secondary structure Class (DSC) method (King and Sternberg 1996). A 3D model of PiGH1-x was generated using the homology modelling server, Protein Homology/analogy Recognition Engine V.2.0 (Phyre^2) (http://www.sbg.bio.ic.ac.uk/phyre2/) (Kelley et al. 2010). The catalytic sites of the putative protein were identified by this modeling server as well. Chimera 1.10 molecular graphics software was then used to render figures (http://www.cgl.ucsf.edu/chimera) (Pettersen et al. 2004).

5.3. Results

5.3.1. Amplification and cloning of a potential ß-glucosidase from *Pythium irregulare*

Knowledge of the partial amino acid sequences of glycosidases G2 and G3 obtained through *de-novo* sequencing (Neculai et al. 2009) allowed us to design degenerate oligonucleotide primers in order to amplify the genes that code for the above mentioned glycosyl hydrolases from *P. irregulare* using both total cell DNA and RNA as templates. Conserved amino acid regions identified in peptide fragments of G2 and G3, with 100% confidence scores, yielded six proteins annotated as ß-glucosidases (PYU1_T003475, PYU1_T003476, PYU1_T013474, PYU1_T013486, PYU1_T013487 and PYU1_T013488) in the *P. ultimum* Genome Database. Alignment of the amino acid and nucleotide sequences of these proteins between themselves and with peptide fragments of G2 and G3, allowed us to accurately predict the 780 bp size of the amplicon obtained after PCR amplification of *P. irregulare* genomic DNA using the degenerate primers we designed (Fig. 5.1A, Fig. 5.2A.).

The 780 bp fragment amplified by PCR was isolated and cloned, after which recombinant plasmids from 30 randomly selected bacterial colonies were sequenced. Nucleotide alignment of all 30 sequences obtained from the 780 bp amplified fragment showed that the cloned fragments could be divided into 3 main groups consisting of: (1) 8 sequences with 97.1% identity, (2) 8 sequences with 99.6% identity and (3) 7 sequences with 98.99% identity. The three main groups of partial sequences all showed similarity to annotated ß-glycosidase sequences from *Pythium ultimum* BR144 and all mapped into the same general region originally used to design degenerate primers. Subsequently, translation of the partial sequence fragment groups (1), (2) and (3) and their alignment with partial peptide fragments of G2 and G3 (Neculai et al. 2009), showed that the nucleotide sequence of Group 1 fragments most likely encodes the ß(1-2) glucosidases G2 and G3 previously isolated from *P. irregulare* (Fig. 5.1A). This is because peptide fragments from G2 and G3 showed similarity to regions of the Group 1 partial sequence that were not near the conserved regions used for degenerate primer design. However, no such homology was observed with any of the other degenerate primer PCR fragments sequenced.

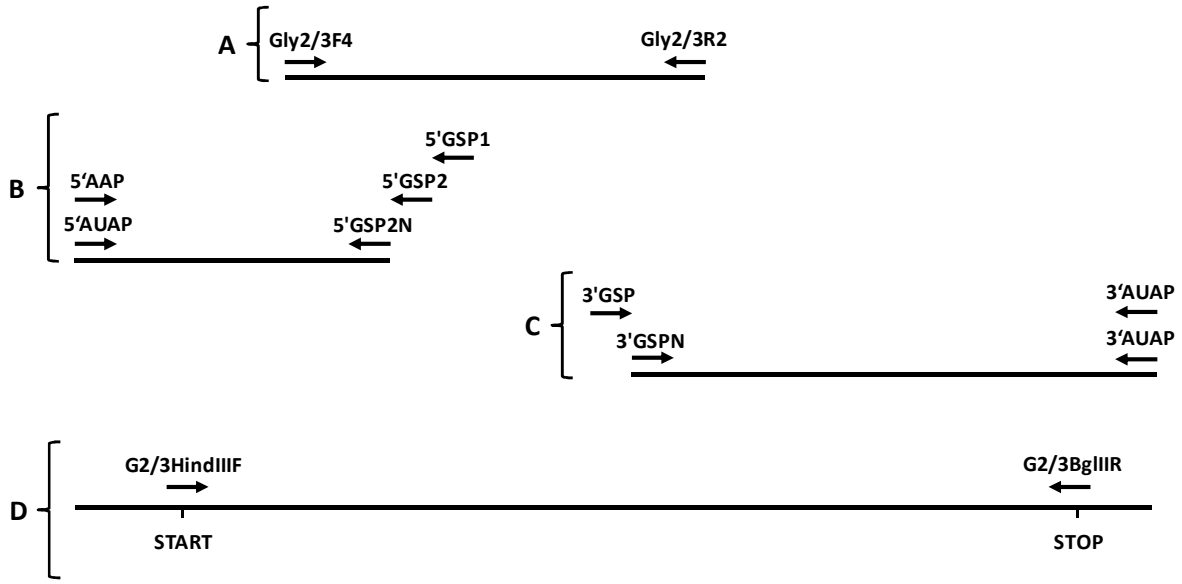

Figure 5.1. Scheme of the strategy used to obtain the full coding sequence of a potential ginsenoside metabolizing glycosidase (PiGH1-x) isolated from *P. irregulare*. At the bottom is the full cDNA nucleotide sequence for the putative glycosidase, including untranslated regions before and after the relative locations of the stop and start codons, which has been obtained after PCR with degenerate primers and RACE experiments (additional information in Materials and Methods). The open reading frame of the protein was 1767 bp. A) Represents a 780 bp fragment isolated from genomic DNA of *P. irregulare* by PCR with degenerate primers Gly2/3F4 and Gly2/3R2. B) Represents a 5'-RACE fragment of 1050 bp amplified with the combination of primers 5'AAP/5'GSP2 and nested primers 5'AUAP/5'GSP2N, with the 5'GSP1 primer being used to synthesize first strand cDNA. C) Represents a 3'-RACE fragment of 630 bp amplified with the combination of primers 3'GSP/3'AUAP and nested primers 3'GSPN/3'AUAP. D) Represents the full assembled cDNA nucleotide sequence for the putative glycosidase with the positions of primers G2/3HindIIIF and G2/3BglIIR which were designed to amplify the full open reading frame of the glycosidase for insertion into pFLAG-CTS expression vector, using HindIII and BglII restriction sites. The oligonucleotide primers utilized are shown in Table 5.1. Primers 5'AAP, 5'AUAP and 3'AUAP were supplied in the 3' and 5' RACE System for Rapid Amplification of cDNA Ends (Invitrogen). All fragments are shown 5' to 3' from left to right.

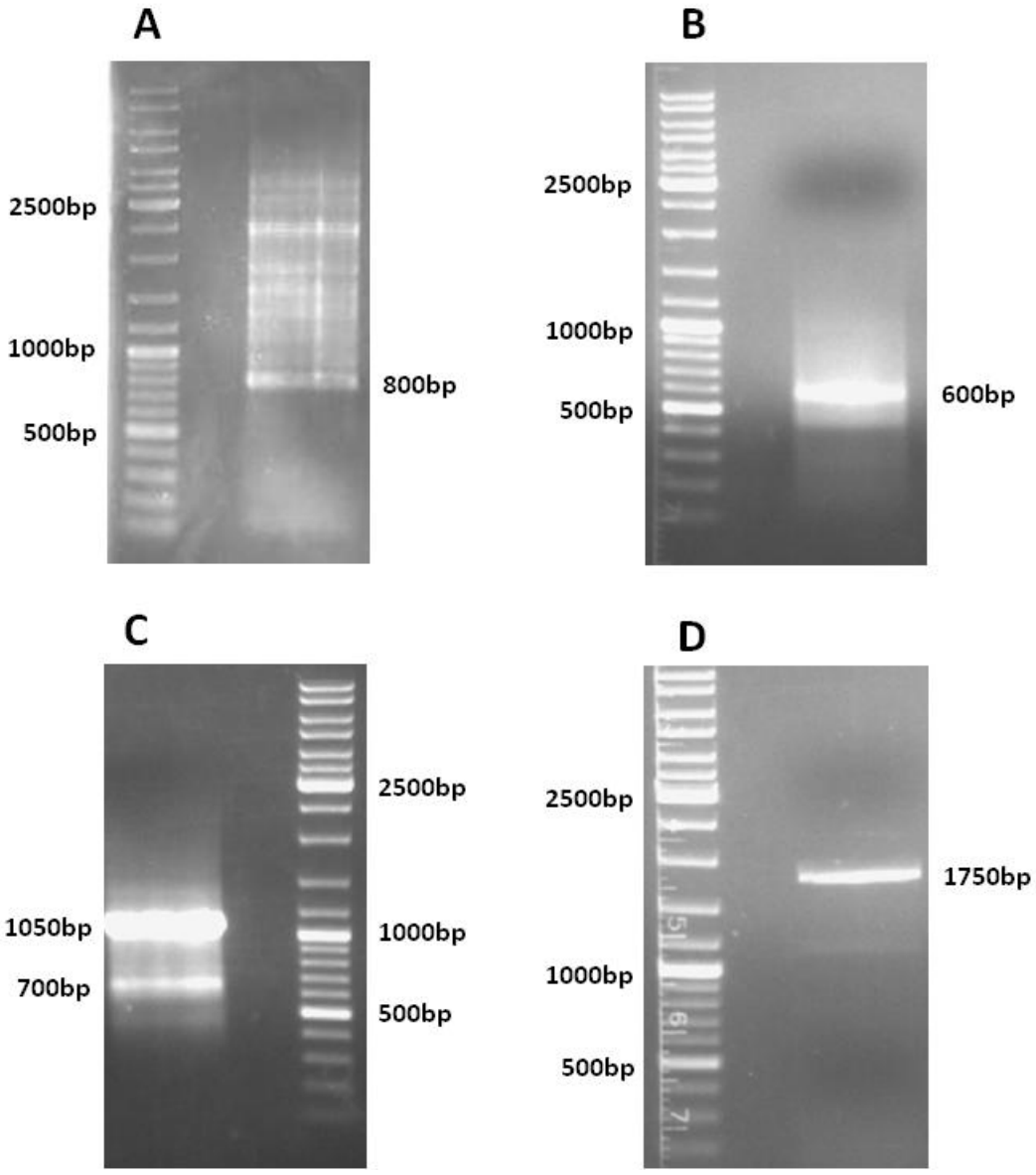

Figure 5.2. PCR amplification of PiGH1-x. A) Amplification products obtained by PCR with degenerate primers from *P. irregulare* genomic DNA. B) Product of 5'RACE amplification of fragment obtained from degenerate primer PCR. C) 1050 bp and 700 bp products of 3'RACE amplification of fragment obtained from degenerate PCR. D) Full cDNA nucleotide sequence of PiGH1-x PCR amplified using primers G2/3HindIIIF and G2/3BglIIR from cDNA constructed from total RNA of *P. irregulare*. The oligonucleotide primers utilized are shown in Table 5.1.

Based on the partial sequence of Group 1 degenerate primer PCR fragments, it was believed that the cDNA coding sequences of at least two glycosidases expressed by *P. irregulare*, would have high homology to the Group 1 partial sequence, because peptide fragments from both G2 and G3 aligned to the translated sequence. As a result, RACE experiments were undertaken to ascertain the full coding cDNA sequences of the potential glycosidases that shared the same conserved Group 1 sequence. 5'RACE yielded an intense amplicon of approximate size 600bp, while 3' RACE yielded an intense amplicon of approximate size 1100 bp and one additional amplicon of approx. size 700 bp (Fig. 5.2B, C). Bands corresponding to fragments of the 3'- and 5'- ends of potential glycosidases, obtained with primers designed from Group 1 fragment sequences, were cloned and 10 colonies containing each fragment were sequenced (Fig. 5.1B, C; Fig. 5.2B, C.)..

Sequencing and alignment of the 5' RACE amplicon revealed that it contained two sequences of 630 bp, while sequencing of the two amplicons obtained from 3'RACE revealed that both contained one identical sequence, however, larger 1050 bp amplicon contained an additional 350bp base pairs of the sequence. Subsequent multiple sequence alignments, revealed the full coding sequence of only one putative glycosidase, because the 3'RACE sequence and only one of the 5'RACE sequences obtained, overlapped with the corresponding nucleotide sequence of the original Group 1 fragment isolated by PCR with degenerate primers (Fig. 5.1B, C). The full-length cDNA sequence of the potential ß-glucosidase, designated PiGH1-x, was then amplified using specific primers with restriction sites that could facilitate cloning of the ORF and expression of recombinant protein (Fig. 1D, Fig. 5.2D).

5.3.2. Sequence analysis of PiGH1-x

cDNA sequence analysis showed that the isolated PiGH1-x ORF encompassed 1767 bp, without any introns, and that it encoded a protein comprising 589 amino acids, with a calculated molecular weight (MW) of 66.1413 kDa and a theoretical isolelectric point (pI) of 6.25 (Fig. 5.3). BLASTp analysis of the NCBI conserved domain database (CDD) using the deduced amino acid sequence of PiGH1-x was then conducted and revealed that PiGH1-x shared conserved amino acid residues with the glycosyl hydrolase (GH) family 1 multifamily domain (Table 5.2). It was also shown that the PiGH1-x ORF had conserved sequences from

```
-160   TGGCCACGCGTCGACTAGTACGGGGGGGGGGGGGGGGGACGCGGTCTTGCTTCTGTCTC
-100   AGTTCAATTCAATCCGTCCTCATTTCCAAAGTCGCTGGGACTCGAGCACTACTCTCGCCC
-40     GAACCATCGACTCCTGGTTTTGGCCGCATTCCTACCCATCATGAAGTGTCTGCAACTGCT
                                                  M  K  C  L  Q  L  L      7
21     TCTGGCTGGCGTCTCGGCCGTGCTCGCGACTGTGAGTGCGAGCGCTGTCGTCACCACCTC
         L  A  G  V  S  A  V  L  A  T  V  S  A  S  A  V  V  T  T  S     27
81     CGCGAGTGCCAAGCGCTGCTTCCCGGACGACTTCCTCTTTGGCTCTGCCACCGCCGCATA
         A  S  A  K  R  C  F  P  D  D  F  L  F  G  S  A  T  A  A  Y     47
141    CCAAGTGGAGGGCGCTTGGAACGAGACCGGCCGAACGCCGTCAATCTGGGACGACTTCTG
         Q  V  E  G  A  W  N  E  T  G  R  T  P  S  I  W  D  D  F  C     67
201    TCGCGAGAAGCCCGGTCTTCAGTGCTCGAACGTCGCCGACGACTTCTACCACCGGTACGT
         R  E  K  P  G  L  Q  C  S  N  V  A  D  D  F  Y  H  R  Y  V     87
261    GAGCGACATCCAGACGATGGTCGACTCGGGATTGGACTCGTTCCGCTTCAGCATCTCCTG
         S  D  I  Q  T  M  V  D  S  G  L  D  S  F  R  F  S  I  S  W    107
321    GTCGCGCGCCATGAACTGGGACCCTGCGACCAAGAAGATGAAGCCCAACCCGCAAGGCAT
         S  R  A  M  N  W  D  P  A  T  K  K  M  K  P  N  P  Q  G  I    127
381    CGCCTTCTACCACGCGCTCATCGACGAGCTCAAGCGCAACAATATCGTGCCGATCTTGAC
         A  F  Y  H  A  L  I  D  E  L  K  R  N  N  I  V  P  I  L  T    147
441    GCTCTACCACTGGGACCTCCCGAGCGAATTGCACAGTGAGCTCAAGCCGCAGGGTTGGCT
         L  Y  H  W  D  L  P  S  E  L  H  S  E  L  K  P  Q  G  W  L    167
501    CAACCGCGAGATCATCGATCACTTCGTTGAGTACTCGGAGCTCATATTCAACGAGTTTGG
         N  R  E  I  I  D  H  F  V  E  Y  S  E  L  I  F  N  E  F  G    187
561    CAAGAAGGTGGACATGTGGACGACGTTCAATGAGCCGCTGTCGTTCGTCTCCCAGGGCTA
         K  K  V  D  M  W  T  T  F  N  E  P  L  S  F  V  S  Q  G  Y    207
621    CGCAACGGGCATGTCGGCTCCAGGATACACCAACTCCAAGACGAACGCGTACGTTGTCGC
         A  T  G  M  S  A  P  G  Y  T  N  S  K  T  N  A  Y  V  V  A    227
681    GCACAACGTGCTGCTCTCGCACGGCAAGGCGGTGCAGCGCTTCCGCGAGCTCAAGAAGAG
         H  N  V  L  L  S  H  G  K  A  V  Q  R  F  R  E  L  K  K  S    247
741    CAACGTCGTCCATGAGAAGGCGCGCATCGGTATCGTGATTGTCGACCACTTCTACTACCC
         N  V  V  H  E  K  A  R  I  G  I  V  I  V  D  H  F  Y  Y  P    267
801    TCTCGACCCGAGCAACCCGCGCGACGTCATTGCGGCTGAGCGCGCGATCCAGTTTGGATT
         L  D  P  S  N  P  R  D  V  I  A  A  E  R  A  I  Q  F  G  F    287
861    CGGCTGGTTCTTCATTCCCATAGTGACTGGCAAGTATCCAGACGTGATGCGCGAACGTGT
         G  W  F  F  I  P  I  V  T  G  K  Y  P  D  V  M  R  E  R  V    307
921    CGGTGACCGCCTGCCAGAGTTCACGGCGGAGGAAGCTGCGATGGTAAAGGACTCGTACGA
         G  D  R  L  P  E  F  T  A  E  E  A  A  M  V  K  D  S  Y  D    327
981    CCTCTTCATGCTCAACCACTACTCATCCCACACTGTGACGGACTGCGACTCCGAAACGTC
         L  F  M  L  N  H  Y  S  S  H  T  V  T  D  C  D  S  E  T  S    347
1041   GCTCGTCAAGTGCAGCGATTTGTCCCTCGGATGGGAACAGGATATGGGCGTCGACAGTAC
         L  V  K  C  S  D  L  S  L  G  W  E  Q  D  M  G  V  D  S  T    367
1101   GCGTGCGCCAGACGGTGCGCGTCTGTCCAGCAAGAACAGCCTCGGCGAGTACAACTGCAA
         R  A  P  D  G  A  R  L  S  S  K  N  S  L  G  E  Y  N  C  K    387
1161   GTGGTTCACGGGATACCCGGCAGGCTACCTGGAAATGATCAAGTGGATGCACAAGTACAA
         W  F  T  G  Y  P  A  G  Y  L  E  M  I  K  W  M  H  K  Y  N    407
1221   CACAAAGGCGGACATCTTACTCACCGAGAACGGCTGGTGCGGCAACGAGACCATCGACAA
         T  K  A  D  I  L  L  T  E  N  G  W  C  G  N  E  T  I  D  N    427
1281   CCAGGACCAACTCTGGTACTTCCAGAGCTACATCGGCGAAGTCTACAAGGCGATCAACGA
         Q  D  Q  L  W  Y  F  Q  S  Y  I  G  E  V  Y  K  A  I  N  E    447
1341   ACTCAAGATCCCCATCATTGGGTACACTGCGTGGTCGTTCATGGACAACTACGAGTGGGG
         L  K  I  P  I  I  G  Y  T  A  W  S  F  M  D  N  Y  E  W  G    467
1401   CTCATTCAAGCCTCGCTTTGGACTCTACTACGTCAATTTCACGTCCGAGACCGGCAAGGC
         S  F  K  P  R  F  G  L  Y  Y  V  N  F  T  S  E  T  G  K  A    487
1461   GGATGAGGTCACCCCAGGATCAAACGCCTTGGCACGCATCCCACGTCCTGCGGCCAAATG
         D  E  V  T  P  G  S  N  A  L  A  R  I  P  R  P  A  A  K  W    507
1521   GTACGCGCAAGTGGCGAAGACCAAGTGCCTCGACGGCTTTGAGATTGAAGGCGTGCCAGT
```

```
          Y  A  Q  V  A  K  T  K  C  L  D  G  F  E  I  E  G  V  P  V    527
1581  CTTGGCAGGAGTCAGCGACGTTACTGGTACCAGCTCTGGCAGCAGCTTTAAGACGTTCGC
          L  A  G  V  S  D  V  T  G  T  S  S  G  S  S  F  K  T  F  A    547
1641  ACTCTGGGGGCTGGTGCTGGGTGTTGTTGTCGGCGTACCAGCGATCGCTTTCTTTGTCAA
          L  W  G  L  V  L  G  V  V  V  G  V  P  A  I  A  F  F  V  K    567
1701  GAGCCGTCGCTCTCGTCAGAGCTCGCTGCTCCGCGCGGGCGAGAACACGCCGCTCGTGCG
          S  R  R  S  R  Q  S  S  L  L  R  A  G  E  N  T  P  L  V  R    587
1761  TGGACAGTAAAGTAGGCGAGTTCGTTCGCTGATATTCAGAATGAGCTCTTCGCAAATAGT
          G  Q  *                                                       589
1821  GGTTTTTGGTGTATGTACTGATAATAATATCAATACTTTTTTGGTATCATGAAAAAAAAA
1881  AAAAAAAAAAAAAGTACTAGTCGACGCGTGGCC
```

Figure 5.3. Full length cDNA coding sequence and deduced amino acid sequence of potential ginsenoside metabolizing glycosidase (PiGH1-x) isolated from *P. irregulare*. Nucleotides and amino acid residues are numbered from the first ATG codon (**bold**) of the assembled consensus nucleotide sequence and the first methionine residue of the predicted protein sequence, respectively. The termination codon TAA is marked with an *asterisk* and the untranslated regions (5' and 3' end) are indicated in *grey italic font*. Conserved Glutamine residues in the catalytic domain are indicated in ***bold italic font***. The putative glycosidase sequence is composed of 589 amino acids, with a predicted molecular weight (MW) of 66.1413 kDa and isoelectric point (pI) of 6.25. Dark shaded letters indicate amino acid sequence obtained through 5'RACE, light shaded letters indicate amino acid sequence obtained from 3'RACE and unshaded letters show amino acid sequence obtained from degenerate PCR, experiments.

Table 5.2. Conserved protein domains present in ORF of PiGH1-x. The complete open reading frame (ORF) of the potential ginsenoside metabolizing glycosidase (PiGH1-x) was compared to the conserved domain database (CDD) administered by NCBI, using BLASTp analysis, in order to ascertain the potential domain superfamily of the enzyme. All other enzymes listed also belonged glycosyl hydrolase family 1.

Domain Name	Accession	Description	Interval	E-Value
*Glyco_hydro_1	pfam00232	Glycosyl hydrolase family 1	34-515 aa	5.65e-150
BglB	COG2723	ß-glucosidase/6-phospho-ß-glucosidase/ß-galactosidase	34-518 aa	3.24e-119
BGL	TIGR03356	ß-galactosidase	35-508 aa	2.82e-127
PLN02814	PLN02814	ß-glucosidase	1-509 aa	1.35e-98
PRK13511	PRK13511	6-phospho-ß-galactosidase (Provisional)	34-515 aa	1.95e-88

* Indicates glycosyl hydrolase multi-domain superfamily according to the Carbohydrate-Active Enzyme classification server (CAZy).

4 separate glycosyl hydrolase superfamilies described as ß-glucosidases and ß-galactosidases (Table 5.2). An additional BLASTp analysis of the *Pythium ultimum* BR 144 proteome (Pythium Genome Database) and the Universal Protein Resource database (UniProt) revealed that the highest values of similarity in alignments with the PiGH1-x ORF corresponded to a candidate ß-glycosidase from *Pythium ultimum* (BR144) (PYU_T013486) exhibiting 66.89% of identical amino acids in an alignment that covered 100% of the sequence (E value, 9.7e-222). Furthermore, after the database survey, the PiGH1-x protein sequence was shown to have the highest sequence identity to 3 other candidate ß-glycosidases from *Pythium ultimum* (PYU1_T013487, PYU1_T013488 and PYU1_T013474) all of which were used to design the original degenerate PCR primers that were utilized in the extraction of the initial fragment of the enzyme. Interestingly, the NCBI non-redundant protein sequence database yielded protein matches with lower sequence identity and alignment coverage and as such, was not taken in to account in the database survey.

5.3.3. Molecular modeling of PiGH1-x

The Phyre[2] molecular modeling server program revealed that the X-ray crystallographic structure of wheat beta-glucosidase c2dgaA, isolated by Sue et al. (2006), is the best template for homology modeling of the PiGH1-x coding sequence. The beta-glucosidase c2dgaA showed a 36% amino acid sequence identity and 82% sequence coverage with PiGH1-x, however, 452 amino acid residues or 77% of the PiGH1-x sequence were modeled with 100% confidence using cdgaA as a template. The structural coordinates generated for the 3D model were visualized using Chimera 1.10 software, which revealed that the structure of PiGH1-x contained the typical $(\alpha/ß)_8$ barrel folding common to glycosyl hydrolase family 1 (Davies and Henrissat 1995) (Fig. 5.4). The predicted PiGH1-x 3D structure also revealed potential binding sites for glucose residues with the involvement of Glu 198 and Glu 416 residues that could reduce bonds between a docked ligand (Fig. 5.3, Fig. 5.4).

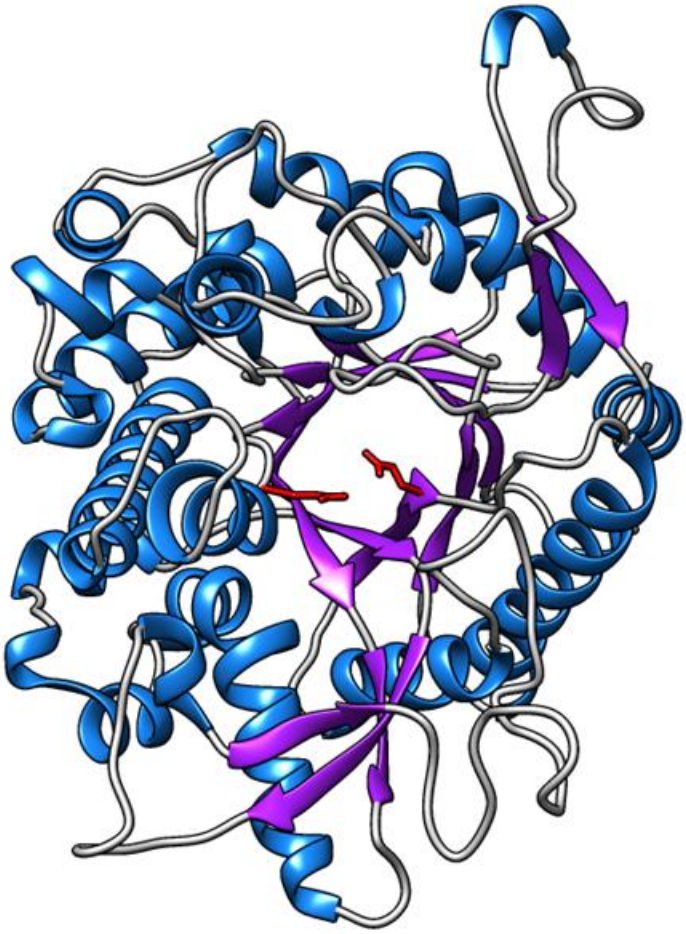

Figure 5.4. Predicted tertiary structure of PiGH1-x. 3D structure of PiGH1-x predicted using Phyre[2], α-helices are coloured *blue*, ß-sheets are coloured *purple*, and linking amino acid chains are coloured *white*. The conserved Glu 198 and Glu 416 residues in the catalytic domain are represented as *red sticks*.

5.4. Discussion

The focus of this study was to amplify and express the full coding sequence of one or both of the ginsenoside metabolizing ß(1-2)- glucosidases designated as G2 or G3 previously isolated by Neculai et al. (2009). The culmination of this work was the determination of the complete nucleotide and deduced amino acid sequences of a gene designated PiGH1-x, since at this time we cannot fully distinguish if it encodes G2 or G3. PiGH1-x was shown to be homologous to the glycoside hydrolase family 1 based on its amino acid sequence similarities to conserved motifs in the Conserved Domain Database (CDD) (Table 5.2) and 3D modelling Fig. 5.4. This supports the conclusion that PiGH1-x belongs to the same GH family as the G2 and G3 ginsenosidases previously described (Neculai et al. 2009). Furthermore, PiGH1-x was shown to have sequence similarities with conserved motifs indicating that it likely possesses ß-glucosidase activity and it showed amino acid sequence similarity to other enzymes annotated as potential ß-glucosidases (Table 5.2, Table 5.3). All of this showed that PiGH1-x likely has ß-glucosidase activity similar to ginsenosidases G2 and G3. This also falls in line with recent studies showing that cloned ginsenoside-hydrolyzing family 1 glycosyl hydrolases can convert ginsenoside Rb1 into either Rd or GXVII (Wang et al. 2011; Cui et al. 2013), which requires the same (1→2) and (1→6) ß-glucosidase catalytic activities observed in the three ginsenoside metabolizing proteins isolated by Neculai et al. (2009).

Alignment of sequenced peptide fragments from G2 and G3 to the full coding sequence of PiGH1-x, however, did not allow us to clearly decipher if the PiGH1-x protein encoded ginsenosidase G2 or G3, or if it was a novel ß-glucosidase never before isolated in *P. irregulare*. This was because peptide fragments from G2 and G3 that fully aligned to the translated PiGH1-x protein sequence all aligned to the same regions of the protein. This may occur because sequence similarity between the two proteins is potentially very high. Furthermore, the PEAKS software (Ma et al. 2003, 2005) used to compute the original G2 and G3 peptide sequences from MS/MS data, did not have access to sequence information for any members of the Oomycota as none had been sequenced at the time. This means that prediction of peptide sequences for G2 and G3, isolated from the oomycete *P. irregulare*, may not have been precise enough to separate the two proteins due to a lack of protein scaffolds.

In either case, only further characterization of the PiGH1-x protein will allow us to answer this question. To do this we will attempt to express recombinant PiGH1-x using the pFLAG-CTS vector in order to further characterize the protein. Successful expression of PiGH1-x will, firstly, allow us to determine the molecular mass of the mature protein and its isoelectric point. This is necessary because the calculated molecular mass of 66.1413 kDa for PiGH1-x is higher than that of both G2 and G3 (Neculai et al. 2009), which if confirmed will mean that PiGH1-x is not identical to either G2 or G3. However, differences between predicted (based on sequence information) and observed (based on denaturing gel electrophoresis) molecular masses have been shown to exceed 10% in a model organism (Link et al. 1997), which may mean that expressed PiGH1-x may still share identity with either G2 or G3. Recombinant protein expression of PiGH1-x will also allow us to study the catalytic specificity of the enzyme, by testing its activity on various chromogenic substrates measured by ONP and PNP release (Park et al. 2010; Cui et al. 2013), and its ability to deglycosylate ginsenosides. Furthermore, primers specific to PiGH1-x will be used to test if production of this glucosidase in *P. irregulare* is induced or up-regulated in the presence of ginsenosides.

This is important, because previous studies have shown that while some glycosidases are constitutively expressed by *P. irregulare in vitro,* the profile of glycosidases produced in the presence of ginsenosides is altered and includes ginsenoside metabolizing ginsenosidases G1, G2 and G3 (Neculai et al. 2009, Ivanov and Bernards 2012). If production of PiGH1-x is induced by exposure of *P. irregulare* to ginsenosides then this will help to confirm whether PiGH1-x in fact shares identity with one of ginsenosidases G2 or G3. If this is confirmed and production of PiGH1-x is up-regulated by ginsenosides, this may mean that the enzyme can exhibit a greater specificity to deglycosylating the ß (1→2) glucosidase linkages in ginsenosides. This will have great commercial pharmaceutical applications as this enzyme might be more efficient at converting common ginsenosides than the currently available recombinant ginsenoside metabolizing glycosyl hydrolases obtained mostly from microbial sources (Kim et al. 2007; Noh and Oh 2009; Noh et al. 2009, An et al. 2012; Cui et al. 2013). Furthermore, knowing the coding sequence of ginsenosidase G2 or G3 will have great implications for the study of the pathogenic interaction between *P. irregulare* and ginseng plants (Neculai et al. 2009, Bernards et al. 2010). This is because it has been shown that the ability of different strains of *P. irregulare* to metabolize common ginsenosides into

ginsenoside F2 *in vitro* is positively correlated to the ability of the organism to infect ginseng (Ivanov and Bernards 2012). Therefore, having the ability to track and manipulate the expression of one of the enzymes responsible for extracellular ginsenoside metabolism in *P. irregulare* may be invaluable.

5.5. Conclusion

The identified putative ß-glucosidase designated as PiGH1-x is the first potential ginsenoside metabolizing family 1 glycosyl hydrolase sequenced from *P. irregulare*. However, a recombinant ß-glucosidase (PiGH1-x) will need to be constructed and expressed in the future, in order to functionally characterize this enzyme and test its substrate specificity and suitability for metabolizing ginsenosides. This is important because the enzymatic transformation of ginsenosides using recombinant glycosidases is one of the most promising ways to produce pharmaceutically active minor ginsenosides in large quantities (Park et al. 2010, Cui et al. 2013). Furthermore, knowledge of the full sequence of this enzyme, will allow us to test if production of this glucosidase by *P. irregulare* is induced*, in vitro*, in the presence of ginsenosides. If proven this could have biological applications in the mitigation of disease caused by *P. irregulare* on ginseng plants (see Bernards et al. 2010; Ivanov and Bernards 2012) and also, could mean this recombinant enzyme may be more efficient at biotransforming common ginsenosides then currently available recombinant proteins.

5.5. References

Altschul, S.F., Gish, W., Miller, W., Myers, E.W., Lipman, D.J., 1990. Basic local alignment search tool. J. Mol. Biol. 215, 403-410.

An, D.S., Cui, C.H., Sung, B.H., Yang, H.C., Kim, S.C., Lee, S.T., Im, W.T., Kim, S.G., 2012. Characterization of a novel ginsenoside-hydrolyzing alpha-L-arabinofuranosidase, AbfA, from *Rhodanobacter ginsenosidimutans* Gsoil 3054T. Appl. Microbiol. Biotechnol. 94, 673-682.

Attele, A.S., Wu, J.A., Yuan, C.S., 1999. Ginseng pharmacology: Multiple constituents and multiple actions. Biochem. Pharmacol. 58, 1685-1693.

Attele, A.S., Zhou, Y.P., Xie, J.T., Wu, J.A., Zhang, L., Dey, L., Pugh, W., Rue, P.A., Polonsky, K.S., Yuan, C.S., 2002. Antidiabetic effects of *Panax ginseng* berry extract and the identification of an effective component. Diabetes 51, 1851-1858.

Benson, D.A., Cavanaugh, M., Clark, K., Karsch-Mizrachi, I., Lipman, D.J., Ostell, J., Savers, E.W., 2013. GenBank. Nucleic Acids Res. 41, D36-46.

Bernards, M.A., Ivanov, D.A., Neculai, A.M., Nicol, R.W., (2010) Ginsenosides: Phytoanticipins or host recognition factors? Recent Advances in Phytochemistry 41, 13-32.

Cheng, L.Q., Kim, M.K., Lee, J.W., Lee, Y.J., Yang, D.C., 2006 Conversion of major ginsenoside Rb1 to ginsenoside F2 by *Caulobacter leidyia*. Biotechnol. Lett. 28, 1121-1127.

Cheng, L.Q., Na, J.R., Kim, M.K., Bang, M.H., Yang, D.C., 2007. Microbial conversion of ginsenoside Rb1 to minor ginsenoside F2 and gypenoside XVII by *Intrasporangium* sp. GS603 isolated from soil. J. Microbiol. Biotechnol. 17, 1937-1943.

Chi, H., Lee, B.H., You, H.J., Park, M.S., Ji, G.E., 2006. Differential transformation of ginsenosides from *Panax ginseng* by lactic acid bacteria. J. Microbiol. Biotechnol. 16, 1629-1633.

Christensen, L.P., 2008. Chapter 1 Ginsenosides: Chemistry, biosynthesis, analysis, and potential health effects. Adv. Food Nut. Res. 55, 1-99.

Cui, C-H., Kim, S-C., Im, W-T., 2013. Characterization of the ginsenoside-transforming recombinant [beta]-glucosidase from Actinosynnema mirum and bioconversion of major ginsenosides into minor ginsenosides. Appl. Microbiol. Biotechnol. 97, 649-659.

Davies, B., Henrissat, B., 1995. Structures and mechanisms of glycosyl hydrolases. Structure. 3, 853-859.

Dong, A., Ye, M., Guo, H., Zheng, J., Guo, D., 2003. Microbial transformation of ginsenoside Rb1 by *Rhizopus stolonifer* and *Curvularia lunata*. Biotechnol. Lett. 25, 339-344.

Han, Y., Sun, B., Hu, X., Zhang, H., Jiang, B., Spranger, M.I., Zhao, Y., 2007. Transformation of bioactive compounds by *Fusarium sacchari* fungus isolated from the soil-cultivated ginseng. J. Agric. Food Chem. 55, 9373-9379.

Hostettmann, K., Marston, A., 1995. Saponins. Chemistry and Pharmacology of Natural Products. Cambridge University Press, Cambridge, U.K, pp. 329-337.

Ivanov, D.A., Bernards, M. A., 2012. Ginsenosidases and the pathogenicity of *Pythium irregulare*. Phytochemistry 78, 44-53.

Jia, L., Zhao, Y.Q., 2009. Current evaluation of the millennium phytomedicine-ginseng (I): etymology, pharmacognosy, phytochemistry, market and regulations. Curr. Med. Chem. 16, 2475-2484.

Karikura, M., Miyase, T., Tanizawa, H., Taniyama, T., Takino, Y., 1991. Studies on absorption, distribution, excretion and metabolism of ginseng saponins. VII. Comparison of the decomposition modes of ginsenoside-Rb1 and -Rb2 in the digestive tract of rats. Chem. Pharm. Bull. (Tokyo) 39, 2357-2356.

Kelley, L.A., Mezullis, S., Yates, C.M., Wass, M.N., Sternberg, M.J.E., 2015. The Phyre2 portal for protein modelling, prediction and analysis. Nat. Protoc. 6; 845-848.

Kiefer, D., Pantuso, T., 2003. Asian ginseng improves psychological and immune function. Am. Fam. Physician 68, 1539-1542.

Kim, M.K., Lee, J.W., Lee, K.Y., Yang, D.C., 2005. Microbial conversion of major ginsenoside Rb1 to pharmaceutically active minor ginsenoside Rd. J. Microbiol. 43, 456-462.

Kim, S.J., Lee, C.M., Kim, M.Y., Yeo, Y.S., Yoon, S.H., Kang, H.C., Koo, B.S., 2007. Screening and characterization of an enzyme with beta-glucosidase activity from environmental DNA. J. Microbiol. Biotechnol. 17, 905-912.

King, R.D., Sternberg, J.D., 1996. identification and application of the concepts important for accurate and reliable protein secondary structure prediction. Prot. Sci. 5; 2298-2310.

Lévesque, C.A., Brouwer, H., Cano, L., Hamilton, J.P., Holt, C., Huitema, E., Raffaele, S., Robideau, G.P., et al., 2010. Genome sequence of the necrotrophic plant pathogen *Pythium ultimum* reveals original pathogenicity mechanisms and effector repertoire. Genome Biol. 11, R73.

Liang, Y., Zhao, S., 2007. Progress in understanding of ginsenoside biosynthesis. Plant Biology 10, 415-421.

Ligor, T., Ludwiczuk, A., Wolski, T., Buszewski, B., 2005. Isolation and determination of ginsenosides in American ginseng leaves and root extracts by LC-MS. Anal Bioanal Chem. 383, 1098-1105.

Link, A.J., Robison, K., Church, G.M., 1997. Comparing the predicted and observed properties of proteins encoded in the genome of *Escherichia coli* K-12. Electrophoresis. 18, 1259-1313.

Lombard, V., Ramulu, H.G., Drula, E., Coutinho, P.M., Henrissat, B., 2014, The carbohydrate-active enzymes database (CAZy) in 2013. Nucleic Acids Res. 42, D490-D495.

Ma, B., Zhang, K., Hendrie, C., Liang, C., Li, M., Doherty-Kirby, A., Lajoie, G., 2003. PEAKS: powerful software for peptide de novo sequencing by tandem mass spectrometry. Rapid Commun. Mass Spectrom. 17, 2337–2342.

Ma, B., Zhang, K., Liang, C., 2005. An effective algorithm for peptide *de novo* sequencing from MS/MS spectra. J. Comput. Syst. Sci. 70, 418–430.

Marchler-Bauer, A., Derbyshire, M.K., Gonzales, N.R., Lu, S., Chitsaz, F., Geer, L.Y., Geer, R.C., He, J., Gwadz, M., Hurwitz, D.I., et al., 2015. CDD: NCBI's conserved domain database. Nucleic Acids Res. 43, 222-226.

Neculai, M.A., Ivanov, D., Bernards, M.A., 2009. Partial purification and characterization of three ginsenoside-metabolizing [beta]-glucosidases from *Pythium irregulare*. Phytochemistry 70, 1948-1957.

Noh, K.H., Oh, D.K., 2009. Production of the rare ginsenosides compound K, compound Y, and compound Mc by a thermostable [beta]-glycosidase from *Sulfolobus acidocaldarius*. Biol. Pharm. Bull. 32, 1830–1835.

Noh, K.H., Son, J.W., Kim, H.J., Oh, D.K., 2009. Ginsenoside compound K production from ginseng root extract by a thermostable [beta]-glycosidase from *Sulfolobus solfataricus*. Biosci. Biotechnol. Biochem. 73, 316–321.

Park, S.Y., Bae, E.A., Sung, J.H., Lee, S.K., Kim, D.H., 2001. Purification and characterization of ginsenoside Rb1-metabolizing [beta]-glucosidase from *Fusobacterium* K-60, a human intestinal anaerobic bacterium. Biosci. Biotechnol. Biochem. 65, 1163-1169.

Park, C-H., Yoo, M-H., Noh, K-H., Oh, D-K., 2010. Biotransformation of ginsenosides by hydrolyzing the sugar moieties of ginsenosides using microbial glycosidases. Appl. Microbial. Biotechnol. 87, 9-19.

Pettersen, E.F., Goddard, T.D., Huang, C.C., Couch, G.S., Greenbilt, D.M., Meng, E.C., Ferrin, T.E., 2004. UCSF Chimera - A visualization system for exploratory research and analysis. J. Comput. Chem. 25; 1605-1612.

Predy, G.N., Goel, V., Lovlin, R.E., Basu, T.K., 2006. Immune modulating effects of daily supplementation of COLD-fX (a proprietary extract of North American ginseng) in healthy adults. J. Clin. Biochem. Nutr. 39, 160-165.

Qi, L.W., Wang, C.Z., Yuan, C.S., 2010. American ginseng: potential structure–function relationship in cancer chemoprevention. Biochem. Pharmacol. 80, 947-954.

Qu, C., Bai, Y., Jin, X., Wnaga, Y., Zhang, K., You, J., Zhang, H., 2009. Study on ginsenosides in different parts and ages of *Panax quinquefolius*. L. Food Chem. 115, 340-346.

Ruan, C.C., Zhang, H., Zhang, L.X., Liu, Z., Sun, G.Z., Lei, J., Qin, Y.X., Zheng, Y.N., Li, X., Pan, H.Y., 2009. Biotransformation of ginsenoside Rf to Rh1 by recombinant β-glucosidase. Molecules 14, 2043-2048.

Sanger, F., Nicklen, S., Coulson, A.R., 1977. DNA sequencing with chain terminator inhibitors. Proc. Natl. Acad. Sci. U.S.A. 74, 5463-5467.

Shi, W., Wang, Y., Li, J., Zhang, H., Ding, L., 2007. Investigation of ginsenosides in different parts and ages of *Panax ginseng*. Food Chem. 102, 664-668.

Shin, H.Y., Lee, J.H., Lee, J.Y., Han, Y.O., Han, M.J., Kim, D.H., 2003. Purification and characterization of ginsenoside Ra-hydrolyzing beta-D-xylosidase from *Bifidobacterium breve* K-110, a human intestinal anaerobic bacterium. Biol. Pharm. Bull. 26, 1170-1173.

Sue, M., Yamazaki, K., Yajima, S., Nomura, T., Matsukawa, T., Iwamura, H., Miyamoto, T., 2006. Molecular and structural characteriazation of hexameric beta-D-glucosidase in wheat and rye. Plant Physiology. 141, 1237-1247.

Tawab, M.A., Bahr, U., Karas, M., Wurglics, M., Schubert-Zsilavecz, M., 2003 Degradation of ginsenosides in humans after oral administration. Drug Metab. Dispos. 31, 1065-1071.

Teng, R., Li, H., Chen, J., Wang, D., He, Y., Yang, C., 2002. Complete assignment of 1H and 13C NMR data for nine protopanaxatriol glycosides. Magn. Reson. Chem. 40, 483-488.

The UniProt Consortium, 2015. UniProt: a hub for protein information. Nucleic Acids Res. 43, D204-D212.

Thompson, J.D., Gibson, T.J., Plewniak, F., Jeanmougin, F., Higgins, D.G., 1997. The CLUSTAL-X windows interface: flexible strategies for multiple sequence alignment aided by quality analysis tools. Nucleic Acids Res. 25, 4876-4882.

Wang, C.Z., Mehendale, S.R., Yuan, C.S., 2007. Commonly used antioxidant botanicals: active constituents and their potential role in cardiovascular illness. Am. J. Chin. Med. 35, 543-558.

Wang, C.Z., Yuan, C.S., 2008. Potential role of ginseng in the treatment of colorectal cancer. Am. J. Chin. Med. 36, 1019-1028.

Wang, L., Liu, Q.M., Sung, B.H., An, D.S., Lee, H.G., Kim, S.G., Kim, S.C., Lee, S.T., Im, W.T., 2011. Bioconversion of ginsenosides Rb1, Rb2, Rc and Rd by novel β-glucosidase hydrolyzing outer 3-O glycoside from Sphingomonas sp. 2F2: cloning, expression, and enzyme characterization. J. Biotechnol. 156, 125-133.

Wen, J., Zimmer, E.A., 1996. Phylogeny and biogeography of *Panax* L. (the ginseng genus, *Araliaceae*): inferences from ITS sequences of nuclear ribosomal DNA. Mol. Phylogenet. Evol. 6, 167-177.

Yousef, L.F., Bernards, M.A., 2006. *In vitro* metabolism of ginsenosides by the ginseng root pathogen *Pythium irregulare*. Phytochemistry 67, 1740-1749.

Zhao, X., Gao, J., Song, C., Fang, Q., Wang, N., Zhao, T., Liu, D., Zhou, Y., 2012. Fungal sensitivity to and enzymatic deglycosylation of ginsenosides. Phytochemistry 78, 65-71.

Zhou, W., Yan, Q., Li, J.Y., Zhang, X.C., Zhou, P., 2008. Biotransformation of *Panax notoginseng* saponins into ginsenoside compound K production by *Paecilomyces bainier* sp. 229. J. Appl. Microbiol. 104, 699-706.

Chapter 6: General Discussion and Future Directions

6.1. General discussion

The main goals of this research project were to evaluate the potential roles of extracellular ginsenosidases and of the ginsenosides these enzymes generate, in the ginseng-*Pythium irregulare* pathosystem. The interactions between these two organisms were probed on various biological scales, ranging from the whole organism to the molecular level. This led to new perspectives on how potential ecological interactions between these organisms could function and also led to the development and implementation of new methods for the tracking of root pathogen infection *in vivo*.

Previously, *in vitro* studies of *P. irregulare* had shown that the growth of this organism is stimulated in the presence of ginsenosides (Nicol et al. 2002; 2003) and that it produces specific glucosidases (termed ginsenosidases) that catalyze the conversion of the common 20 (S)-protopanaxadiol ginsenosides to ginsenoside F2 (Yousef and Bernards 2006; Neculai et al. 2009). Taking this into account, a working hypothesis on the role of ginsenosides and ginsenosidases in the ginseng-*P. irregulare* pathosystem was conceptualized by Bernards et al. (2010). It was hypothesized that initial degradation of ginsenosides and the formation of products like ginsenoside F2 may signal the presence of ginseng roots to *P. irregulare* and lead to the alteration of the glycosidases secreted by the organism into the soil, resulting in the expression of more specific ginsenosidases. The degradation of ginsenosides in the rhizosphere was then believed to form a gradient of ginsenoside F2 that could lead *P. irregula*re to the ginseng root. The induction of *P. irregulare* ginsenosidases in cultures supplemented with ginsenosides was therefore, taken as possible evidence that these enzymes play an important part in the recognition of host roots by this pathogen and that they are important in the infection cycle.

This aspect of the interaction between ginseng and *Pythium* was the first to be evaluated during the course of this research project. To do this it was determined whether there was a correlation between the production of extracellular ginsenosidases by different strains of *P. irregulare* and the ability of those strains to infect ginseng. These experiments (Chapter 2) showed that the pathogenicity of unique isolates of *P. irregulare* on ginseng roots correlated with their ability to deglycosylate 20 (S)-protopanaxadiol ginsenosides via extracellular ginsenosidases. However, it must be noted, that this did not prove that

extracellular ginsenosidases were needed for infection. This is because *Pythium ultimum,* an organism closely related to *P. irregulare,* showed a relatively poor ability to deglycosylate ginsenosides yet readily infected ginseng plants. Nevertheless, this finding did support the initial hypothesis proposed by Nicol et al. (2002) that *P. irregulare* uses ginsenosides as a host recognition/growth factor.

To further test whether ginsenosides do, in fact, serve as a host recognition factor for *P. irregulare*, the ability of ginsenosides to act as signaling molecules (i.e. chemo-attractants/ inhibitors) was evaluated *in vitro*. To do this, the differential growth effects of pure ginsenosides Rb1, Re and F2 as well as a purified total ginsenoside mixture (GSF) were evaluated on *P. irregulare* by observing pathogen growth on a minimal media agar plate toward a point source of ginsenosides (Chapter 4). The data obtained from this experiment however, did not provide definitive answers on whether the growth *P. irregulare* was due to ginsenosides acting as chemoattractants or host recognition factors.

As expected from previous studies, the protopanaxatriol ginsenoside Re showed no effect on the growth of *P. irregulare* (Nicol et al 2003; Yousef and Bernards 2006), yet the protopanaxadiol ginsenoside Rb1 and GSF both stimulated the growth of *P. irregulare* to the same extent when applied in the same concentration (see Supporting Information). Therefore it was shown that ginsenoside Rb1 is involved in growth stimulation but is not the only ginsenoside having this effect. The *in vitro* assay however, also provided some contradictory results when it was observed that ginsenoside F2 caused a well defined zone of inhibition and limited *P. irregulare* growth. This effect diminished over time but *P. irregulare* hyphae never grew through the ginsenoside point source.

From this data it remains unclear why *P. irregulare* invests the energy to convert 20 (S)-protopanaxadiol ginsenosides into ginsenoside F2, when in fact the growth of this organism is visibly inhibited when it encounters the pure compound. It is possible that *P. irregulare* adjusts its metabolism in the presence of ginsenosides, and its reaction to the compound F2 requires this metabolic shift in order to circumvent the potential deleterious effects that it can have on growth. This metabolic shift may be part of a physiological change in the pathogen that facilitates the infection of ginseng, as suggested by the strong correlation between *P. irregulare's* ability to convert ginsenosides into ginsenoside F2 and its pathogenicity (Chapter 2).

In conjunction with the *in vitro* experiments utilizing pure ginsenosides, the infection rate of *P. irregulare* on ginseng roots before and after exposure to ginsenosides was determined *in vivo* using chlorophyll fluorescence imaging, in order to see if ginsenosides serve as a virulence factor/chemoattractant on the whole plant scale. In order to do this, a new method was adapted to track the infection of a root pathogen, by monitoring the slow induction chlorophyll fluorescence parameter ΦNO (Chapter 3; Ivanov and Bernards *submitted*). This parameter measures the quantum yield of non-regulated quenching processes in photosystem II (PSII) and was shown to be the most sensitive of the slow induction chlorophyll fluorescence parameters at detecting biotic stress, *in vivo*. Furthermore, determination of ΦNO was shown to be as effective in monitoring disease progression in ginseng as the measurement of the maximum quantum efficiency of PSII (Fv/Fm) (Chapter 3; Ivanov and Bernards *submitted)* which has been previously used to study fungal/oomycete plant pathogen infections *in vivo* in a number of different species like bean (*Phaseolus vulgaris*) (Chaerle et al. 2007), wheat (*Triticum aestivum*) (Kuckenberg et al. 2009), lettuce (*Lactuca sativa*) (Prokopová et al. 2010) and even American ginseng where a decrease in Fv/Fm has been correlated to increasing disease load of *P. irregulare* (Chapter 2: Ivanov and Bernards 2012). However, ΦNO was monitored in the *in vivo* study because there is no need for dark adaptation of plants before measuring this parameter and because it can be monitored during steady state illumination at a wide range of light intensities (Klughammer and Schreiber 2008).

For the purposes of our *in vivo* studies, ΦNO was used to monitor the disease severity of *P. irregulare* on American ginseng plants which were treated with a relatively high dose of ginsenosides after their roots were dipped into a solution of GSF prior to planting in a pot-based experiment (Fig. 4.2) (Chapter 4).This experiment indicated that infection by the pathogen was delayed in ginsenoside treated plants compared to control plants which were not treated with ginsenosides. These results were surprising since Nicol et al. (2003) previously demonstrated that the *in vitro* exposure to ginsenosides increased *P. irregulare* growth, and by extension it was predicted that increased ginsenoside concentrations would cause the pathogen to grow faster and consequently locate and infect ginseng plants quicker. Instead it appeared that ginsenosides present in the rhizosphere, in the dosage applied, may have provided temporary protection for one-year old plants by delaying infection. This conclusion was supported by data from two-year old plants, which showed no infection at all

relative to the control, meaning this protective effect could be exaggerated and may have provided even longer term protection for hardier two-year old plants.

Alternatively however, the presence of ginsenosides in relatively large doses in the rhizospere may have simply altered the growth pattern of the pathogen in the soil, as seen when *P. irregulare* is grown in the presence of ginsenosides in liquid culture (Nicol et al. 2002; 2003) and on agar plates with point sources of pure ginsenosides. In either case it remains unclear whether the delayed infection of *P. irregulare* on ginsenoside treated plants was due to a protective effect from ginsenosides or from a modification of *P. irregulare* growth as observed in the *in vitro* assays. The results, however, suggest that the latter is correct, and that ginsenosides serve to alter the growth and metabolism of this organism which may serve to (ultimately) facilitate infection.

The data obtained from the *in vivo* and *in vitro* studies examining the role of ginsenosidases and ginsenosides in the ginseng-*P. irregulare* pathosystem all point to the involvement of the extracellular enzymes secreted by the pathogen in the infection process. For this reason, in conjunction with the above experiments, amino-acid sequence data obtained by Neculai et al. (2009) from trypsin digest peptide fragments of purified ginsenosidases G2 and G3 was used to attempt to clone and sequence these enzymes in order to functionally characterize them. This work culminated in the identification of a putative ß-glucosidase designated as PiGH1-x, which was the first potential ginsenoside metabolizing family 1 glycosyl hydrolase ever sequenced from *P. irregulare* (Chapter 5).

At this time, however, it is still unclear whether the protein PiGH1-x represents G2, G3 or an as of yet uncharacterized ß-glucosidase. All knowledge of the structure of this protein, to date, has been derived from *in silico* analysis and the only firm information available is that the amino acid sequence encoding this protein is homologous to protein sequences encoding glycosyl hydrolase family 1 enzymes, which are the same family of enzymes the partially purified G2 and G3 belong to (Neculai et al. 2009). Further information about this enzyme will require the expression of a recombinant ß-glucosidase (PiGH1-x) for functionalcharacterization and testing it's suitability for metabolizing ginsenosides. This is important because the enzymatic transformation of ginsenosides using recombinant glycosidases is one of the most promising ways to produce pharmaceutically active minor ginsenosides in large quantities and could result in commercial utilization of this recombinant protein (Park et al. 2010; Cui et al. 2013).

6.2. Summary and future directions

From the data obtained during the course of this research project it has become clear that the common 20 (S)-protopanaxadiol ginsenosides, secreted by ginseng plants into the rhizoshpere, alter the growth pattern of the pathogen in the soil delaying initial infection of seedlings (Fig. 6.1) (Chapter 4). Furthermore, it has been established that there is a correlation between the virulence of *P. irregulare* on ginseng and ginsenosidase activity (Fig 6.1) (Chapter 2). The presence of protopanaxadiol ginsenosides may also, act as a trigger for the production of the specific ginsenoside metabolizing ß-glucoisdases G1, G2 and G3 (Neculai et al. 2009), one of which may be the sequenced ß-glucosidase from *P. irregulare* PiGH1-x (Chapter 5). However, the exact metabolic trigger for the production of these specific glycosidases is still unknown. Previously, it had been suggested by Bernards et al. (2010) that the main ginsenoside product obtained from combined G1, G2 and G3 activity *in vitro,* ginsenoside F2 acts as the main chemoatractant/growth stimulator. Data obtained during this project raises doubts about this assertion, due to the *in vitro* inhibition of *P. irregulare* growth caused by ginsenoside F2. Nevertheless, even though ginsenoside F2 initially inhibits the growth of *P. irregulare in vitro,* this inhibition is overcome with time.

The inhibition in growth may be overcome through a physiological/structural change in *P. irregulare* signalled by exposure to ginsenoside F2 which may be related to signalling and increased pathogenicity (Fig. 6.1) (Chapter 4). A vital fluorescent stain could therefore, be used to monitor changes in structure according to Thrane et al. (1999) who elucidated a clear stress response to antifungal agents in *P. ultimum* using this method. In addition, to date the response of *P. irregulare* to ginsenosides has only been tested on hyphae, however, while most *Pythium* spp. can directly infect using hyphae, they also infect using zoospores (Hendrix and Campbell 1973). Zoospores from many oomycete species have been shown to utilize secondary metabolites and other chemical cues in order to locate plant roots (Latijnhouwers et al. 2003; Hardham 2007). Therefore, the chemoattractant potential of pure ginsenosides and GSF must be evaluated on zoospores from *P. irregulare* to see if presence of ginsenosides in the rhizosphere could attract zoospores to facilitate infection.

Cloning of the genes encoding glycosidases G1, G2 and G3 and the functional characterization of their corresponding enzymes will also need to be carried out in the future in order to better study this pathosystem. The further characterization of the ß-glucosidase PiGH1-x and the determination of whether this enzyme codes for G2 or G3 will be the

natural extension of this work. However, to date, sequence information obtained from tryptic digest fragments of G1 indicate this to be a novel ß-glucosidase with no known analogs in the NCBI non-redundant protein database (Neculai et al. 2009). Knowledge about the genes of glycosidase G1, G2 and G3 will, allow for analysis of their gene expression in various isolates of *P. irregulare*. Furthermore, selective down regulation (e.g. through RNAi technology) of the genes may allow for a better understanding of their role in the pathogenicity of these organisms on ginseng. If the proteins are necessary for recognition of roots and infection, selective down regulation may cause a virulent strain to become avirulent.

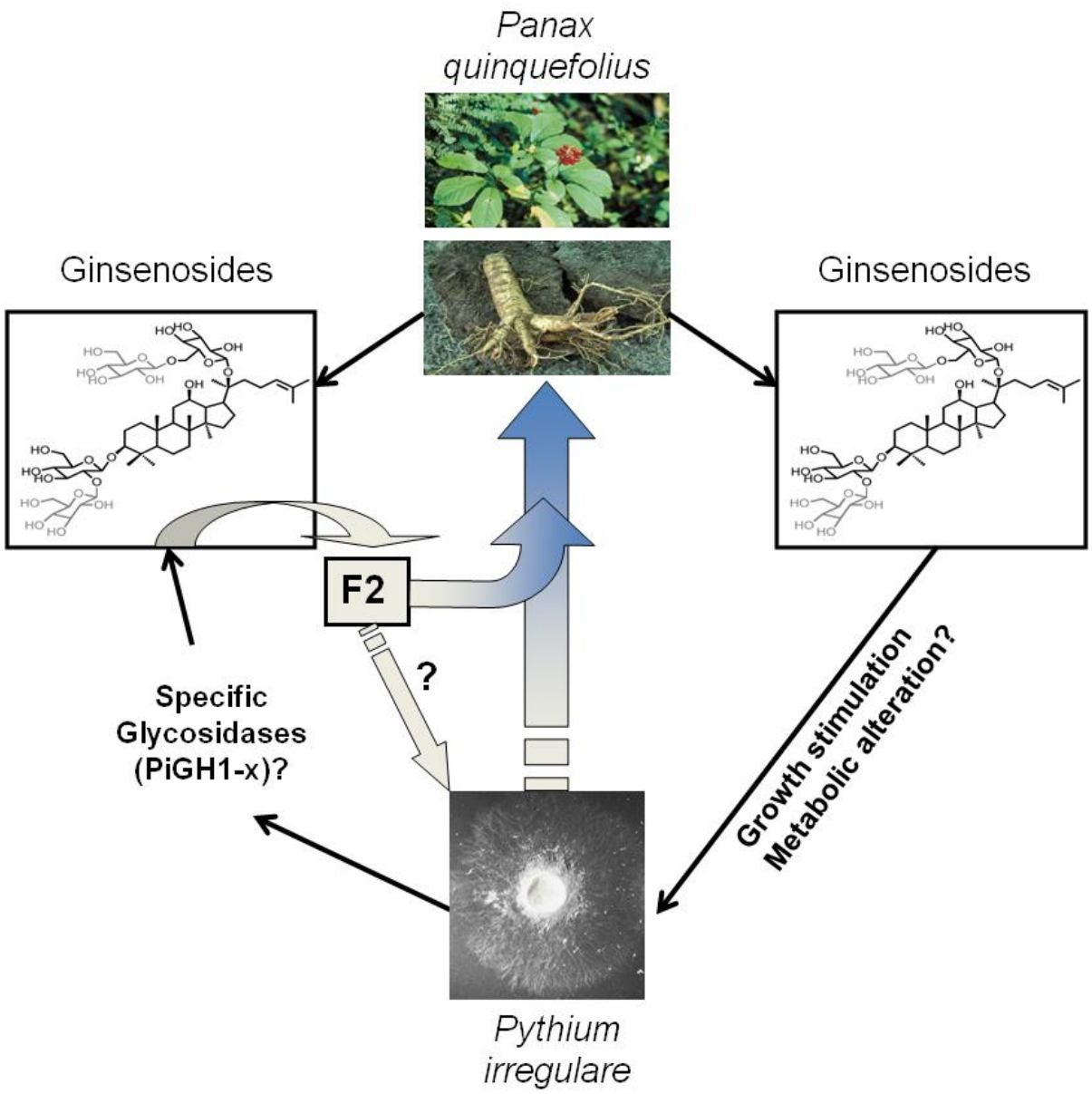

Figure 6.1. Potential roles of ginsenosides in the interaction between ginseng *and Pythium irregulare*. Ginseng plants secrete/leach ginsenosides into the rhizosphere. When ginsenosides are encountered by the pathogen this elicits growth of the organism through an as of yet unknown mechanism. The sensing of ginsenosides may also be used as a signal by *P. irregulare* resulting in a change of glycosidases secreted by the organism into the rhizosphere, resulting in the expression of more specific ginsenosidases, one of which may be ß-glucosidase PiGH1-x, by *Pythium irregulare*, which convert common 20(S)-protopanaxadiol ginsenosides into ginsenoside F2. The role of ginsenoside F2 is still unclear through it is believed that it may elicit a physiological/structural change in *P. irregulare* which may be related to signaling and increased pathogenicity of the organism towards ginseng.

6.3. References

Bernards, M.A., Ivanov, D.A., Neculai, A.M., Nicol, R.W., (2010) Ginsenosides: Phytoanticipins or host recognition factors? Recent Advances in Phytochemistry 41, 13-32.

Chaerle, L., Hagenbeek, D., Vanrobeys, X., Van Der Straeten, D., 2007. Early detection of nutrient and biotic stress in *Phaseolus vulgaris*. Int. J. Remote Sens. 28, 3479-3492.

Cui, C-H., Kim, S-C., Im, W-T., 2013. Characterization of the ginsenoside-transforming recombinant [beta]-glucosidase from Actinosynnema mirum and bioconversion of major ginsenosides into minor ginsenosides. Appl. Microbiol. Biotechnol. 97, 649-659.

Hardham, A.R., 2007. Cell biology of plant-oomycete interactions. Cell. Microbiol, 9, 31-39.

Hendrix F.F., Campbell, W.A., 1973. Pythiums as plant pathogens. Annu. Rev. Phytopathol. 11, 77-98.

Ivanov, D.A., Bernards, M.A., 2012. Ginsenosidases and the pathogenicity of *Pythium irregulare*. Phytochemistry 78, 44-53.

Klughammer, C., Schreiber, U., 2008. Complimentary PSII quantum yields calculated from simple chlorophyll fluorescence parameters measured by PAM fluorometry and the saturation pulse method. PAM Application Notes 1, 27-35.

Kuckenberg, J., Tartachnyk, I., Noga, G., 2009. Temporal and spatial changes of chlorophyll fluorescence as a basis for early and precise detection of leaf rust and powdery mildew infections in wheat leaves. Precision Agric. 10, 34–44.

Latijnhouwers, M., de Wit, P.J.G.M., Govers, F., 2003. Oomycetes and fungi: similar weaponry to attack plants. Trends Microbiol. 11, 462-469.

Neculai, M.A., Ivanov, D., Bernards, M.A., 2009. Partial purification and characterization of three ginsenoside-metabolizing [beta]-glucosidases from *Pythium irregulare*. Phytochemistry 70, 1948-1957.

Nicol, R.W., Traquair, J.A., Bernards, M.A., 2002. Ginsenosides as host resistance factors in American ginseng (*Panax quinquefolius*). Can. J. Bot. 80, 557-562.

Nicol, R.W., Yousef, L., Traquair, J.A., Bernards, M.A., 2003. Ginsenosides stimulate the growth of soilborne pathogens of American ginseng. Phytochemistry 64, 257-264.

Park, C-H., Yoo, M-H., Noh, K-H., Oh, D-K., 2010. Biotransformation of ginsenosides by hydrolyzing the sugar moieties of ginsenosides using microbial glycosidases. Appl. Microbial. Biotechnol. 87, 9-19.

Prokopová, J., Spundova, M., Sedlarova, M., Husickova, A., Novotny´ , R., Dolezal, K., Naus, J., Lebeda, A., 2010. Photosynthetic responses of lettuce to downy mildew infection and cytokinin treatment. Plant Physiol. Biochem. 48, 716–723.

Thrane, C., Olsson, S., Nielson, T.H., Sørensen, J., 1999. Vital fluorescent stains for detection of stress in *Pythium ultimum* and *Rhizoctonia solani* challenged with viscosinamide from Pseudomonas fluorescens DR54. FEMS Microbiol. Ecol. 30, 11-23.

Yousef, L.F., Bernards, M.A., 2006. *In vitro* metabolism of ginsenosides by the ginseng root pathogen *Pythium irregulare*. Phytochemistry 67, 1740-1749.

SUPPORTING INFORMATION

Table S3.1. Changes in the chlorophyll fluorescence parameters ΦPSII, ΦNPQ and ΦPSII. over time measured at an actinic irradiance of PAR 414 µmol photons m^{-2} s^{-1} for one-year old ginseng plants inoculated with different strains of *P. irregulare* (Table 2), compared to Fv/Fm determined after a saturating light pulse for the same treatments. Measurements were taken every 3 days for 15 days total. All values are expressed as Mean ± SE, N = 5 for Fv/Fm, ΦPSII, ΦNPQ and ΦNO measurements.

	Isolate no.				
	Control	BR 901	BR 486	BR 962	BR 1068
Fv/Fm - 1 year old Ginseng plants					
Day 0	0.774 ± 0.005	0.760 ± 0.012	0.782 ± 0.004	0.752 ± 0.009	0.781 ± 0.006
Day 3	0.714 ± 0.017	0.740 ± 0.014	0.755 ± 0.007	0.757 ± 0.006	0.756 ± 0.007
Day 6	0.763 ± 0.006	0.647 ± 0.103	0.766 ± 0.003	0.727 ± 0.009	0.759 ± 0.005
Day 9	0.761 ± 0.008	0.589 ± 0.128	0.742 ± 0.008	0.600 ± 0.130	0.731 ± 0.014
Day 12	0.731 ± 0.015	0.583 ± 0.133	0.734 ± 0.007	0.534 ± 0.131	0.451 ± 0.112
Day 15	0.697 ± 0.020	0.578 ± 0.132	0.716 ± 0.018	0.402 ± 0.150	0.330 ± 0.158
ΦNO - 1 year old Ginseng plants					
Day 0	0.322 ± 0.020	0.318 ± 0.014	0.332 ± 0.019	0.335 ± 0.019	0.371 ± 0.009
Day 3	0.401 ± 0.049	0.301 ± 0.018	0.309 ± 0.013	0.295 ± 0.013	0.345 ± 0.030
Day 6	0.316 ± 0.017	0.304 ± 0.016	0.300 ± 0.018	0.297 ± 0.025	0.323 ± 0.029
Day 9	0.277 ± 0.009	0.444 ± 0.128	0.309 ± 0.016	0.403 ± 0.137	0.327 ± 0.028
Day 12	0.298 ± 0.013	0.460 ± 0.126	0.304 ± 0.013	0.472 ± 0.130	0.585 ± 0.117
Day 15	0.325 ± 0.019	0.422 ± 0.133	0.308 ± 0.019	0.624 ± 0.142	0.712 ± 0.155
ΦNPQ - 1 year old Ginseng plants					
Day 0	0.342 ± 0.030	0.274 ± 0.033	0.241 ± 0.025	0.258 ± 0.026	0.252 ± 0.036
Day 3	0.217 ± 0.055	0.313 ± 0.048	0.290 ± 0.023	0.389 ± 0.078	0.382 ± 0.031
Day 6	0.302 ± 0.025	0.344 ± 0.052	0.297 ± 0.026	0.390 ± 0.050	0.422 ± 0.029
Day 9	0.352 ± 0.027	0.283 ± 0.076	0.288 ± 0.034	0.351 ± 0.088	0.436 ± 0.029
Day 12	0.397 ± 0.027	0.239 ± 0.067	0.352 ± 0.029	0.307 ± 0.077	0.258 ± 0.075
Day 15	0.326 ± 0.035	0.345 ± 0.091	0.343 ± 0.036	0.248 ± 0.102	0.149 ± 0.084
ΦPSII - 1 year old Ginseng plants					
Day 0	0.335 ± 0.025	0.409 ± 0.029	0.426 ± 0.012	0.408 ± 0.020	0.377 ± 0.037
Day 3	0.383 ± 0.031	0.386 ± 0.040	0.401 ± 0.019	0.395 ± 0.020	0.273 ± 0.037
Day 6	0.382 ± 0.020	0.351 ± 0.048	0.403 ± 0.017	0.313 ± 0.029	0.255 ± 0.038
Day 9	0.371 ± 0.026	0.272 ± 0.068	0.403 ± 0.021	0.246 ± 0.067	0.238 ± 0.045
Day 12	0.305 ± 0.033	0.301 ± 0.077	0.344 ± 0.025	0.221 ± 0.060	0.157 ± 0.050
Day 15	0.348550.035	0.233 ± 0.070	0.349 ± 0.031	0.160 ± 0.088	0.138 ± 0.078

Table S3.2. Changes in the chlorophyll fluorescence parameters ΦPSII, ΦNPQ and ΦPSII over time measured at an actinic irradiance of PAR 414 µmol photons m^{-2} s^{-1} for **two-year old** ginseng plants inoculated with different strains of *P. irregulare* (Table 2), compared to Fv/Fm determined after a saturating light pulse for the same treatments. Measurements were taken every 3 days for 15 days total. All values are expressed as Mean ± SE, N = 5 for Fv/Fm, ΦPSII, ΦNPQ and ΦNO measurements.

	Isolate no.				
	Control	BR 901	BR 486	BR 962	BR 1068
Fv/Fm - 2 year old Ginseng plants					
Day 0	0.758 ± 0.008	0.744 ± 0.013	0.751 ± 0.014	0.753 ± 0.010	0.761 ± 0.012
Day 3	0.777 ± 0.005	0.714 ± 0.015	0.740 ± 0.013	0.725 ± 0.019	0.706 ± 0.015
Day 6	0.783 ± 0.005	0.742 ± 0.015	0.734 ± 0.015	0.689 ± 0.033	0.748 ± 0.009
Day 9	0.774 ± 0.008	0.720 ± 0.015	0.737 ± 0.017	0.637 ± 0.082	0.637 ± 0.053
Day 12	0.789 ± 0.004	0.763 ± 0.005	0.745 ± 0.012	0.561 ± 0.121	0.622 ± 0.107
Day 15	0.773 ± 0.010	0.752 ± 0.011	0.741 ± 0.011	0.326 ± 0.152	0.527 ± 0.134
ΦNO - 2 year old Ginseng plants					
Day 0	0.278 ± 0.010	0.273 ± 0.022	0.282 ± 0.015	0.274 ± 0.015	0.277 ± 0.013
Day 3	0.281 ± 0.013	0.299 ± 0.030	0.280 ± 0.011	0.296 ± 0.031	0.304 ± 0.020
Day 6	0.256 ± 0.010	0.264 ± 0.012	0.267 ± 0.008	0.349 ± 0.068	0.260 ± 0.012
Day 9	0.260 ± 0.010	0.266 ± 0.019	0.260 ± 0.011	0.361 ± 0.099	0.331 ± 0.047
Day 12	0.255 ± 0.013	0.219 ± 0.025	0.253 ± 0.009	0.449 ± 0.108	0.391 ± 0.118
Day 15	0.241 ± 0.008	0.239 ± 0.027	0.247 ± 0.007	0.699 ± 0.159	0.512 ± 0.152
ΦNPQ - 2 year old Ginseng plants					
Day 0	0.488 ± 0.038	0.453 ± 0.039	0.501 ± 0.029	0.482 ± 0.029	0.481 ± 0.041
Day 3	0.412 ± 0.057	0.450 ± 0.035	0.476 ± 0.043	0.473 ± 0.042	0.439 ± 0.040
Day 6	0.485 ± 0.030	0.421 ± 0.040	0.511 ± 0.037	0.391 ± 0.058	0.517 ± 0.030
Day 9	0.448 ± 0.044	0.441 ± 0.046	0.463 ± 0.044	0.413 ± 0.083	0.500 ± 0.055
Day 12	0.380 ± 0.042	0.505 ± 0.048	0.478 ± 0.045	0.383 ± 0.076	0.463 ± 0.090
Day 15	0.442 ± 0.038	0.440 ± 0.068	0.503 ± 0.042	0.214 ± 0.121	0.337 ± 0.118
ΦPSII -2 year old Ginseng plants					
Day 0	0.235 ± 0.043	0.274 ± 0.035	0.216 ± 0.027	0.244 ± 0.033	0.242 ± 0.041
Day 3	0.307 ± 0.052	0.251 ± 0.036	0.244 ± 0.044	0.232 ± 0.032	0.261 ± 0.041
Day 6	0.259 ± 0.033	0.315 ± 0.039	0.222 ± 0.038	0.261 ± 0.035	0.222 ± 0.032
Day 9	0.292 ± 0.045	0.293 ± 0.049	0.277 ± 0.039	0.227 ± 0.038	0.168 ± 0.041
Day 12	0.364 ± 0.036	0.276 ± 0.035	0.258 ± 0.042	0.168 ± 0.056	0.146 ± 0.042
Day 15	0.317 ± 0.039	0.321 ± 0.051	0.249 ± 0.041	0.087 ± 0.055	0.149 ± 0.052

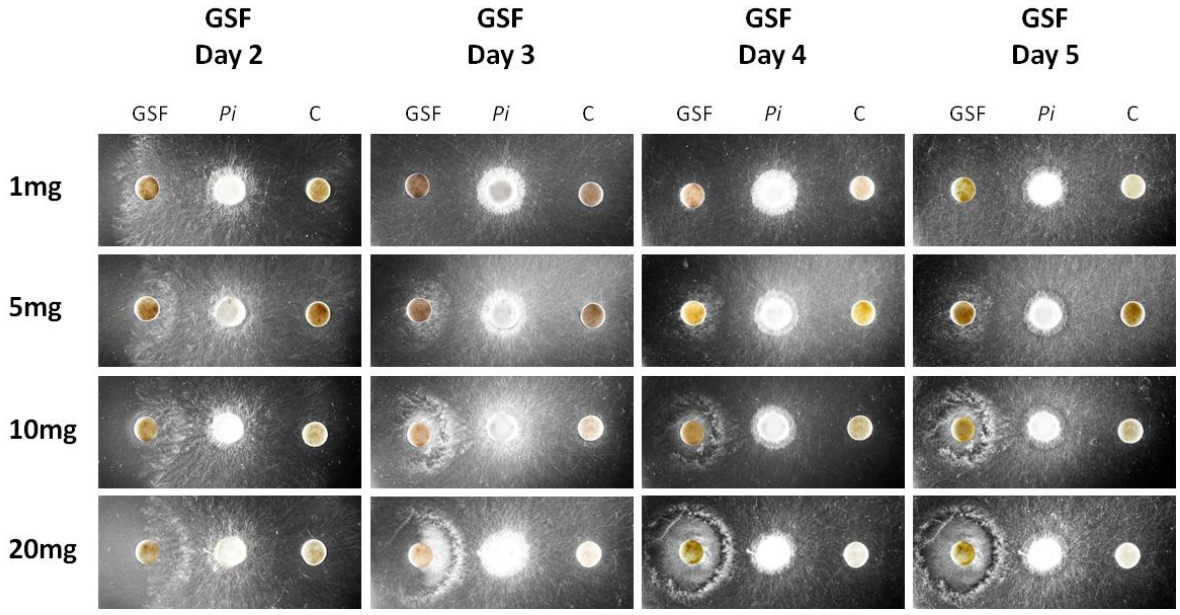

Figure S4.1. Effect of purified ginsenoside extract (GSF) on *Pythium irregulare* BR 1068 growth *in vitro*. Representative images of 90 mm petri dishes filled with Czapek Dox Mineral Agar containing 6 mm antibiotic-assay discs placed an equal distance from an 8 mm diameter plug of *P. irregulare* BR 1068 are portrayed. Discs on the left in each column are infused with 100 µL of either 1, 5, 10 or 20 mg mL^{-1}, purified ginsenoside extract (GSF). All discs on the right in each column are controls infused with 100 µL MeOH. Experiment was performed in triplicate (N = 3). Images shown are representative of a single plate, for each treatment, monitored every 24 hours (Day 1) for 120 hours (Day 5). 24 hour images are not included because mycelia had not reached filters and no effects were seen in any treatments. All ginsenosides were dissolved in MeOH.

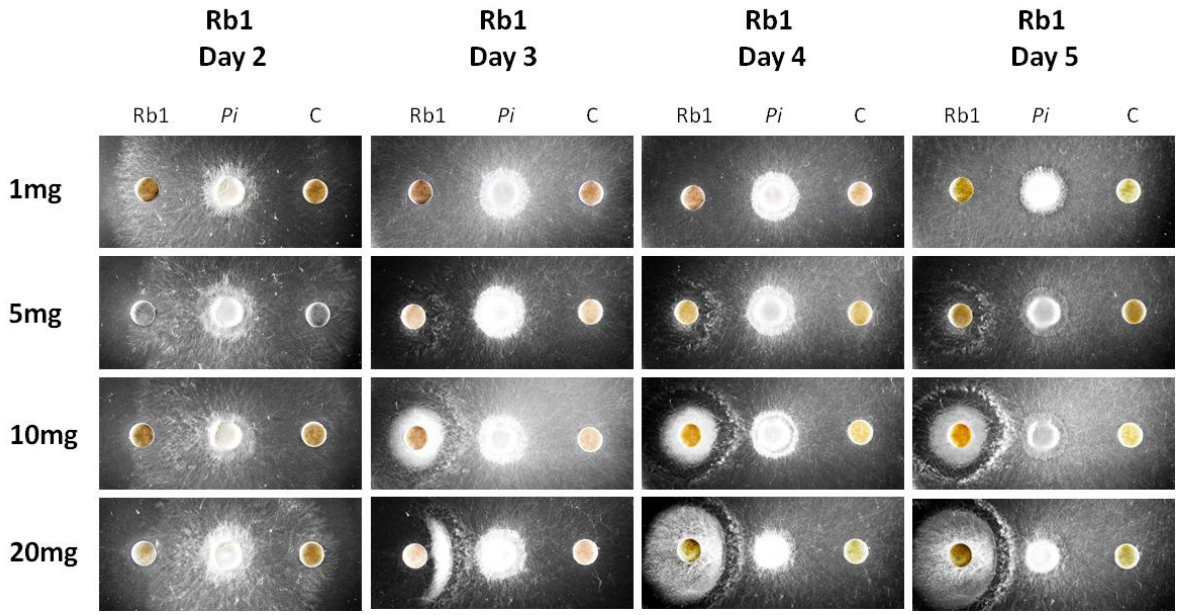

Figure S4.2. Effect of pure ginsenoside Rb1 on *Pythium irregulare* BR 1068 growth *in vitro*. Representative images of 90 mm petri dishes filled with Czapek Dox Mineral Agar containing 6 mm antibiotic-assay discs placed an equal distance from an 8 mm diameter plug of *P. irregulare* BR 1068 are portrayed. Discs on the left in each column are infused with 100 µL of either 1, 5, 10 or 20 mg mL^{-1}, pure ginsenoside Rb1. All discs on the right ineach column are controls infused with 100 µL MeOH. Experiment was performed in triplicate (N = 3). Images shown are representative of a single plate, for each treatment, monitored every 24 hours (1 day) for 120 hours (5 days). 24 hour images are not included because mycelia had not reached filters and no effects were seen in any treatments. All ginsenosides were dissolved in MeOH.

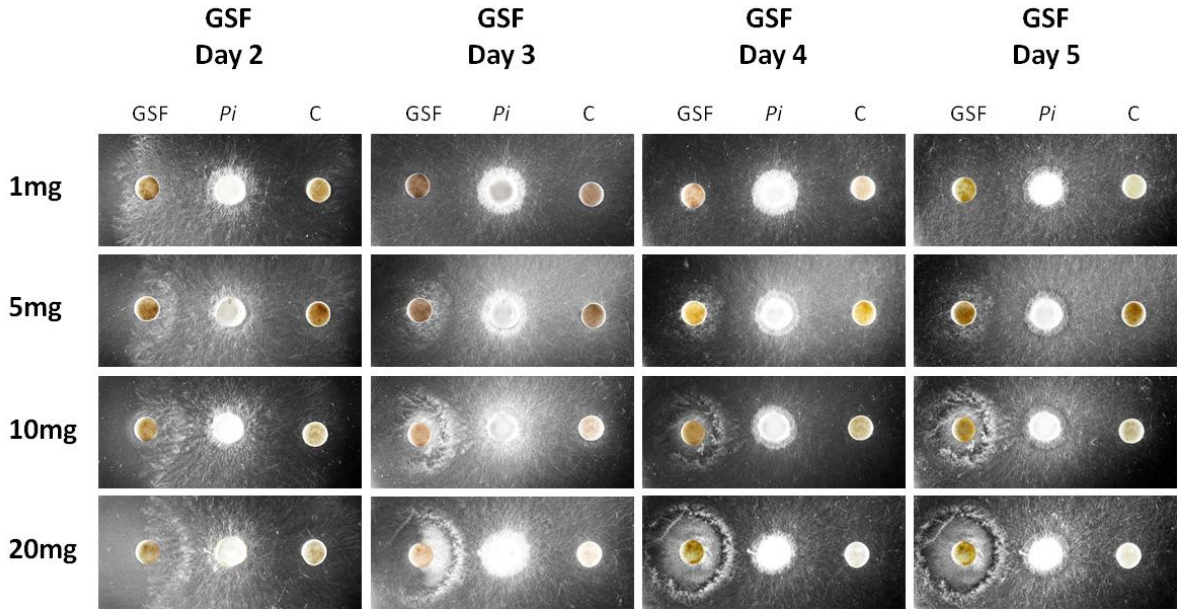

Figure S4.3. Effect of pure ginsenoside Re on *Pythium irregulare* BR 1068 growth *in vitro*. Representative images of 90 mm petri dishes filled with Czapek Dox Mineral Agar containing 6 mm antibiotic-assay discs placed an equal distance from an 8 mm diameter plug of *P. irregulare* BR 1068 are portrayed. Discs on the left in each column are infused with 100 µL of either 1, 2, 5 or 10 mg mL^{-1}, pure ginsenoside Re. All discs on the right in each column are controls infused with 100 µL MeOH. Experiment was performed in triplicate (N = 3). Images shown are representative of a single plate, for each treatment, monitored every 24 hours (1 day) for 120 hours (5 days). 24 hour images are not included because mycelia had not reached filters and no effects were seen in any treatments. All ginsenosides were dissolved in MeOH.

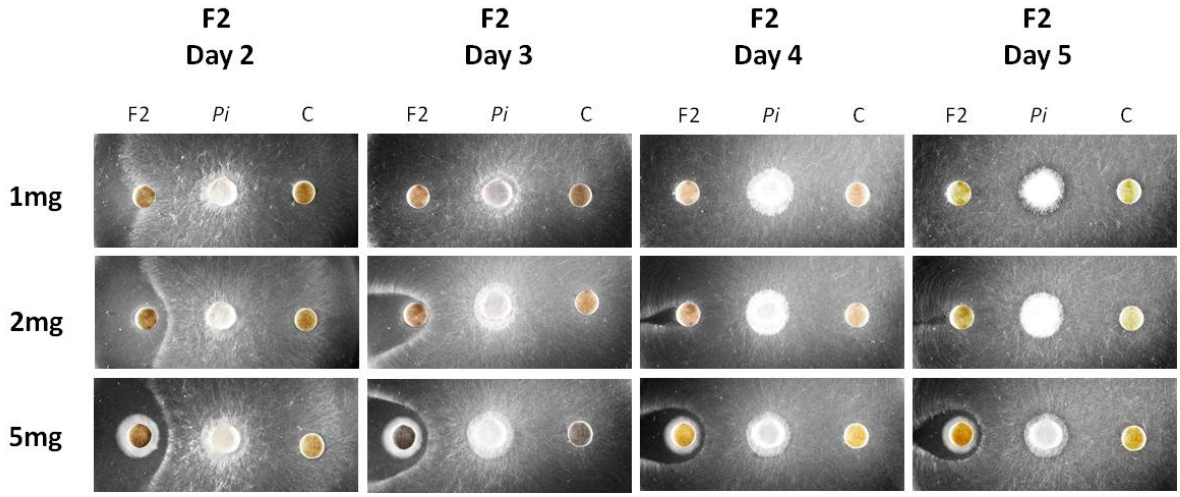

Figure S4.4. Effect of pure ginsenoside F2 on *Pythium irregulare* BR 1068 growth *in vitro*. Representative images of 90 mm petri dishes filled with Czapek Dox Mineral Agar containing 6 mm antibiotic-assay discs placed an equal distance from an 8 mm diameter plug of *P. irregulare* BR 1068 are portrayed. Discs on the left in each column are infused with 100 µL of either 1, 2 and 5 mg mL^{-1}, pure ginsenoside F2. All discs on the right in each column are controls infused with 100 µL MeOH. Experiment was performed in triplicate (N = 3). Images shown are representative of a single plate, for each treatment, monitored every 24 hours (1 day) for 120 hours (5 days). 24 hour images are not included because mycelia had not reached filters and no effects were seen in any treatments. All ginsenosides were dissolved in MeOH.

CURRICULUM VITAE

Post-secondary Education

Graduate Degree Ph.D. (2009 - Present)
University of Western Ontario, London, ON, Canada

Undergraduate Degree B.Sc. (2004 - 2009)
University of Western Ontario, London, ON, Canada

Professional Experience

Teaching Assistant (2009 - 2015)
University Of Western Ontario – Department of Biology

Research Assistant (2007 - 2008)
Agriculture and Agri-Food Canada (Southern Crop Protection and Food Research Centre), London, ON, Canada

Research Assistant (2005)
University of Western Ontario – Department of Physical Therapy

List of Publications and Presentations

a. Articles published or accepted in refereed journals

Ivanov, D.A., and Bernards, M.A. (2012) Ginsenosides and the pathogenicity of *Pythium irregulare*. Phytochemistry **78**: 44-53

Bernards, M.A., **Ivanov, D.A.**, Neculai, A.M., and Nicol, R. (2010) Ginsenosides: Phytoanticipins or host recognition factors? Gang, D.R. (ed.), *The Biological Activity of Phytochemicals*, Recent Advances in Phytochemistry **41**:13-32.

Neculai, A.M., **Ivanov, D**., and Bernards, M.A. (2009) Partial purification and characterization of three ginsenoside-metabolizing β-glucosidase from *Pythium irregulare*. Phytochemistry **70**:1948-1957.

b. Non-refereed contributions (Conference and Poster presentations)

Ivanov, D.A* and Bernards, M.A. (2014) Using chlorophyll fluorescence imaging to track and measure Pythium irregulare infection of American ginseng. Presented at the 9th Summer Colloquium on Plant Ecophysiology Parque Katalapi, Pichiquillaipe, Puerto Montt, Chile January 18-20. *Oral Presenter.

Ivanov, D.A* and Bernards, M.A. (2012) Ginsenosides and the pathogenicity of *Pythium irregulare.* Presented at the 51st Meeting of the Phytochemical Society of North America, University of Western Ontario, London ON, August 11-15. *Poster Presenter

Ivanov, D.A* and Bernards, M.A. (2012) Ginsenosides and the pathogenicity of *Pythium irregulare.* Presented at the 3rd Banff Conference on Plant Metabolism, Banff AB, June 28-July 2. *Poster Presenter

Ivanov, D.A*, and Bernards, M.A. (2011) Extracellular glycosidases of *Pythium irregulare.* Presented at the Joint Plant Canada Conference, St. Mary's University, Halifax NS, July 17-21. *Oral Presenter

Ivanov, D.A.*, and Bernards, M.A. (2010) The role of extracellular glycosidases in the *Pythium irregulare* - ginseng pathosystem**.** Presented at the Eastern Regional Meeting of the Canadian Society of Plant Physiologists, Brock University, St. Catherines ON, December 3-4, 2010. *Poster presenter

Bernards, M.A*, **Ivanov**, **D**., Neculai, A., Yousef, L., and Nicol, R. (2009) The Ecological Role(s) of Ginsenosides. Presented at the 49th Meeting of the Phytochemical Society of North America, Towson University, Towson MD, August 8-12, 2009. *Oral presenter

Awards and Scholarships

a. Scholarships

NSERC Postgraduate Scholarship D (2013-2015)

Ontario Graduate Scholarship (2011-2012)

Ontario Graduate Scholarship (2010-2011)

b. Awards

Department of Biology Travel Award (2014)
University of Western Ontario

Best Poster Award
51st Meeting of the Phytochemical Society of North America (2012)

Department of Biology Travel Award (2012)
University of Western Ontario